INSTITUT FÜR HYDROLOGIE
ALBERT-LUDWIGS-UNIVERSITÄT FREIBURG IM BREISGAU

Marc Haering

# The Impact of Groundwater Recharge on Dissolved Gaseous Components
-
# A Process-Oriented Approach

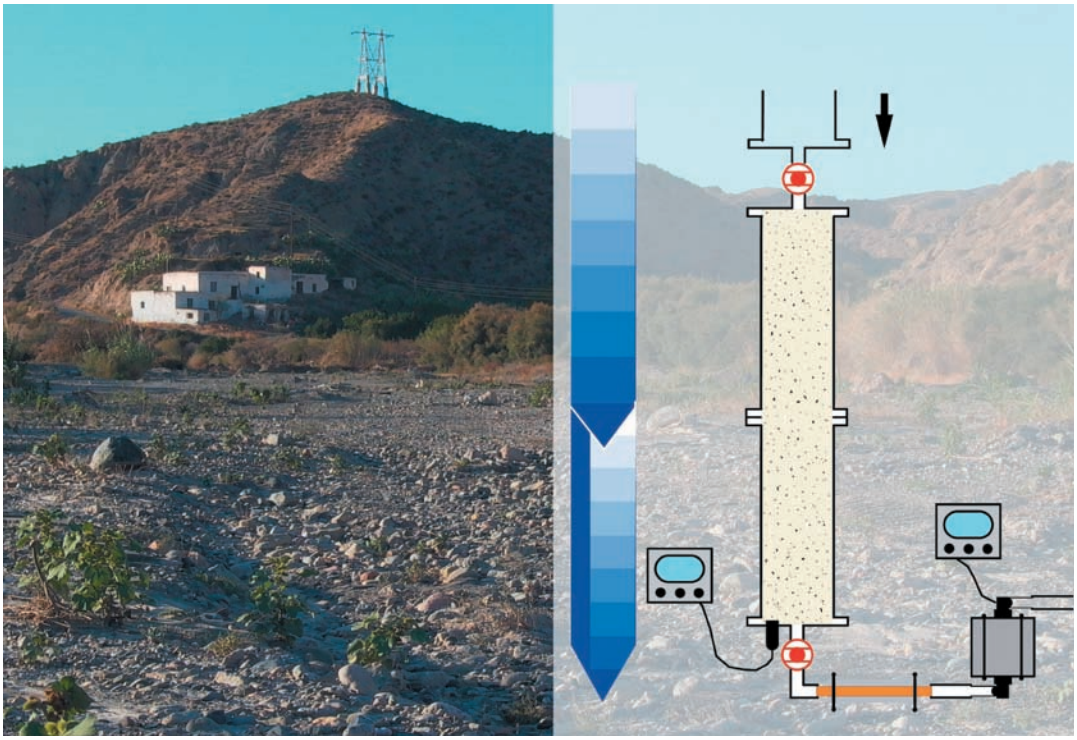

Diplomarbeit unter der Leitung von Prof. Dr. Ch. Leibundgut
Freiburg im Breisgau, April 2006

**I**NSTITUT **F**ÜR **H**YDROLOGIE
**A**LBERT-**L**UDWIGS-**U**NIVERSITÄT **F**REIBURG IM **B**REISGAU

Marc Haering

# The Impact of Groundwater Recharge on Dissolved Gaseous Components
-
# A Process-Oriented Approach

Referent: Prof. Dr. Christian Leibundgut
Koreferent: Dr. Christoph Külls

Diplomarbeit unter der Leitung von Prof. Dr. Ch. Leibundgut
Freiburg im Breisgau, April 2006

## Acknowledgements

I would like to thank Prof. Dr. Christian Leibundgut for his patronage of the work and a greatly formative education. Without both, this work would not have been realizable. Sincere thanks go to my co-referent and supervisor, Dr. Christoph Külls, for initiating this work, for taking the time to develop inspiring discussions, and for solving problems with patience and deliberateness. I also would like to thank Dr. Jens Lange, from who I learned to share and to deepen the fascination for hydrological processes in semi-arid and arid regions.

The funding of project WADE (GOCE-CT-2003-506680-WADE) by the European Commission, Sixth Framework Programme (2002-2006) is acknowledged. Thanks go to Hydrosiotop GmbH, for the fast analyses of samples taken on the field trip. Cordial thanks go to the WADE team, in particular to Dr. Gerardo Benito for assistance during the field trip, and Ainhoa Lorenzo for preparation of the field trip as well as for continuous sampling.

I would sincerely like to thank Prof. Dr. Werner Aeschbach-Hertig (IUP, Heidelberg) for his ardent collaboration regarding the realization of experimental investigations, and Dr. Lazlo Palcsu for his devoted assistance during the whole time of investigations in Freiburg, as well as for analyses.

I would like to express my gratitude to the following people, that have contributed a lot to the realization of this work:

Emil Blattmann, for the construction of the column setup; Jochen Wenninger for the analyses of stable isotopes; Volker Abraham, for saving the experimental data, almost lost; Jürgen Strub for support in the poster layout; Carlette Orellana, for proof-reading and for the patience and sacrifice she brought me; Andrea Wachtler, for last-minute layout problems. Cordial thanks go to my parents and my friends, for supporting and encouraging me devotedly.

*„Die Natur ist das einzige Buch, das auf allen Blättern großen Gehalt bietet“*

(Johann Wolfgang von Goethe)

# Contents

# List of Figures

# List of Tables

## List of Tables in the Annex

## Abbreviations

| | |
|---|---|
| Ar | Argon |
| CFCs | Chlorofluorocarbons |
| He | Helium |
| $^{2}H$ | Deuterium |
| $^{3}H$ | Tritium |
| Kr | Krypron |
| Ne | Neon |
| $^{18}O$ | Oxygen 18 |
| $SF_6$ | Sulfur hexafluoride |
| Xe | Xenon |
| a.s.l. | above sea level |
| GMWL | Global Meteoric Waterline |
| GWR | Groundwater Recharge |
| IAEA | International Atomic Energy Association |
| IHF | Institute of Hydrology Freiburg |
| IUP | Insitute of Environmental Physics Heidelberg |
| MMWL/A | Mediterranean Meteoric Waterline according to Anza et al. |
| UNEP | United Nations Environment Programme |
| USGS | United States Geological Survey |

## Summary

This study aims at investigating the impact of hydrological processes on the comportment of gaseous components in groundwater. Distinguishable processes of groundwater recharge in semi-arid and arid regions, such as direct and indirect recharge, are detected by evaluating characteristical patterns of CFCs and $SF_6$. Together with information gained from insitu parameters and water chemistry as well as supporting data from Tritium and stable isotopes $^{18}O$ and $^{2}H$, the groundwater in the alluvial aquifer of an ephemeral stream is characterized in terms of origin, recharge altitude, residence times and dominant processes. In addition, the identification of excess air and noble gas patterns, subject to relevant groundwater recharge processes, is conducted inductively in laboratory column experiments.

The study site chosen for this work is situated within the Province of Almeria in southeast Spain, which is regarded as one of Europe's most arid regions. The Rio Andarax Basin has a catchment size of 2200 km² and shows a semi-arid/mediterranean climate with an annual air temperature average of 18 °C and about 160 mm of rainfall. Being situated within the Betic Cordillera, the catchment is surrounded by four major mountain ranges, mainly consisting of Pre-Cenozoic mica slate, phyllite and dolomite. A Neogene Basin extends among the major elevations with an average thickness of 500 meters. All the streams in the catchment are ephemeral. The main stream, Rio Andarax, however, is permanently flowing at its source. Occasional flooding contributes recharge to the detritic aquifer and sometimes reaches the Mediterranean Sea superficially.

The fourteen water samples taken on a field trip within the frame of project WADE (EU-funded GOCE-CT-2003-506680-WADE) could be differentiated regarding their chemical properties and assigned to a fissured dolomite aquifer and several shallow and deep detritic aquifers of the Neogene sequence. Analyses of the stable isotopes $^{2}H$ and $^{18}O$ give information of recharge elevations and recharge processes. Most groundwaters exhibit an altitude shift, meaning that rainfall occured at elevations higher than the actual sampling point. This altitude shift is most pronounced for groundwater in the alluvium of Rio Andarax. The temporal behavior of stable isotopes gave evidence, that the shallow detritic aquifer below the river bed of Rio Andarax is recharged by floods.

CFC-analyses determined three major ranges of residence times in groundwater. Young groundwater with residence times around 15 years could be found in the active channel of Rio Andarax. Groundwater originating in the Pre-Cenozoic basement and the detritic aquifer in the eastern part of the basement showed intermediate residence times around 30 years. Finally a groundwater with no traces of recent recharge was found in a molasse aquifer. In addition, CFC-analyses determined groundwater with itermediate and long residence times to be mixing waters composed of young and old water. Groundwater from the detritic aquifers below the river bed of Rio Andarax point to a piston-type flow distribution, indicating focused indirect recharge. For some samples, analyses of $SF_6$ indicated a potential presence of high excess air concentrations in fissured aquifers and in aquifers with rapid, focused recharge.

The measurements of CFCs and $SF_6$ concentrations in groundwater from different aquifers within the Rio Andarax basin have demonstrated that a determination of mean residence times in groundwater bodies is possible with a relatively high precision. It is

suggested to measure all CFCs and $SF_6$ in order to better interpret dinstinct behaviors and obtain objective results. That way, additional information on dominant processes in aquifers, such as presence of excess air, detection of anaerobic environments and identification of relevant mass transport processes, can as well be obtained.

Nevertheless it is important to integrate conventional hydrologic methods in the use of gases as environmental tracers. Information gained from insitu parameters and water chemistry as well as supporting data from Tritium and stable isotopes $^{18}O$ and $^{2}H$ remain crucial to reliably interpret CFCs, $SF_6$ and noble gas measurements. In addition, field investigations on catchment boundaries, potential recharge areas, geological and hydrogeological units, etc., as well as construction properties of the sampled wells and boreholes avoid a misinterpretation.

The identification of excess air and noble gas patterns, subject to direct and indirect recharge processes was conducted in three experimental setups, designed at the IHF. The first experiment simulated direct recharge to groundwater with a precipitation rate smaller or equal to the infiltration rate of the sand used for the investigations. Two other experiments simulated indirect recharge processes to groundwater, representing an applied hydrostatic pressure of 160 hPa and 300 hPa. Investigations were carried out in cooperation with the IUP, and analyses were done at the Edelgas-MS Laboratory of IUP, Heidelberg.

Acrylic glass columns were filled up to 100 cm above the bottom with fine sorted quartz sand. Samples were fused into copper tubes at the bottom outlet of the columns. A fluorimeter was connected subsequently to the copper tube sampler, measuring fluorescence tracers added to the water to determine appropriate times for sampling and controlling outflow temperature. At the outflow of the fluorimeter, an electronic balance was positioned to weigh the cumulated amount of outflow per time. The applied hyrostatic head was monitored with a pressure sensor at the bottom of the column.

Experimental investigations could successfully simulate the formation of excess air. Almost all samples, that have been analyzed so far show concentrations higher than water in equilibrium with air. The amount of supersaturation ranges from 4.8% to 14.6% $\Delta Ne$. A high supersaturation of water could be found in samples taken out of the saturated zone at the bottom of the column. One sample taken towards the end of the inestigations shows no relative $\Delta He$ excess, although it steamed from water that has moved under the same ponded conditions to the bottom of the column. Observations during the experiments showed, that the effective hydrostatic pressure does not necessarily correspond to the applied hydrostatic head and might reveal a potential discrepancy between nature and laboratory.

Keywords:

environmental tracers - groundwater recharge - noble gases - excess air - chlorofluorocarbons - age dating - Almeria

## Zusammenfassung

Das Ziel dieser Arbeit ist, den Einfluss hydrologischer Prozesse auf das Verhalten von Gasen im Grundwasser zu untersuchen. Dabei wird ein besonderes Augenmerk auf die direkten und indirekten Grundwasserneubildungsprozesse in Trockengebieten gerichtet und durch charakteristische Gaszusammensetzungen unterschieden. Hydrochemische und isotopenhydrologische Untersuchungen sollen die Interpretation des Verhaltens von Gasen unterstützen und gemeinsam alluviale Grundwässer hinsichtlich ihrer Herkunft, Neubildungshöhe, mittleren Verweilzeit und weiteren relevanten Prozessen beschreiben. Des Weiteren wird der in der Natur oft beobachtete Gasüberschuss (excess air) im Grundwasser untersucht. In einem Laborversuch werden die oben erwähnten Neubildungsprozesse möglichst naturnah nachgestellt, um eventuelle charakteristische Verhaltensmuster von Edelgaszusammensetzungen im Wasser aufzudecken.

Das Forschungsgebiet dieser Arbeit liegt im Südosten Spaniens, genauer in der Provinz Almeria, die weithin als eine der trockensten Regionen Europas angesehen wird. Das 2200 km² große Einzugsgebiet des Rio Andarax erstreckt sich in einem semi-ariden, mediterranen Klima, mit einer mittleren Jahrestemperatur von 18°C und mittleren jährlichen Niederschlägen von ca. 160 mm. Vier große, von Ost nach West verlaufende Höhenzüge grenzen das Gebiet ab. Sie sind Teil der betischen Cordilleren und bestehen hauptsächlich aus Dolomiten, Phyliten und Glimmerschiefern des frühen Känozoikum. Das sich dazwischen erstreckende Becken besteht aus einer Abfolge von Sedimenten und Konglomeraten mit Mächtigkeiten von ca. 500 m. Alle Flüsse im Einzugsgebiet sind ephemer, lediglich im Rio Andarax kann nah an der Quelle ganzjährig Abfluss beobachtet werden. Rio Andarax weist jährlich Abflussereignisse auf, die weit in das Einzugsgebiet hineinreichen und teilweise in das Mittelmeer entwässern.

Die vierzehn Wasserproben, die im Gelände entnommen wurden, können durch ihre Hauptinonenzusammensetzung unterschieden und verschiedenen Grundwasserleitern des Einzugsgebietes zugeordnet werden. Durch die Auswertung der stabilen Isotope Deuterium und $^{18}O$ kann angenommen werden, dass sich das Neubildungsgebiet der untersuchten Grundwässer in höheren Lagen befindet. Die stärkste Abweichung vom anzunehmenden Höhengradienten isotopischer Zusammensetzung weisen die Proben auf, die aus dem Alluvium des Rio Andarax entnommen wurden. Monatliche Messungen der stabilen Isotope im Flusswasser, in einem Piezometer im ephemeren Teil des Flussbetts, sowie auf angrenzenden Plantagen haben gezeigt, dass das Alluvium durch indirekte Grundwasserneubildung bei Hochwasserereignissen gespeist wird.

Durch die Messungen von FCKWs im Grundwasser können drei Altersgruppen von Wässern unterschieden werden. Die jüngsten Wässer mit mittleren Verweilzeiten um die 15 Jahre befinden sich unter oder in unmittelbarer Nähe des aktiven Flussbetts. Grundwässer im trockeneren Osten des Einzugsgebietes sowie Grundwasser des Karstaquifers weisen Verweilzeiten um die 30 Jahre auf. Eine Grundwasserprobe, die ausserhalb der oberirdischen Einzugsgebietsgrenze entnommen wurde, weist fast keine FCKW- und $SF_6$- Konzentrationen auf. Ihr Alter wird je nach Modellvorstellung auf 50 bis 200 Jahre geschätzt. Der Vergleich von FCKW-Gehalten untereinander deutet darauf hin, dass Wässer mit mittleren und langen Verweilzeiten durch Mischungsprozesse im Aquifer beeinflusst sind. Grundwasserproben, die unter dem aktiven, ephemeren Flussbett des Rio Andarx

entnommen wurden, weisen hingegen ein pistonflow-ähnliches Fliessverhalten auf. Dies deutet erneut darauf hin, dass die oberflächennahen Grundwasserleiter unter dem ephemeren Flussbett bevorzugt durch indirekte Neubildungsmechanismen gespeist werden. Die gemessenen $SF_6$-Konzentrationen zeigen im Gegensatz zu den FCKW-Werten ein eher unbeständiges Bild auf. Proben aus dem Karstaquifer sowie eine Probe aus dem tiefergelegenen Grundwasserleiters des Alluviums enthalten hohe Konzentrationen, die auf das Vorhandensein von excess air schliessen lassen könnten. Andere Proben hingegen stimmen mit den aus FCKW errechneten Verweilzeiten überein.

Die Datierung von Grundwasser mit FCKWs hat gezeigt, dass die Bestimmung von Verweilzeiten vergleichsweise genau ist. Um jedoch zuverlässige Aussagen treffen zu können, empfielt es sich, stets alle Industriegase in die Interpretation mit einzubeziehen. Auf diese Weise können auch zusätzliche Aquifereigenschaften aufgedeckt werden, wie zum Beispiel Mischungsprozesse und Fliessverhalten durch das Anwenden von Stofftransportmodellen oder anaerobe Verhältnisse durch die relativ stärkere Dergradierung von F-11. Auch das eventuelle Vorhandensein von Luftüberschuss kann auf diese Weise aufgezeigt werden, und sollte unbedingt in der Interpretation von Verweilzeiten berücksichtigt werden.

Auch bleibt es nach wie vor wichtig, konventionelle hydrologische Methoden in die Interpretation von Industriegasen einzubeziehen. Diese Arbeit zeigt, dass gewonnene Erkenntnisse aus chemischen und isotopenhydrologischen Analysen, Feldbegehungen sowie Informationen über die beprobten Brunnen unerlässlich sind, um zuverlässige Aussagen über das Verhalten von Gasen im Grundwasser treffen zu können.

Die Auswirkung von Neubildungsmechanismen auf Excess air und Edelgaszusammensetzungen wird in drei Laborversuchen nachgestellt. In einem ersten Versuch wird die direkte Grundwasserneubildung durch Beregnung mit Intensitäten kleiner oder gleich der Infiltrationskapazität des verwendeten Sandes simuliert. In zwei weiteren Versuchen werden durch einen definierten Überstau indirekte Neubildungsprozesse nachgestellt, wie sie in ephemeren Flussbetten während Abflussereignissen vorzufinden sind.

Säulen aus Plexiglas werden bis auf eine Höhe von 100 cm mit feinem Quarzsand befüllt. Wasserproben werden am unteren Auslass der Säulen in Kupferrohren abgeklemmt und im Institut für Umweltphysik der Universität Heidelberg auf Edelgase analysiert. Einflussgrössen wie Raumtemperatur, Wassertemperatur und Druck wurden ständig überwacht und aufgezeichnet. Zusätzlich wird das für die Versuche verwendete Wasser mit Fluoreszenzstoffen markiert und mit einem Fluorimeter online gemessen, um den geeigneten Zeitpunkt für Probeentnahmen abzugreifen.

Mit den Laborversuchen kann der Gasüberschuss in Wasser erfolgreich erzeugt werden. Fast alle Proben, die bis zum Zeitpunkt der Bearbeitung dieser Arbeit ausgewertet wurden, weisen Edelgaskonzentrationen auf, die über der Gleichgewichtskonzentration von Wasser im Austausch mit der Atmosphäre liegen. Die Gasübersättigung der Wasserproben reicht für Neon von 4.8% bis 14.6%. Hohe Gasübersättigungen stammen aus Proben, die zu Anfang des Säulenversuchs entnommen wurden. Das Wasser aus der letzten Probe weist deutlich kleinere Gasübersättigungen auf, Helium zeigt sogar seine Gleichgewichtskonzentration mit der Atmosphäre auf. Beobachtungen während der Versuche haben jedoch gezeigt, dass der tatsächlich gemessene Druck am Boden der Säule nicht unter allen

Bedingungen mit dem eingestellten wasserstand übereinstimmt. Diese Tatsache zeigt die Grenzen einer möglichst naturnahen Nachbildung des Laborversuchs auf.

# 1 Introduction

## 1.1 Motivation

Groundwater is a vital resource, in steadily increasing demand by man. An increasing conversion of substances and energy within the anthroposphere, and its spacial closeness to groundwater sytems makes potable water become a more and more vulnerable resource. Enormous infrastructural projects in the water sector of countries suffering from water scarcity, including constructions of dams and pipelines, cannot deny the fact that the resource water has to be treated sustainable, in order to prevent a serious impact on its quality and quantity. Because of the inaccessibility of groundwater systems, the degree of interference caused by pollution is difficult to be estimated. For the evaluation of disturbances, dynamics and geochemical processes within the aquifer have to be understood. In order to protect the groundwater resource, reliable informations on relevant hydrological processes, such as groundwater recharge, groundwater flow rate and direction, as well as mean residence times in the groundwater body, have to be acuired. The knowledge of hydrological and hydrochemical conditions affecting subsurface water is crucial for a sustainable development within the water sector.

Alongside conventional hydrogeological methods, chemical and isotopic hydrology is often applied in order to understand aquifer properties and processes relevant for groundwater. New methods are constantly being studied to improve determination techniques. Dissolved gases have been used as tracers for the determination of residence times, recharge temperatures and elevations, or to study interactions of groundwater with surface water. The chemically inert noble gases, as well as some anthropogenic produced gases, seem to be ideal tracers of physical transport in the subsurface. Their behavior is essentially geochemically conservative, and modern analytical methods are capable of detecting small quantities. Nevertheless, a well observed phenomenon going by the name of „excess air“ does have an influence on the comportment of gases in water, and therefore might falsify results of investigations. However, the excess air component itself probably conveys informations about aquifer characteristics.

The study site chosen for this work is one among four catchments being investigated within the project WADE (Floodwater Recharge of Alluvial Aquifers in Dryland Enviroments). WADE aims at estimating groundwater recharge in semi-arid and arid catchments to provide scientific information on water resource availability in dryland areas. Situated within the Province of Almeria, which is widely regarded as one of Europe’s most arid regions, the Rio Andarax basin suits the problems mentioned above. Along the coast, the region suffers from seawater intrusion into the aquifers as a result of an over-use of water resources with a high number of private wells and boreholes. The risk of a potential contamination grows, regarding the fact that hydraulic gradients between the water table of aquifers and the sea level decrease.

To draw a conclusion, the motivation of this work is to develope practical solutions for improved integrated water resource managment. The challenge is to detect processes relevant for groundwater by applying and improving hydrological techniques of determination.

## 1.2 Objectives

The objective target of this study is to investigate the impact of hydrological processes on the comportment of gaseous components in groundwater. Distinguishable processes of groundwater recharge in semi-arid and arid regions, such as direct and indirect recharge shall be detected by evaluating patterns of gaseous compositions, more precisely CFCs, SF6 and the noble gases He, Ne, Ar, Kr and Xe.

The application of these gases as hydrological tracers shall be verified, their potentials and boundaries shall be revealed. In addition, conventional hydrological methods of determination are consulted in order to validate gas patterns. In detail, questions that follow the objective target are:

- The process-oriented approach to determination techniques with noble gases, CFCs and SF6.
- The characterization of groundwater in the alluvial aquifer of an ephemeral stream, in terms of origin, recharge altitude, residence times and dominant processes.
- The identification of excess air and noble gas patterns, subject to relevant groundwater recharge processes, more precicely direct and indirect recharge.

Therewith, the statement shall be done, whether or not gained cognitions helped to improve analysis and interpretation of gaseous components in groundwater.

Implementing objective targets is done deductively by catchment-hydrological investigations, as well as inductively by experimental laboratory investigations. In the semi-arid basin of Rio Andarax, southeast Spain, groundwater samples are taken directly from below the river bed of an ephemeral stream, as well as beside the river bed, in order to cover the two relevant recharge processes. In an experimental setup, direct and indirect recharge processes to groundwater are simulated, as nature-oriented as possible.

## 1.3 State of the Art

Groundwater recharge is well defined by the German Institute for Standardization (DIN). DIN 4049 (1993) gives two different definitions for the term groundwater recharge (GWR), depending on the approach. GWR can be defined as inward flow of infiltrating water into the saturated zone of an aquifer, if regarded as component of runoff formation. GWR can also be defined as precipitation over area minus evaporation over area minus direct runoff, if regarded as water balance component. According to Leibundgut et al. (1997), direct GWR is understood as areal infiltration of precipitation, whereas indirect GWR occurs linearly along streams and focused in sinks. Being a component of the waterbalance, GWR differs depending on the clime. In arid and semi-arid regions, where rainfall is likely to be short and intense, and evaporation rates are high, indirect GWR is assumed to play an important role.

Several books have discussed the use of dissolved gases as environmental tracers in subsurface hydrology: Noble Gas Geochemistry (Ozima and Podozek, 1983), Dissolved Gases in Subsurface Hydrology (Solomon et al., 1998), Chemical and Isotopic Groundwater Hydrology (Mazor, 2004). All the studies focus mainly on dissolution of noble gases under fully saturated conditions. The occurance of excess air is discussed on the basis of works of Heaton and Vogel (1981), and rely on the belief that the formation of excess air results from complete dissolution of entrapped air in soil during water saturation under hydrostatic pressure. Soil properties as well as rainfall properties are assumed to have an influence on the formation of excess air.

Regarding the fact that water sometimes shows a type of excess air composition not coinciding with the model belief of complete dissolution, new models have been developed. Stute et al. (1995) suggested a partial re-equilibration model, which assumes that an initially dissolved gas excess is partially lost, either to the gase phase of the soil or during flow processes within the aquifer. Aeschbach-Hertig et al. (2000) introduced the model belief of closed-system equilibration, in which a finite volume of water equilibrates with a finite air volume under increasing pressure, resulting in either partial dissolution or complete dissolution.

Further approaches towards a better understanding of excess air and the improvement of noble gas based investigations, were done by Peeters et al., (2002). They suggested to include $^{20}Ne/^{22}Ne$ ratios in nobel gas measurements in order to obtain distinct results between the three model beliefs mentioned above.

Experimental investigations on the formation of excess air were performed by Holocher et al. (2002), in order to reproducibly generate excess air as well as to identify the relevant mechanisms and the underlying physical parameters controlling the excess air formation. Two experimental setups were conducted, a first with unidirectional vertical water flow through the colums, and a second simulating groundwater level fluctuations without active infiltration. The total hydrostatic pressure exerted on the entrapped air was determined to be the dominating parameter for the amount of dissolved air. Secondary parameters having an influence on excess air were determined to be the flow regime, the total amount of entrapped air, entrapped air bubble size, and initial composition of the dissolved gases.

The possibility that excess air itself conveys information about recharge conditions as well as aquifer characteristics is suggested by e.g. Aeschbach-Hertig (2004). If excess air mainly depends on hydrostatic pressure, informations on amplitude of water table fluctuations could be gained, and as a result, help to estimate amounts of recharge and precipitaion.

The Reston Chlorofluorocarbon Laboratory of USGS (URL 1-3) provides detailed information on estimation of residence times in groundwater with CFCs and $SF_6$. The current state of research is mainly based on the work of Plummer and Busenberg (2000). Oster (1994) has studied the comportment of CFCs in groundwater and contributed to the knowledge of microbial degradation of CFCs as well as transport of CFCs in the unsaturated zone. Successful applications of CFCs in hydrological investigations were done by Katz et al. (1995), who used CFCs to study leakage from a sinkhole lake in nothern Florida. Plummer et al. (1998) used CFCs to trace recharge of river water to the aquifer derived from seepage through sinkholes in a river bed.

# 2 Methodology

## 2.1 Gaseous Components in Groundwater

Recently, an increasing number of publications can be found, where measurements of dissolved gases in water are included in hydrological investigations. Dissolved gases in water, useful to study hydrological processes comprise the noble gases He, Ne, Ar, Kr, Xe, their isotopes $^{4}He$, $^{39}Ar$, $^{85}Kr$, $^{81}Kr$, for instance, as well as industrial gases such as CFCs and $SF_6$. Due to the management of simple physical processes, the behavior of this gases display a reliable instrument for hydrological investigations, and can be devided into two major groups: gases that are used to study recharge conditions, and gases that can be used to interpret groundwater age.

In addition, gases that are used as indicators of microbial processes (for instance $O_2$, $CH_4$, $CO_2$, $H_2S$, $N_2O$, $N_2$) are mentioned for the sake of completeness, but will not be dealed within this work.

The main source for the presence of gases in water, is the solution of atmospheric gases. The atmospheric equilibrium concentrations are the result of a gas exchange between air and water. This soultion is well described by Henry‘s law:

$$n_i = \frac{p_i}{k_i} \qquad \text{equation 2.1}$$

where *ni* is the mole fraction of the gas *i* in the liquid phase, *pi* is its partial pressure in gas phase, and *ki* is the Henry law constant, which depends on temperature and salinity. Cosequently a concentration proportionality between the gas phase and air equilibrated water is given by the dimensionless Henry law constant. The equilibrium concentration $C_i$* of the dissolved gas *i* in solution results from

$$C_i^* = p_i \cdot \frac{V_i \cdot \rho_{H2O}(T)}{M_{H2O}} \cdot \frac{1}{k_i} = p_i \beta \qquad \text{equation 2.2}$$

where $V_i$ is the molar volume of the gas *i*, $M_{H2O}$ is the molar mass of water, $\rho_{H2O}(T)$ is its density, and $\beta$ is the Bunsen coefficient.

The Bunsen coefficient $\beta$ is defined as the volume of gas at STP dissolved in unit volume of solution, when partial pressure of the gas is 1 atm. The Henry law constant and the Bunsen coefficient are both functions of temperature and salinity. Literature values of *ki* and $\beta$ for different temperatures and salinities are calculated by empirical formulas, determined by Benson and Krause, (1976) and Weiss, (1971), and several other authors.

The atomic mass of gases has an influence on the solubility. The solubility increases with increasing atomic mass. As a result, in solubility equilibrium with the atmosphere the dissolved gas composition is enriched in the heavy gases relative to atmospheric air (Holocher et al., 2002). The molecular diffusivity of gases, however, decreases with increasing atomic mass.

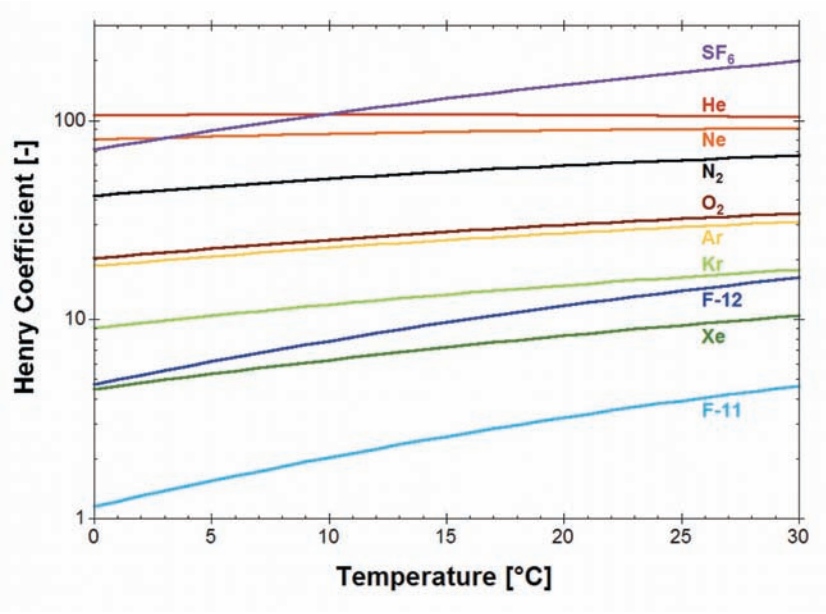


Figure 2.1: Comparison of solubilities for different gases in water (Aeschbach-Hertig, W. 2004). The atomic mass as well as the solubilty decrease with increasing Henry coefficients.

Figure 2.1 compares the solubility of different gases by means of their Henry law constant for different temperatures. Gases with small Henry coefficients have a heavy atomic mass and therefore are high soluble (CFC-11, CFC-12, Kr, Xe). Gases with big Henry coefficients are the least soluble gases with light atomic mass (SF6, He, Ne, N2).

Derived from $\beta$ and *ki,* solubilities of gases decrease with temperature and the sensitivity to temperature increases with the atomic mass (fig 2.1). Hence, the light noble gases He and Ne show only little changes with temperature, the solubility of the heavy noble gases Kr and Xe show a strong temperature dependency.

Thus, the knowlege of salinity, temperature and partial pressure of gas allows to determine its air equilibrium concentration. For the chemically inert noble gases, the equilibrium concentrations give information about the water temperature at the time of infiltration (Stute and Schlosser, 1993).

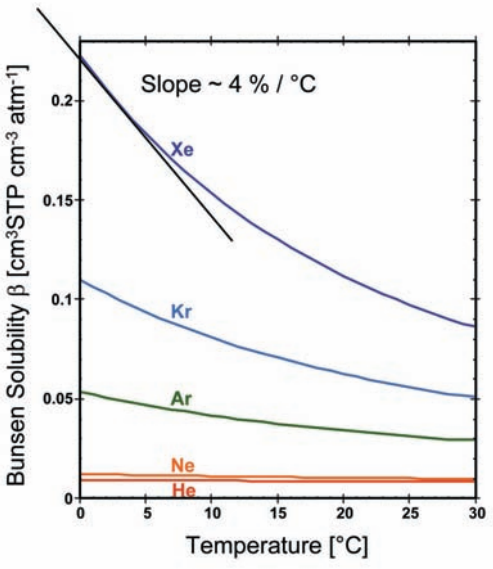


Figure 2.2 Solubility of atmospheric noble gases as a function of temperature (Ozima, M.; Podosek, F. A. 1983)

## 2.2 Estimation of Recharge Temperature with Noble Gases

The noble gases dissolved in groundwater have proved to be useful as environmental tracers. Numerous studies of noble gas concentrations in groundwater were done, to reconstruct past climate conditions (Aeschbach-Hertig, 2000; Heaton and Vogel, 1981; Mazor, 1972; Stute and Schlosser, 1993).

Helium (He), neon (Ne), argon (Ar), krypton (Kr) and xenon (Xe) are elements, which do not interact with other atoms, as their outer shell of electrons is complete. The inert noble gases can be considered to be geochemically concervative tracers, as they are not involved in any chemical or biological activities.

Noble gas concentrations as well as their characteristic isotopic abundances of the well-mixed atmospheric reservoir are known. Thus, the distinct major source of noble gases in groundwater, which is the equilibration with air during infiltration can be determined. Formulas, presented in chapter 2.1 to calculate concentrations of atmospheric noble gases in equilibrated water, can therefore be used as well to estimate recharge tempereratures of groundwater, based on measurements of the dissolved concentrations of atmospheric noble gases. The recharge temperature is the temperature at which groundwater equilibrates with a gas phase. According to Solomon et al. (1998), the final equilibration of infiltrating water with gas, takes place on top of the capillary fringe, above the water table respectively.

The direct proportionality of noble gas solubility in water to the partial pressure in air, gives also information about the recharge altitude. The reason is, that partial pressure of atmospheric gases depend on the barometric pressure, which is linearly correlated to the altitude.

Despite the fact, that the behavior of noble gases is controlled by simple physical processes, additional minor processes responsible for the presence of noble gases in groundwater have to be taken into account, to make estimations of recharge temperature and elevation reliable and accurate. The source of radiogenic gases, steaming from deep-seated origins includes flushing of radiogenic products from aquifer rocks and from mantle-derived gases. It is most pronounced for He, equilibrium concentrations of He in groundwater might be exceeded by several hundred percent (Solomon et al. 1996). In order to include He in temperature estimation, $^{3}He$ must be measured along with $^{4}He$ to identify the source of He by its isotopic composition (Price et al. 2003).

Finally, in addition to the atmospheric and radiogenic sources, a third process affecting concentrations of all noble gases in groundwater goes by the name of „excess air“. Heaton and Vogel (1981) introduced the term „excess air“ in a first methodical study about this ubiquitous process. It manifests in a supersaturation of dissolved atmospheric noble gases in groundwater, with a composition that is often similar to that of atmospheric air.

Both, the additional amount of radiogenic gas as well as the amount of excess air in groundwater have to be determined, and separated from the total measured dissolved gas concentration to estimate recharge temperature with noble gases.

## 2.3 Excess Air

Heaton and Vogel (1981) explained the formation of excess air by dissolution of entrapped air in soil during water saturation. The percolation of water carries along air bubbles to the water table, which finally are dissolved under higher hydrostatic pressure within the aquifer. Soil properties as well as rainfall properties were assumed to have an influence on the formation of excess air.

Numerous field studies (e.g. Stute and Talma, 1998; Aeschbach-Hertig et al., 1999) and conclusive investigations under defined laboratory conditions (Faybishenko, 1995; Holocher et al. 2002) have advanced the knowledge on the formation of excess air to the present state of research.

Excess air, which is reflected in groundwater by concentrations exceeding the atmospheric equilibrium, shows two chracteristical compositions, that essentially differ from each other. A dissolved gas excess of purely atmospheric composition can be found as well as a gas excess, that shows a mass-dependent fractionation relative to atmospheric air.

The gas excess of purely atmospheric composition is described by

$$C_i = C_i^{eq}(T,S,P) + Ax_i \qquad \text{equation 2.3}$$

where $C_i^{eq}$ is the solubility equilibrium concentration of a gas $i$, at a given temperature $T$, salinity $S$, and atmospheric pressure $P$. $A$ is the air/water volume ratio, and $x_i$ the atmospheric mixing ratio of a gas $i$.

The model concept in equation 2.3 assumes, that water percolating into the groundwater is in equilibrium with the atmosphere of the unsaturated zone, and that an additional air volume is completely dissolved (Aeschbach-Hertig et al., 1999). The complete dissolution of an additional amount of air leads to an excess air pattern, as it can be seen in figure 2.3 for unfractionated air. Since the solubilities as well as the temperature dependency of the Henry law constant *ki* of gases increases with increasing molecular weight, the complete dissolution shows a pattern, in which the least soluble light gases show the largest excess.

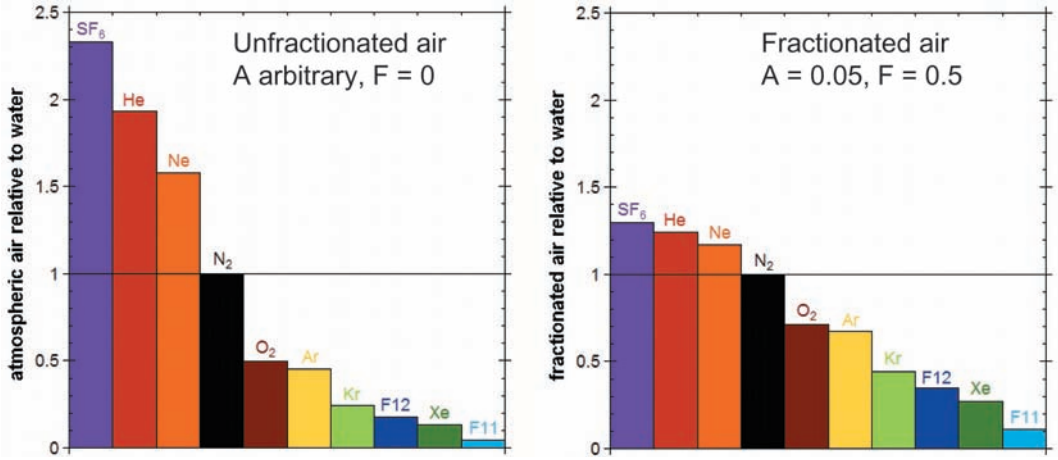


Figure 2.3: Relative composition of excess air, normalized to $N_2$ and relative to air equilibrated water at 15 °C (Aeschbach-Hertig, 2004). Left: unfractionated air for complete dissolution. Right: fractionated air for partial dissolution.

The second characteristical composition of excess air can be found as well in groundwater, and shows a systematic, mass-dependent fractionation relative to atmospheric air. It is described by the equation

$$C_i = C_i^{eq}(T,S,P) + \frac{(1-F)\,Ax_i}{1 + AFx_i / C_i^{eq}} \qquad \text{equation 2.4}$$

where the model parameter F describes the degree of elemental fractionation (Aeschbach-Hertig, 2000).

The model concept in equation 2.4 assumes, that an additional amount of air is partially dissolved. It describes the equilibration of a finite water volume with a finite air volume under increased pressure. Assuming a closed system, air can be completely dissolved, and consequently, for F = 0, equation 2.4 becomes equation 2.3 for pure, unfractionated excess air. If the air volume is not completely dissolved, the excess air composition shows a fractionation pattern (fig. 2.3), depending on the initial air/water volume ratio and the pressure. As a result the difference between gases with high and low solubility is less pronounced compared to unfractionated air, as the heavy noble gases will be enriched in the water phase relative to the light noble gases.

Excess air is often described as the volume of dry air in $cm^3$ STP/kg of water. If not all noble gases are measured, excess air can also be expressed as a relative Ne-excess

$$\Delta Ne\ (\%) = \left[\frac{C_{Ne} - C_{Ne}^{eq}}{C_{Ne}^{eq}}\right] \cdot 100 \qquad \text{equation 2.5}$$

where $C_{Ne}$ is the measured neon concentration in water, and $C_{Ne}^{eq}$ is the neon equilibrium concentration. For the relative expression Ne is used, because of its low solubiltiy and temperature independency.

If measurements of two gases are available, the determination of excess air and recharge temperature can be done using a graphical method. Concentrations of two gases are plotted versus each other, assuming that the excess is not fractionated, the data points are extrapolated towards the equilibrium line. This allows to determine the recharge temperature and the amount of excess air.

An iterative technique for the determination of excess air and recharge temperature is given by the least-square optimization routine NOBLE (Aeschbach-Hertig, et al. 2000). For this technique, several noble gases must be measured. Small amounts of excess air are subtracted from the measured concentrations by fitting the model parameters *A* and *F* (eq. 2.3 and 2.4), and the temperature of recharge is calculated using the solubility data. The procedure is repeated until agreement between all calculated noble gas temperatures is achieved.

Typical amounts of excess air observed in groundwater range from zero to about 30 $cm^3$ STP/kg of water. However such extreme values are only found in palaeogroundwater in semi-arid regions, or in groundwater being artificially recharged (Aeschbach-Hertig, 2004).

## 2.4 Estimation of Residence Times with CFCs and $SF_6$

Chlorofluorocarbons (CFC-11, CFC-12, CFC-113) and sulphur hexafluoride have recently been used for dating of shallow grondwater (Katz et al., 1995; Beyerle et al., 1999; Busenberg and Plummer, 2000). Their properties like stability and non-reactivity make them potentially useful as hydrologic tracers.

Unlike the naturally constant concentrations of noble gases, CFCs and SF6 are anthropogenic released to the troposphere. The results are variable atmospheric input functions, depending on production and release of these industrial gases. Together with the fact, that developing atmospheric concentrations are monitored or reconstructed since the first occurance of CFCs and SF6, the basic requirements, for their use as tracer for mass transport processes in aquifers, are provided.

Air mixing ratios of CFCs in figure 2.4, show a monotone increasing of concentrations through the 1970s and 1980s due to the comparatively high atmospheric lifetimes (approx. 45 years for CFC-11; 87 years for CFC-12; 100 years for CFC-113; (Volk et al., 1997)). CFC-11 and CFC-113 peaked in 1993 and 1994, CFC-12 peaked in 1999, as a result of the agreement of 37 nations to limit CFC release in 1987 (UNEP, 1987). SF6 increases constantly since its began of production in the 1960s. Its estimated atmospheric lifetime varies significantly, depending on the authors, between 800 and 3200 years.

CFCs and SF6 enter the groundwater through precipitation in equilibrium with atmospheric mixing ratios, managed by the same physical processes mentioned above. Recharging water, percolating through the soil to the water table suppresses groundwater within the aquifer, and as a consequence isolates it from the atmosphere. Thus, water will be marked with a distinct CFC, SF6 equilibrium concentration, depending on the year of recharge.

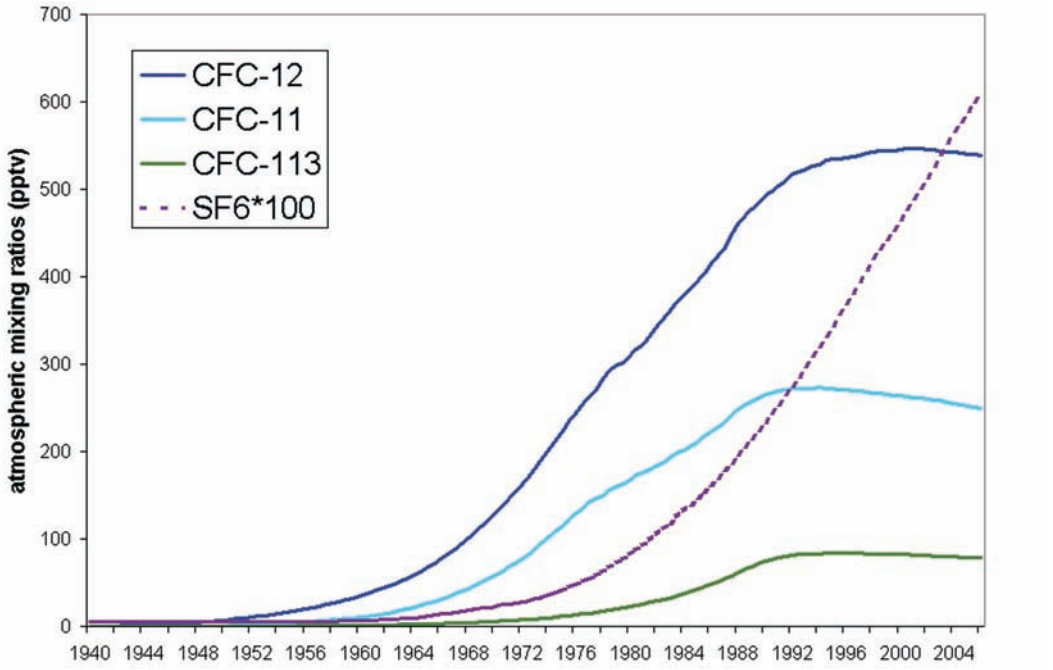


Figure 2.4: Atmospheric mixing ratios of CFC-11, CFC-12, CFC-113, and $SF_6$ for the nothern hemisphere (North America). Mixing ratios are in parts per trillion volume (pptv). Data compiled by the U.S. Geological Survey Chlorofluorocarbon Laboratory (URL 3).

The varying atmospheric mixing ratios of CFCs and $SF_6$, disable an estimation of recharge temperature and the amount of excess air with these industrial gases. Nevertheless, both parameters, temperature at the time of recharge and excess air mask the equilibrium concentration of CFCs and $SF_6$ in groundwater. They therefore have to be determined by measuring the dissoved concentrations of noble gases.

Aeschbach-Hertig (2004) gives a solution to calculate the relative excess $\Delta_i$ of industrial gases from $\Delta_{Ne}$. Assuming complete dissolution for simplicity the excess of a gas *i* can be described as

$$\Delta_i \equiv \frac{C_i^{ex}}{C_i^{eq}} = \frac{H_i \cdot A \cdot x_i}{(P - e) \cdot x_i} = \frac{A}{(P - e)} \cdot H_i \qquad \text{equation 2.6}$$

where $C_i^{ex}$ is the excess concentration of a gas *i*, $C_i^{eq}$ its solubility equilibrium concentration, $H_i$ is the Henry law constant of the gas *i*, *A* is the air/water volume ratio, *(P - e)* is the partial atmospheric pressure for dry air, and $x_i$ is the atmospheric mixing ratio for the gas *i*. Equation 2.6 shows, that the relative excess of a gas in solution is independent of its atmospheric mixing ratio, and proportional to its Henry law constant. Consequently, the relative $SF_6$ excess can be calculated as follows:

$$\Delta_{SF6}\,(\%) = \Delta_{Ne} \cdot \frac{H_{SF6}}{H_{Ne}} \qquad \text{equation 2.7}$$

where $\Delta_{Ne}$ is the relative excess of the measured noble gas Ne, $H_{SF6}$ and $H_{Ne}$ are the Henry law constants for $SF_6$ and Ne, respectively.

Other processes, that might falsify the estimation of mean residence times in groundwater with CFCs and $SF_6$, have been studied by Oster (1994). Atmospheric mixing ratios of industrial gases might be enriched around urban areas, dissolved concentrations of CFCs and $SF_6$ in water might therefore exceed the applied atmospheric mixing ratios. As a consequence investigated groundwater would be dated too young. Microbial degradation is little, however most pronounced for CFC-11, and takes place in anaerobic enviroments. As a consequence, apparent groundwater age might be estimated too old. However this disadvantage can be used as well to detect anaerobic conditions in aquifers, if CFC-11 values are compared to CFC-12 values. With increasing thickness of the unsaturated zone, apparent groundwater ages are estimated too old. The reason is, that air in a deep unsaturated zone is most likely older than air of the modern troposphere. As the gas-water equilibration is assumed to occur above the capillary fringe, a lag time might occur. In case of contamination, water will have concentrations that are greater than that possible for equilibrium. Contamination of groundwater with CFCs is often caused by local point sources, such as leaking sewer lines or septic tanks. In that case, estimation of residence times will not be possible. However, contamination of groundwater from local point sources shows pontential for large scale tracing.

Finally, sorption and hydrodynamic dispersion do have an impact on the age dating technique with CFCs and $SF_6$, however these processes are to the present state considered to have a small effect for CFCs.

If the temperature at the time of recharge, the recharge elevation, and the amount of excess air can be determined, the age dating technique with CFCs and $SF_6$ is considered to be reliable for the estimation of mean residence times of groundwater on a 50 year time scale. Although, atmospheric mixing ratios of CFCs are decreasing, concentrations in water and air are still relatively high compared to a detection limit of 0.3 picograms per kg of water.

Reliable results are obtained, if at least two industrial gases are measured and compared to each other. In addition, the choice of an appropriate model believe of mass transport in aquifers must be applied, to derive an apparent groundwater age from mean residence times. If models, such as the piston flow model, the exponential model or binal mixing models are compared to each other, conclusions about dominant processes in the groundwater can be done, in addition to the estimatation of apparent groundwater age.

# 3 The study site of Almeria

## 3.1 Introduction

The Rio Andarax Basin is one of the four study areas being investigated within the project WADE. During a field trip in September 2005, a delineation of the basin boundaries as well as an investigation of the possibility of different basin boundaries for the groundwater system were carried out. In addition, an identification of different geological units in the study area, characteristics and related soil properties, and an identification of different aquifer units were undertaken. Analyses of the hydrological system and a study of the landuse and anthropogenic factors affecting the hydrological system will also be presented in this chapter, and be brought together with already known facts.

## 3.2 Description of the study site

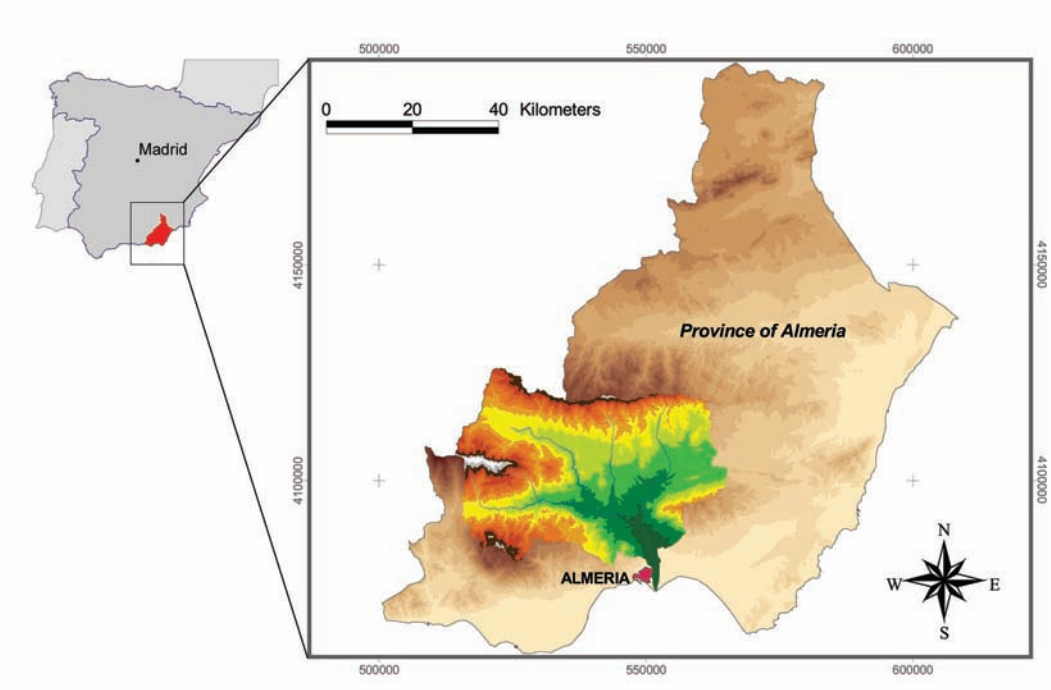


Figure 3.1: Location of the Rio Andarax Basin

The Rio Andarax Basin is located in the southeast of Spain, more precisely in the province of Almeria (fig. 3.1). It extends from W 2°10‘ to 3°00‘ latitude and N 36°50‘ to 37°10‘ longitude. The catchment area size is approximately 2200 km², the catchment length approximately 64 km, resulting in a Horton’s form ratio of $R_f = 0{,}54$.

Rio Andarax Basin is surrounded by four major mountain ranges, all running from east to west. The Sierra de los Filabres delimits the catchment to the north with altitudes up to 2168 m above sea level (Calar Alto). In the western part of the catchment the foothills of Sierra Nevada are located with altitudes up to 2465 m above sea level (Buitre) and in the south of it the Sierra de Gador with altitudes up to 2236 m above sea level (Moron). In the west of Rio Andarax Basin the Sierra Alhamilla is found with altitudes up to 1387 m above sea level (Colativi).

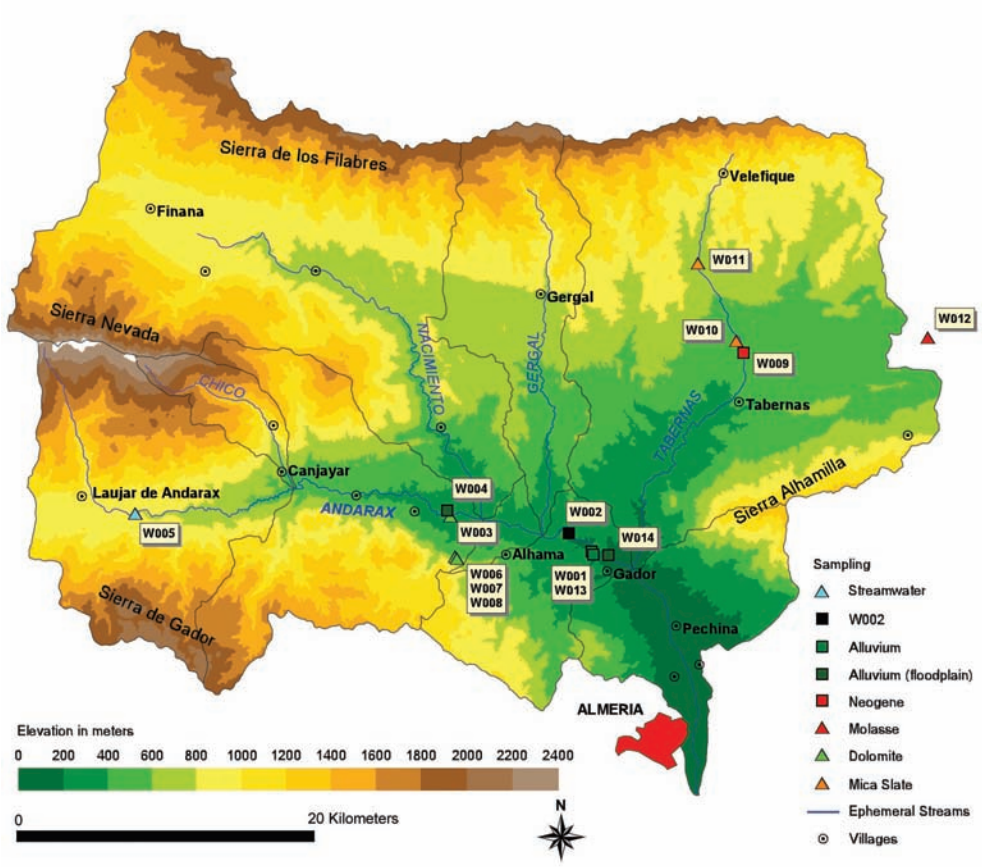


Figure 3.2 The Rio Andarax Basin, its mountain ranges, ephemeral streams and sampling sites.

The basin delineation in figure 3.2 was done based on an existing digital elevation model, provided by CSIC (group Gerardo Benito).

### 3.2.1 Climate

The climate type of Rio Andarax Basin is semi-arid / Mediterranean with annual temperature average of 18°C and about 160 mm/year annual rainfall. It has two raining seasons, a fall rainy season from October to December and a spring rainy season from March to May. Three climate stations in the area are known to measure long term monthly precipitation and temperature, two in Almeria and one in Tabernas. Precipitation data could however, could not be obtained for this work.

### 3.2.2 Geology

The Rio Andarax Basin is situated in the Betic Cordillera, a system which is made up of multiple mountain ranges that generally trend southwest–northeast and represents an uplifted fold-thrust belt. The Basin consists of three major units. The Nevado-Filabride unit, the Alpujarride unit and a Neogene basin.

The Nevado-Filabride unit can be found along the elevations in the northern part, including Sierra Nevada and Sierra de los Filabres. It mostly consists of metamorphic rocks, mainly phyllite, schist, quartzite and gneiss and is chronologically assigned to the Pre-Devonian Period of the Palaeozoic. The Sierra de Gador and the southern margin of Sier-

ra Nevada represent the Alpujarride unit, mainly consisting of siliciclastic and carbonate sediments from the Upper Triassic Period of the Mesozoic. A Neogene Basin extends among the major elevations with an average thickness of 500 meters. The stratigraphy is represented by conglomerates, overlain by marly series from the upper Miocene which locally contain microcrystalline gypsum. In the eastern part of the Basin Molasse partially occurs on surface but is generally overlain by Pliocene stratum consisting of limestone and gravel. In the centre of the basin, the Pliocene strata consist of continental conglomerates or calcareous sinter at the surroundings of Alhama. Quaternary accumulations can be found along the riverbeds and in the alluvial fans, mainly in Sierra de los Filabres.

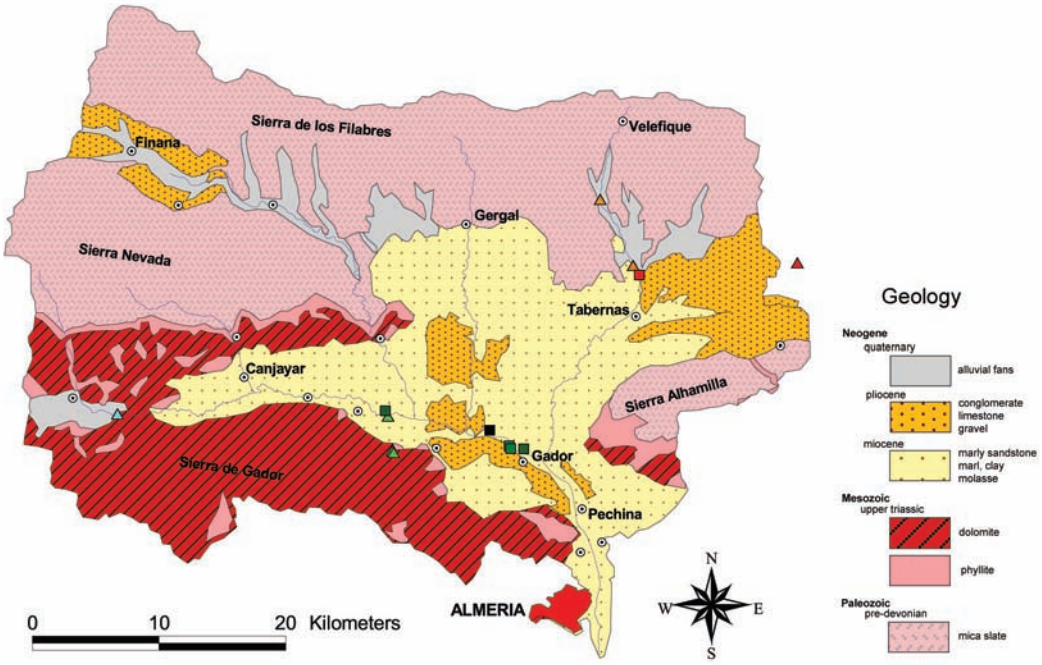


Figure 3.3: Schematized geological map of Rio Andarax Basin prepared from a geological map of Almeria Province (Sacle 1: 200 000), Alvargonzalez, 1967.

### 3.2.3 Hydrogeology

The hydrogeological complexity of the zone is caused by the existence and interaction of different aquifers. Generally, three main hydro-geological units can be differentiated as aquifers.

1) The Pre-Cenozoic Basement on the sides of the valley, consisting of Nevado-Filabrides and Alpujarran units. The Nevado-Filabrides unit generally behaves as an aquiclude being composed of micaschists and quartzites. The Alpujarran unit however contains carbonated formations, in which fissuring and karst formation occurs. This Aquifer usually behaves phreatically, but it is locally confined because of overlaying impermeable strata such as shale.

2) The Pre-Cenozoic Basement at the bottom of the valley, consisting of Alpujarran units, represented by limestone, dolomite and quartzite intercalations. The aquifer is mostly of confined character.

3) A sequence of detritic strata, consisting of several layers of conglomerates partially superposed by quaternary continental deposits. This detritic aquifer is exposed throughout the whole valley and functions as a porous aquifer.

The tectonic activity of the area has an influence on the interaction of the different aquifers. Several overthrusts and folds cause a bigger contact surface between the hydroge-

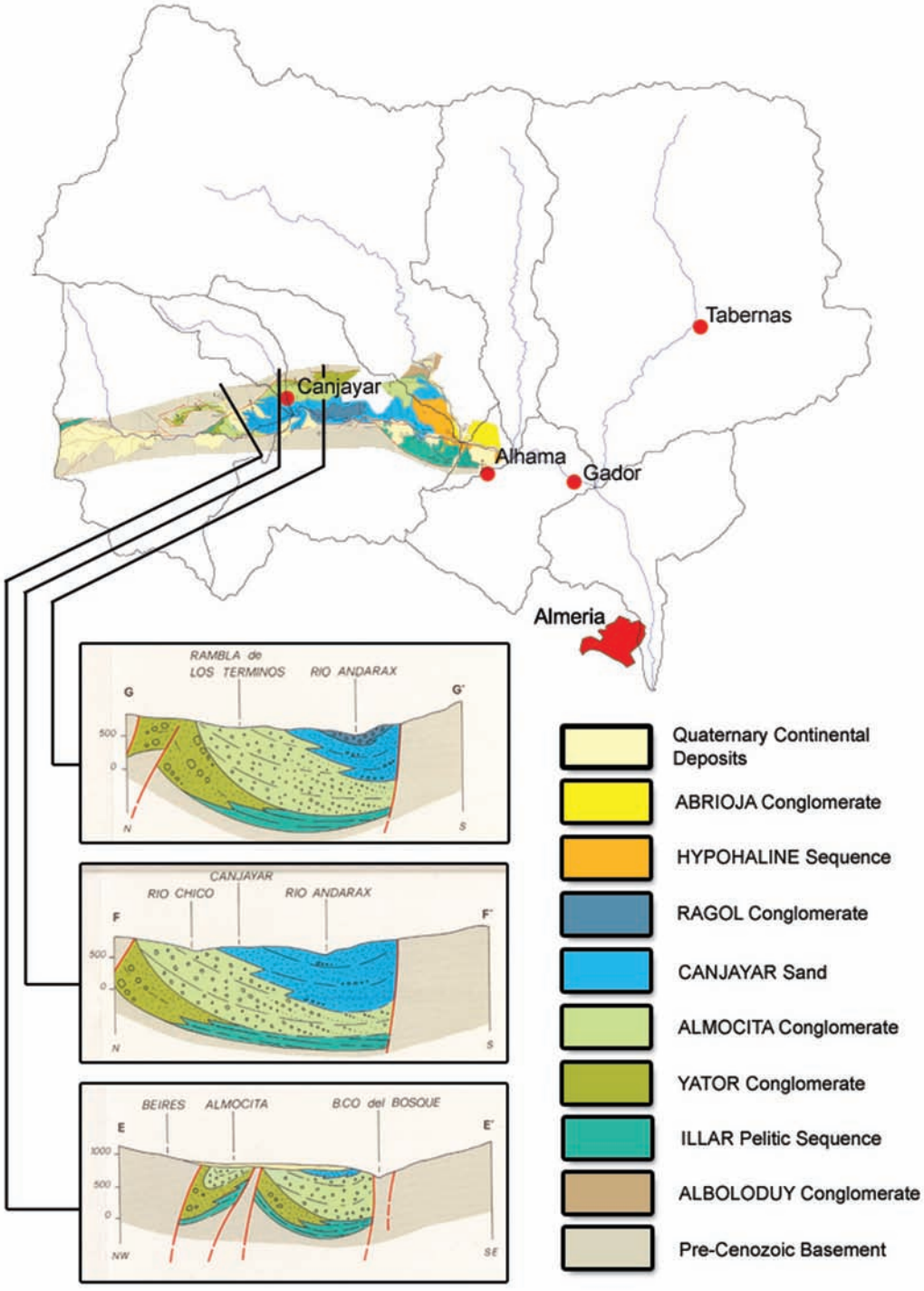


Figure 3.4 Three geological cross sections of the Neogene sequence, Upper Rio Andarax Basin (taken from Bernini M. et al., Geological-Structural Map of Ugijar and Canjayar Basins (Betic Cordillera)).

ological units. A hydraulic interconnection between the detritic aquifer and the fissure aquifer of the Pre-Cenozoic Basement is possible at some points, where the superposed impermeable layer is missing.

Three geological cross sections shown in figure 3.4 provide information about thickness and succession of the Neogene sequence in the upper part of Rio Andarax Basin.

A massive marine pelitic sequence (Illar) composed of light grey marl, locally with thin-bedded turbiditic sandstone in its lower part, lies at the bottom of the valley. Thereupon generally follows a stratum of massive, matrix-supported conglomerates (Yator) showing extensive resedimentation features (debris flow and sliding). Finally, shallow marine homogeneous sand (Canjayar) and alluvial deposit consisting of conglomerate and sandstone with festoons (Ragol) lie on top exposed. They will be partially replaced or overlain further downstream by the Hypohaline sequence, consisting of alluvial conglomerate and sand in its lower part, grading to rhythmic pelites and siltites with fresh water ostracodes and resedimented blocks of gypsum in its uppermost part.

Figure 3.4 shows impressively that the Rio Andarax valley is filled with a major sequence of transmissive to highly transmissive porous material up to 800 m thick. This Negene sediment sequence is complex and heterogeneous. Due to the uplift of single blocks of the Alpujarran unit, contact areas between the Neogene sequence and the Pre-Cenozoic sequence exist.

Therefore, a hydraulic contact is possible that – as mentioned above – has a major impact on the recharge of the whole aquifer system of Rio Andarax. In cross section E-E' the complex folding and fault reveals a possible hydraulic interconnection between the dolomite aquifer of the Pre-Cenozoic Basement and the detritic aquifer of the Neogene sequence.

In the lower part of Rio Andarax Basin, deltaic thick bedded and coarse conglomerate from the Lower Pliocene (Abrioja) and quaternary continental deposits lay on top. Transmissivities were assumed to vary between 150 m²/day for the Pliocene units and 350 – 750 m²/day for the quaternary deposits (IGME-IRYDA, 1977).

### 3.2.4 Geomorphology

The alluvial system of Rio Andarax Basin can be classified as meandering for the better part. The last 20 kilometres however are channeled and can no longer be considered as a natural system. All the river valleys are filled with alluvial material, whereas the gullies surrounding are filled with slope deposits. Alluvial fans at the mouth of small tributaries can rarely be found, as this material has often been removed.

In the Holocene, two developed terrace levels can be found. The upper level is about 3 meters high and has been completely transformed into crops. The lower level is about 1 meter high and can seldom be identified.

The main river bed is covered with sand bars. They are constantly being modified to build non-permanent diversion channels (sand docks) for irrigation purposes.

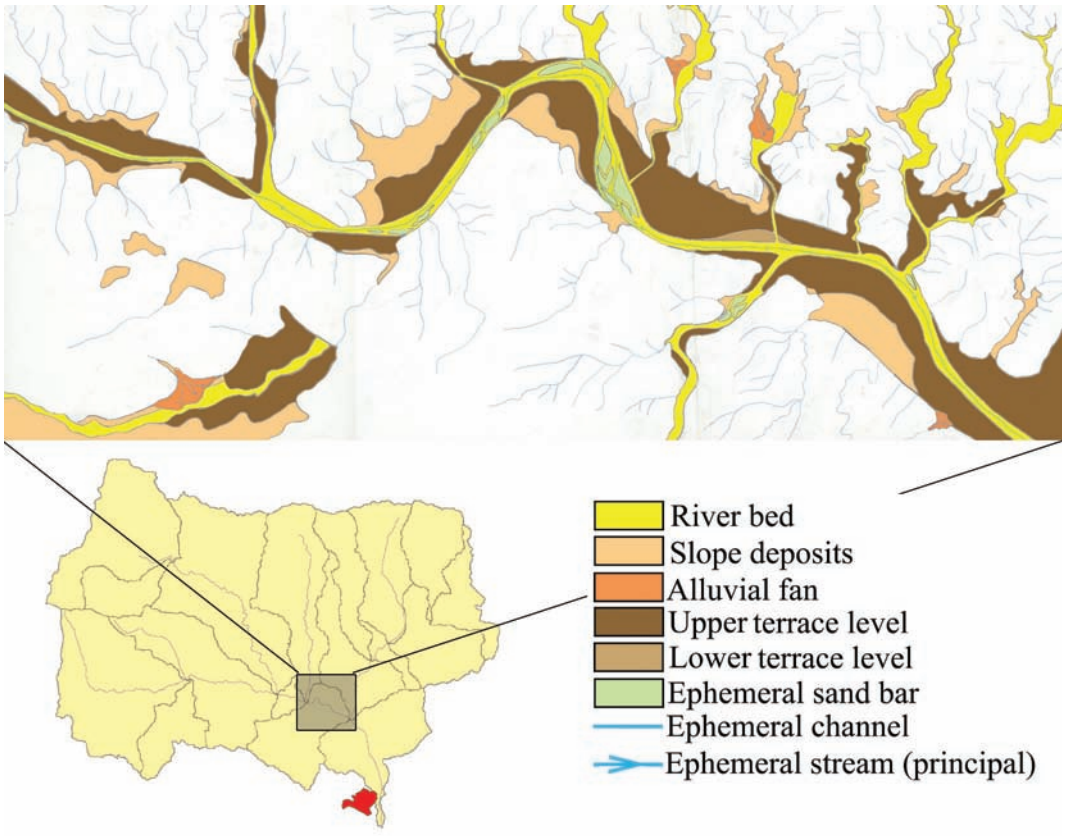


Figure 3.5 Geomorphology of the area being investigated within the project WADE, showing meanders of Rio Andarax and the dominant upper terrace level used for cultivation purposes.

### 3.2.5 Soils

In the Andarax basin two main types of soil can be found. A calcic regosol covering all the Miocene and Pliocene units and a calcic fluvisols covering all the surroundings of the channel, more precisely the terrace system.

In addition the Rambla-type soil, mostly composed by sand with some clay layers, develops in the ephemeral streams which are not run by a flood regulary. This soil is poorly selected, constituted by coarse grains and has no internal structure. Sometimes it can develop a small vegetation cover, and if the flood frequency is low enough, it will be enough to fix the soil.

The Rambla-type soil cannot be found in the river bed of Rio Andarax itself, as the system works regulary to destroy the soil formation by floods.

### 3.2.6 Vegetation and Landuse

The Province of Almeria is widely regarded as one of Europe's most arid regions (Lazaro et al., 2001). In the eastern part of Rio Andarax Basin, the Tabernas desert clearly shows the process of natural desertification and erosion. Although the area may look like it has scarce vegetation, it in fact harbors a fair variety of xerophyte flora accustomed to surviving in semi-arid areas.

This native, semi-natural vegetation is dominated by low scrubland, with pink rock roses (cistus albidus), marjoram (thymus mastichina) and thyme (thymus gracilis).

In the generally parched and treeless landscape of the Neogene Basin, only the numerous dry river beds (ramblas) provide a unique microclimate that is more humid than its surrounding. Here reeds, oleanders, and tamarisks can be seen.

In the mountain ranges however, well preserved holm oaks and some reforested areas of Aleppo and maritime pines can be found.

Figure 3.6 and 3.7: The dry river bed of Rio Andarax with reed and parched srubland on the elevations (left picture). On the right side, an Orthophoto of the study site beeing investigated within the Rio Andarax Basin shows that cultivation is limited to the upper terrace level of Rio Andarax.

Implementation of the Common Agricultural Policy (CAP) in Andalucia has led to a rapid expansion of extensive olive and almond plantations in the eastern, most arid areas of the Rio Andarax Basin, through subsidies provided to encourage agricultural production and aid development of the rural economy (Zukowskyj et al., 2004).

Surrounding the channel of Rio Andarax itself, agriculture focuses on orchards (most of them citrics). Further downstream some greenhouses grow high value products.

Cultivation however is limited to the upper terrace level as can be seen in figure 3.7. Farmers use the drip irrigation system, supplied by local groundwater resources.

Figure 3.8 and 3.9: Greenhouse and orchards beside the ephemeral stream Rio Andarax around the village Gador. The right pictutre vividly shows, that flood water of Rio Andarx is beeing channeled for irrigation purposes.

### 3.2.7 Hydrology

The main stream in the catchment is Rio Andarax, which has its source in the Sierra Nevada and its mouth in the Mediterranean Sea, within the City of Almeria. Its flow direction is west to east. Important tributaries to Rio Andarax are Rio Nacimiento, which has its source in the Sierra de los Filabres, and Rambla de Tabernas, which drains the western part of the catchment.

The rivers in Rio Andarax Basin are ephemeral streams, most of the year they remain dry. But they do transport significant volumes of water after strong rain events or snow melt, normally once a year. However, near to the source of Rio Andarax, permanent runoff can be observed and a gauging station is installed in El Chono, close to Canjayar measuring monthly discharge of the subcatchment with an area of 616 km².

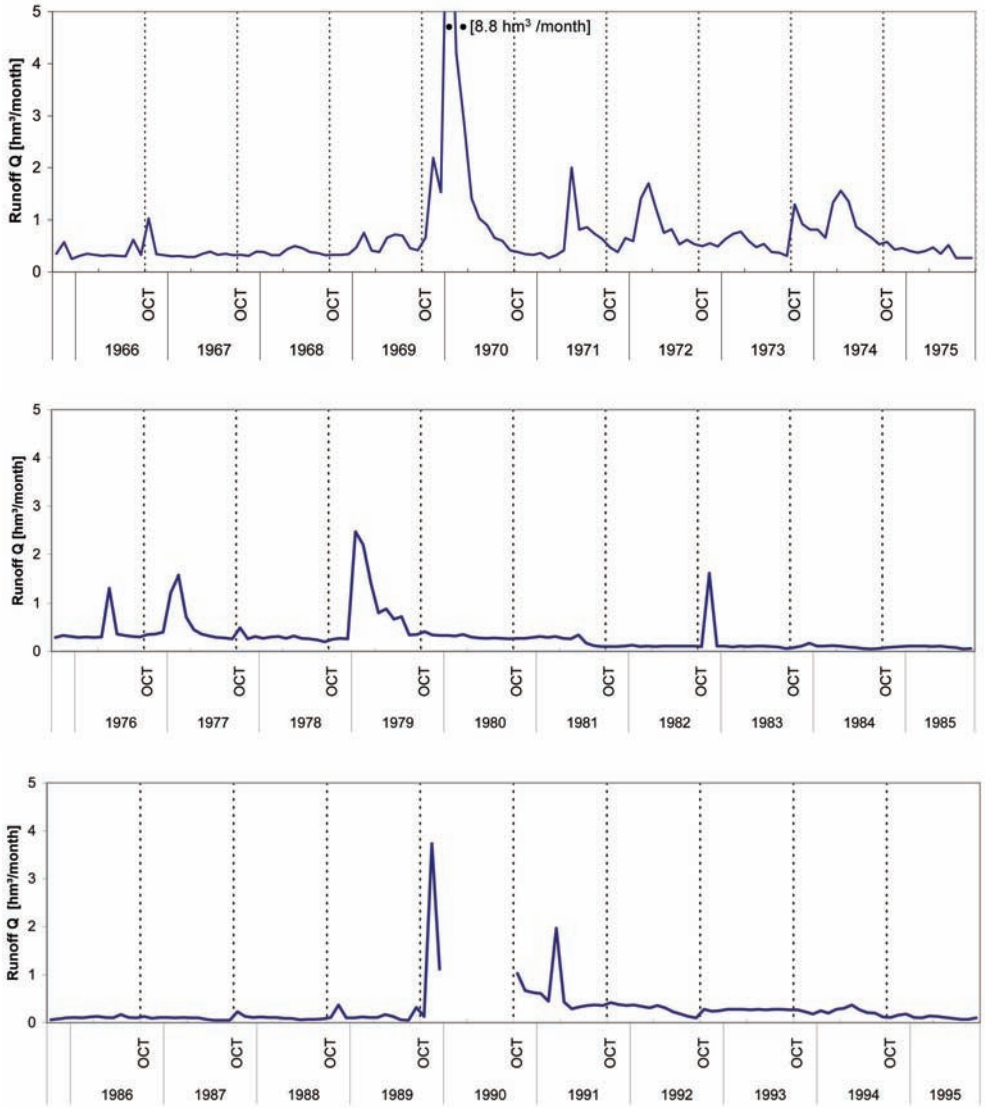


Figure 3.10: Monthly runoff data from the gauging station El Chono. Floods do run every year, the intensity however varies from year to year.

Monthly runoff data records at the gauging station of El Chono provide useful information for the years 1939 – 1996.

The mean annual discharge (MQ) at El Chono gauging station is 0,21 m³/sec which corresponds to 11 mm/year. Discharge varies from 0,03 m³/sec or 2 mm/year (NQ) to 1,59 m³/sec equal to 81 mm/year (HQ). The outcome of this is an area discharge of 0,34 l/sec km².

As shown in figure 3.4, the runoff regime of Rio Andarax is nival with a maximum in March. An increase of runoff from October on identifies the beginning of the rainy season from October to December.

Nevertheless it is worth mentioning that runoff does not decrease to zero during the summertime.

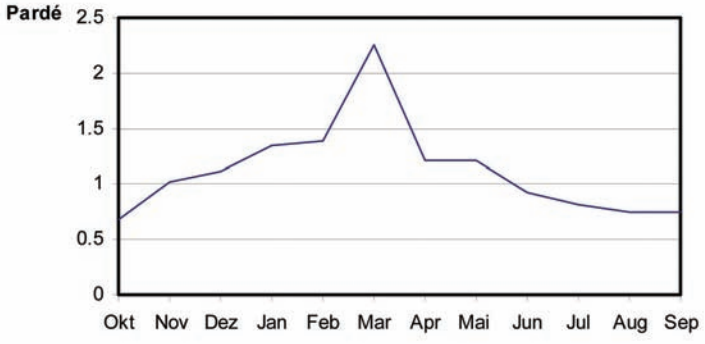


Figure 3.11: Runoff regime of Rio Andarax (Upper part) based on monthly runoff data from El Chono using the Pardé index.

## 3.3 Conclusion

The Rio Andarax Basin has a dry, semi-arid climate with an annual temperature average of 18 °C and about 160 mm of rainfall. All the streams in the catchment are ephemeral. The main stream, Rio Andarax however is permanently flowing at its source. Occasional flooding contributes recharge to the detritic aquifer along the ephemeral parts of the basin and might sometimes reach the Mediterranean Sea superficially, draining a catchment area of 2200 km².

Three high mountain ranges form part of the Andarax river basin, in these mountain ranges snow accumulates during winter time, the snowmelt provides a significant seasonal runoff and recharge potential even in this dry environment.

The fact that the runoff regime of Rio Andarax in figure 3.11 does not decrease to zero during the summertime indicates a storage capacity in the Nevado-Filabrides and Alpujarran units of Sierra Nevada.

Consequentially, an important source of recharge in the upper part of the basin can be identified. The regular inflow into the Andarax detritic aquifer amounts to important volumes of water compared to the sporadic sources.

A possible direct contact between the detritic and the fissure aquifer of the Pre-Cenozoic Basement could be of major importance for the water balance. Recharge to the karstified Alpujarran units in the mountain ranges could trigger for major groundwater flow systems. Direct contact between both aquifers could as a matter of fact be pointed out in the area of Gador by evaluating thermal differences in groundwater temperature (Pulido Bosch, 1992).

# 4 Field Investigations

## 4.1 Introduction

From September 20th to September 22nd 2005, water samples were taken from several wells, boreholes, springs and the main stream of Rio Andarax Basin and analyzed for their chemical composition.

Analysis focused on temperature, electric conductivity, pH-value and the major ions to better understand the hydrogeology of the Rio Andarax basin. Further, groundwater samples were taken to be analysed in the laboratory of Hydroisotop GmbH, Schweitenkirchen for stable isotopes $^{2}H$ / $^{18}O$ and the radioactive isotope tritium $^{3}H$ to determine and locate possible recharge as well as areas contributing to the groundwater system. Finally, water samples were taken for the analysis of CFCs and $SF_6$ for age dating purposes and to determine the amount of noble gases and excess air in groundwater.

The target of the sampling on this first field trip was to improve the understanding of the hydrogeology of the basin, as well as the determination of areas contributing water to the aquifers, and to receive a first impression of the comportment of gases at different locations underneath, beside and apart from the ephemeral stream.

## 4.2 Sampling Locations

The sampling locations were carefully choosen to cover all sources of water and processes relevant to characterize the groundwater in the alluvial aquifer in terms of origin, recharge altitude, residence time and dominant recharge processes. However it must be mentioned, that the access to wells and boreholes was difficult and therefore modified the choice of sampling locations.

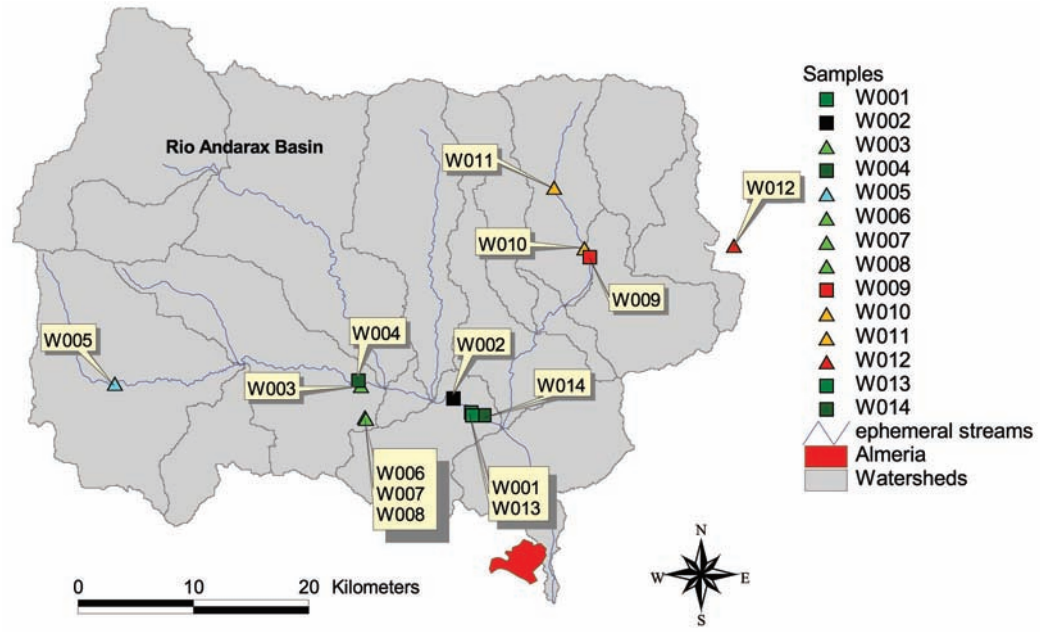


Figure 4.1: Sampling Locations within the Rio Andarax Basin that were choosen for the field investigations from September 20th to September 22nd 2005.

When procurable, farmers and owners of the sampled wells and boreholes were interviewed to obtain a better understanding of the well properties and facts, that may help to assign the sample location to the hydrogeological system. As a matter of fact, properties and facts could most of the time only be estimated, as the owners could rarely be found and communication difficulties occured.

Here is, in summary, a short description of each sampling location that is shown in figure 4.1. The symbol and color assigned to each sampling point has been done based on their chemical properties and is kept throughout this chapter for a concise layout.

W001 is a sample taken out of a piezometer installed in the riverbed of Rio Andarax. This piezometer has been installed within the project WADE. It is drilled through-quaternary alluvial deposits and reaches the watertable at a depth of 20 meters in the Pleistocene conglomeratic units.

W002 was taken at one of the major pumping stations for water supply in the area. It is reaching a deep aquifer, a clear hydrogeological assignment however could not be done because of the reasons mentioned before.

W003 is an irrigation well at the border of the riverbed of Rio Andarax on the upper terrace level. Based on the fact of high pumping rates, it is assumed to reach a deep detritic aquifer.

W004 is a sample, that was taken from a well on a citric plantation on the upper terrace level. The borehole is situated some 50 meters away from the river bed of Rio Andarax. Soils on the plantation terrace consist of marl with embedded gypsum.

W005 is a stream water sample from Rio Andarax. As mentioned in Chapter 3.2.7 Rio Andarax is permanent running close to its source, at the foothills of Sierra Nevada.

W006 - W008 are samples taken out of a major pumping station for water supply. The pumping station is situated at the foothills of Sierra de Gador, and therefore assigned to the Pre-Cenozoic Basement aquifer on the sides of the valley consisting of Alpujarride unit. At the sampling point, an exposure of fault could be observed with hydrothermal shale stratum overlaying a conglomerate with dolomite embedment and calcite/iron hydroxide along the fissures.

W009 is an irrigation well situated in the eastern part of the Rio Andarax catchment. The well is drilled into the river bed of Rio Tabernas and reaches the water level of the detritic aquifer at a depth of 50 meters. The Tabernas river carries floods mor sporadic than Rio Andarax. Interviewed farmers at the sampling point didn't remember seeing a flood since the past 6 years.

W010 is water taken from a well known spring in the area. The spring is caught in a subterranean corridor and drains the foothills of Sierra de los Filabres.

W011 is a sample taken out of an irrigation well on an drip-irrigated olive plantation at the foothills of Sierra de los Filabres. Soils on the plantation consist of fine sand with a high amount of mica slate corresponding to the Nevado-Filabride unit.

W012 is water taken from a big pumping station probably reaching into a molasse aquifer. The sample was taken outside the surface catchment border. The well is situated

in a plain, where no major ephemeral streams could be identified.

W013 is an irrigation well at the border of the river bed of Rio Andarax on the second terrace level. It reaches the water table of the deep detritic aquifer at around 50 meters.

W014 is water sampled from a small irrigation well on a citric plantation, around 30 meters away from the river bed of Rio Andarax. It reaches the water table of the shallow detritic aquifer at 20 meters depth.

Further sampling locations were chosen only for the analysis of stable isotopes 18O and 2H in terms of their temporal behavior. As mentioned before, some sampling locations were difficult to access, and therefore the monthly sampling was moved to other locations.

W005a is a stream water sample from Rio Andarax. The location is further downstream, close to the village of Canjayar.

W014a is a sample taken on the upper terrace level of Rio Andarax, next to the sampling point W014. The sample is taken out of a piezometer which has been installed within the project WADE and reaches the watertable of the shallow detritic aquifer at 20 meters.

W016 is a sampling point situated 500 meters upstream of W001 on the Left Bank of Rio Andarax. The borehole reaches the watertable of the shallow detritic aquifer at around 20 meters depth. The sampling point was choosen, because the watertable at the piezometer W001 sank below the drilled depth in novembre 2005.

## 4.3 Sampling Procedure

At all sample points, water was collected in 500ml polyethylene bottels for hydrochemical analysis on major ions and tritium, and in 100ml polyethylene bottels for the analysis on stable isotopes 18O and 2H. At 9 out of the 14 sampling points water was additionally collected for analysis on CFC-11, CFC-12, CFC-113, SF6 and noble gases. For the analysis of gaseous components in water, careful prevention of contamination must be taken while sampling. Therefore the sampling procedure is pictured and described here in detail.

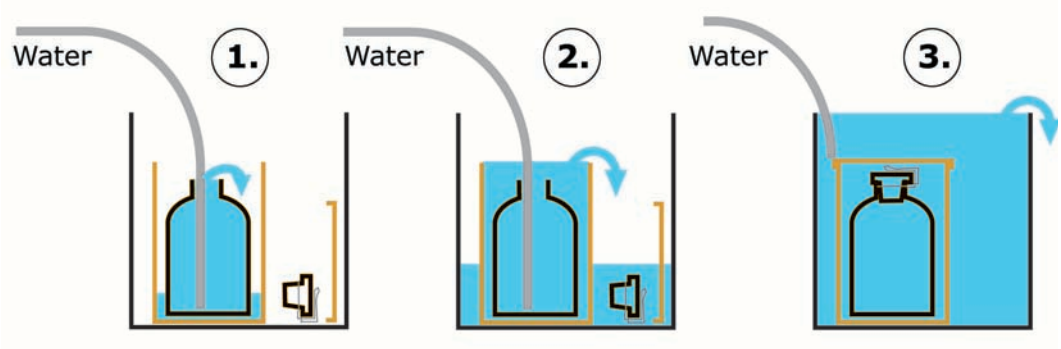


Figure 4.2: Sampling Procedure for CFCs, SF6 and noble gases. The figure shows a glas bottle inside a brazen can and the filling procedure inside a five liter bucket. 1. Bottle, can and caps are placed in the bucket, the tube is insert to the bottom of the glass bottle. 2. Bottle and can are filled until they overflow into the bucket. 3. Bottle and can are closed under water and then removed.

Water for the analysis on gaseous components was collected in glass bottles with metal closure, embedded in a brazen can. The filling procedure was carried out in a five liter bucket.

To make sure not to sample water that has stayed for a long time inside the borehole, pumping started before the actual sampling, according to the dimension of the borehole and the pumping rate. After the well has been purged, the can and bottle were placed inside the bucket and then the end of the tubing from the pump was inserted all the way to the bottom of the glass bottle. The bottle was then filled with water until it overflowed into the brazen can. The proccedure was continued, until the can and the bucket were overflowed. If air bubbles were present they were disloged by slight tapping.

All parts of the closure were put into the bucket in order to flush them with sampling water as well as to remove air bubbles.

The tube was then removed from the bottle, which was tightly capped underwater in order to keep the water in the bottle from coming into contact with air. Afterwards the brazen can was closed, likewise underwater.

After having tightly closed both the glass bottle and the brazen can, they were removed from the bucket and packed for shipping.

## 4.4 Chemical Analyses

Groundwater samples were analyzed on major ions at the Institute of Hydrology Freiburg (IHF). The samples of stable isoptopes 18O and Deuterium that were taken during the sampling period were analyzed by Hydroisotop Laboratory in Schweitenkirchen. Further samples of the stable isotopes, taken monthly for the investigation on their temporal behaviour were analyzed at the IHF with the Isotope Ratio Mass Spectrometer, Type Delta S, produced by Finnigan. Analysis of Tritium, CFCs, SF6 and noble gases were conducted by Hydroisotop Laboratory, Schweintenkirchen.

### 4.4.1 In Situ Parameters

At all sampling points, the in situ parameters water temperature, electric conductivity and pH-value were measured. The results are presented in Table 4.1.

The in situ parameters helped determine different types of groundwater. Generally, samples of the dolomite aquifer showed a relatively low electric conductivity of 870 µs/cm to 950 µs/cm and a high temperature between 28 °C and 29,2 °C. Samples from the alluvium and the detritic aquifer nearby the village of Gador are in the range of 1272 µs/cm to 1724 µs/cm and have temperatures between 17,5 °C and 19 °C.

The sample W003, which was as mentioned before assumed to derieve from the deep detritic aquifer, has a signature alike the samples out of the dolomite aquifer. It has a slightly higher electric conductivity and a slightly lower temperature.

Sample W-002, which was taken from a major pumping station on the Left Bank of Rio Andarax, shows an unexpected signature, too. Through its high electric conductivity, it could be assigned to the samples taken nearby out of the detritc aquifer. The temperature

of 24 °C however is to high too be assigned to the detritic aquifer and too low to be assigned to the Pre-Cenozoic Basement aquifer on the sides of the valley.

The lowest electric conductivity is measured at W005, the stream water sample of Rio Andarax. Its temperature of 17.5 °C coincides with most of the samples taken out of the detritic aquifer along the ephemeral stream of Rio Andarax.

A relatively high electric conductivity of 2290 µs/cm was measured at the sampling point W004 on a drop-irrigated plantation close to the village of Bentarique. Waters both high in conductivity and temperature were also found in the surrounding of Tabernas.

PH-values varied from pH 7,4 in the alluvium/detritic aquifer to pH 8,1 in the sample of upper Rio Andarax river water and in the sample of a spring close to Tabernas.

Table 4.1: The in situ parameters electric conductivity, water temperature and pH-value measured during the field investigations in Rio Andarax Basin.

| Sample ID | Electric Conductivity [µs/cm] | Water Temperature [°C] | pH-Value |
|---|---|---|---|
| W001 | 1272 | 17.5 | 7.4 |
| W002 | 1432 | 24.0 | 7.4 |
| W003 | 947 | 28.0 | 7.8 |
| W004 | 2290 | 22.5 | 7.7 |
| W005 | 693 | 17.5 | 8.1 |
| W006 | 889 | 28.6 | 7.5 |
| W007 | 878 | 28.9 | 8.0 |
| W008 | 892 | 29.2 | 7.8 |
| W009 | 1455 | -9999 | 7.2 |
| W010 | 830 | 22.0 | 8.1 |
| W011 | 973 | 21.7 | 7.4 |
| W012 | 1938 | 29.9 | 7.9 |
| W013 | 1335 | 19.0 | 7.4 |
| W014 | 1724 | 17.6 | 7.3 |

### 4.4.2 Major Ions

In investigating an area with a diversity of geological units and soil properties as it was shown in chapter 3, the composition of major ions in groundwater can give useful information in terms of determination of sources and areas contributing to the different aquifer units.

The hydro-chemistry of the samples can be visualized with Schoeller and Piper diagrams. The Schoeller diagrams shows the absolute profile of major ions on a logarithmic scale, while the Piper diagram shows the complementary percentages of cations and anions.

A Schoeller plot in figure 4.3 shows three essentially different types of water:

1) The river sample W005, the sample from Sierra de Gador W006 and the sample from the irrigation well in the valley close to Bentarique W003 all show relatively low ionic concentrations of sodium/potassium and chloride. W005 shows lower concentrations of calcium and sulphate than W006 and W003. This can be explained by a shorter contact time of the water with the substrate. These waters are declared as dolomite waters and can therefore be used as an end member for mixing approaches.
2) The water sample W012 shows relatively low concentrations of magnesium and sulphate and compared to all the other samples very high concentrations of sodium/potassium and chloride. The water was taken out of a strongly productive well, probably reaching into a molasse aquifer in the east of Tabernas, not far away from the watershed. It might be considered as an end member as well, if the sampling point lays within the subsurface catchment borders.
3) Sample W010 and W011 show a much more balanced run of the curve. These samples were taken at the bottom of Sierra de los Filabres, in the north of Tabernas. They represent the waters coming from the Nevado-Filabride unit and will therefore be used as end members.

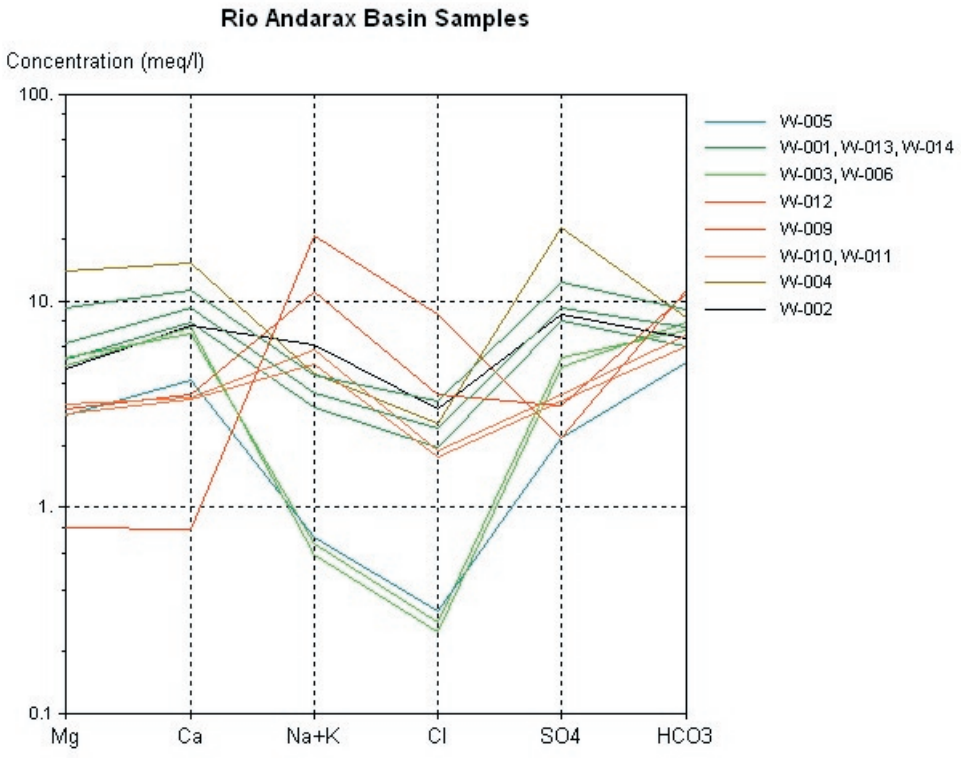


Figure 4.3: Determination of different water types with a Schoeller plot.

The water samples taken out of the alluvium and the detritc aquifer close to the village of Gador, W001, W013 and W014 have a similar composition and always lay in between differentiated type W003, W005, W006 and the sample W004 taken on the Left Bank

upper terrace level of Rio Andarax. They can be regarded as mixing waters. The same distribution of groups is evident in the Piper graph pictured in figure 4.4 representing the samples from Rio Andarax.

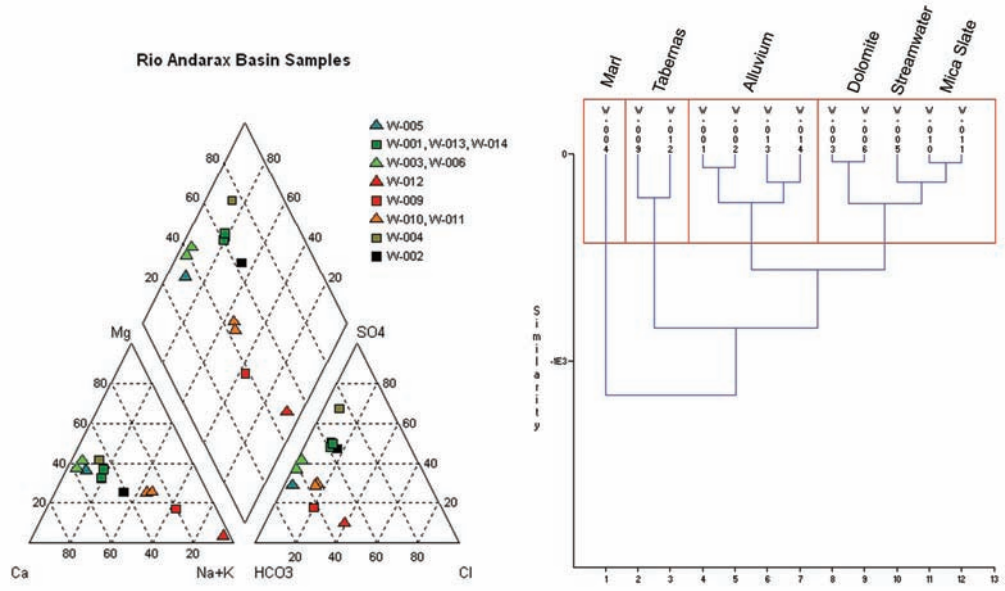


Figure 4.4 and 4.5: on the left: The Piper plot shows the different chemical signatures of the waters that have been sampled so far. Triangles represent end members that could be used in further investigations to identify and to quantify possible hydraulic interconnection and recharge. On the right: A cluster analysis of the samples using Ward's method.

Water samples taken during the field trip coincide with the chemical composition already known in this area. Samples out of the detritic aquifer have a tendency to be a little higher in the content of magnesium and calcium and much higher in their content of sodium/ potassium and chloride, in comparison to the waters of the dolomite aquifer.

W002 and W004 are an exception to the other samples taken out of the detritic aquifer in this area. Apart from showing a higher temperature as mentioned before, W002 has a higher concentration of sodium. The water is possibly influenced by a hydraulic interconnection with the detritic aquifer of Tabernas. W004 attracts attention because of higher magnesium, calcium and sulphate values. Nitrate was also found to be high in water from that sample.

The cluster analysis was done using the Ward's method which is distinct from all other methods because it uses an analysis of variance approach to evaluate the distances between clusters. In short, this method attempts to minimize the Sum of Squares of any two (hypothetical) clusters that can be formed at each step (Ward, 1963).

It identified 4 major groups of water and gave in summary the following classification of samples.

**Group 1: Karst**
It consists of water from the dolomite aquifer in the mountain range of the Sierra de Gador, the stream water of Rio Andarax originating in the Sierra Nevada with its dolomite

and mica slate formations, and finally water from the mountain ranges of Sierra de los Filabres, mica slate respectively.

The dolomite aquifer has a distinct hydro-chemical fingerprint with a Ca/Mg ratio close to 1.2 – 1.5, a low Chloride content and still significant concentrations of sulphate that may be of sedimentary or of hydrothermal origin (fissure coatings with iron oxides and sulphides). The Sierra Nevada stream water is very similar to this group hydro-chemically, sulphate concentrations are somewhat lower. The mica slate member is characterized by higher Na+K concentrations and higher chloride concentrations, sulphate is lower than in the dolomite groups but still significantly present.

**Group 2: Alluvium**
It consists of water samples from wells of plantaions on the upper terrace level and water out of the river bed of Rio Andarax. In both groups, a sample from the deep detritic aquifer and a sample from the shallow detritic aquifer can be found.

The cation composition of these waters is similar to group 1, however, sulpahte concentrations are higher.

**Group 3: Tabernas**
The groundwater of the Tabernas sub-basin forms a single group that contains the end members W009 and W012.

**Group 4: Marl**
Finally, the groundwater W004 beneath the Marl sediments with embedded gypsum has a distinctly different hydro-chemical fingerprint with high concentrations of sulphate.

Regarding the origin of groundwater in the alluvial aquifer, it is obvious that the group 2 is influenced by the group 1 (dolomite) and by group 4 (marls) taking into account the cation and anion characteristics of both groups as shown in figures 4.3, 4.4 and 4.5.

### 4.4.3 Stable Isotopes

#### *4.4.3.1 Spatial distribution of spot samples*

The analysis of stable isotopes sampled from boreholes and stream water in September 2005 were done by Hydroisotop GmbH, Schweitenkirchen.

The concentrations are given in δ-units calculated with respect to VSMOW (Vienna Standart Mean Ocean Water) expressed in part permil (Eq. 4.1)

$$\delta\ sample\ (‰) = \left[ \frac{R_{sample} - R_{VSMOW}}{R_{VSMOW}} \right] \cdot 1000 \qquad \text{equation 4.1}$$

where $R_{sample}$ and $R_{VSMOW}$ are the isotopic ratios of the sample and of the VSMOW, respectively. The accuracy of the measurements is ± 1.5‰ in $\delta^2H$ and ± 0.15‰ in $\delta^{18}O$.

Samples in figure 4.6 point to W005, the stream water of Rio Andarax as being the most depleted source. The sample W012 from a borehole reaching into the molasse aquifer at

the eastern watershed shows the heaviest signature. Groundwater samples do well align on a regression line with a slope close to 6 (5.8, $R^2 = 0{,}81$), which could indicate evaporation effects. Slopes around 6 can also be observed in precipitaion records from Cities around the area of investigation. Precipitation samples from 2000, 2001 of Murcia and Palma in the north east of the study area both show a regression line with a slope of 6.5 (GNIP data; IAEA/WMO, 2004).

However the interpretation of slopes from regression lines of short term precipitation records is not recommended for a determination of local meteoric water lines, as evaporation effects could occur in the sample collector, particulary during precipitation events with low rainfall.

Nevertheless longterm precipitation records for Gibraltar from January 1962 to December 1995 have been evaluated by Vandenschrick et al (2002) and found to align on a regression line of 6.19 with a coefficient of determination $R^2 = 0.83$). They therefore have been considered as a local meteoric water line (LMWL).

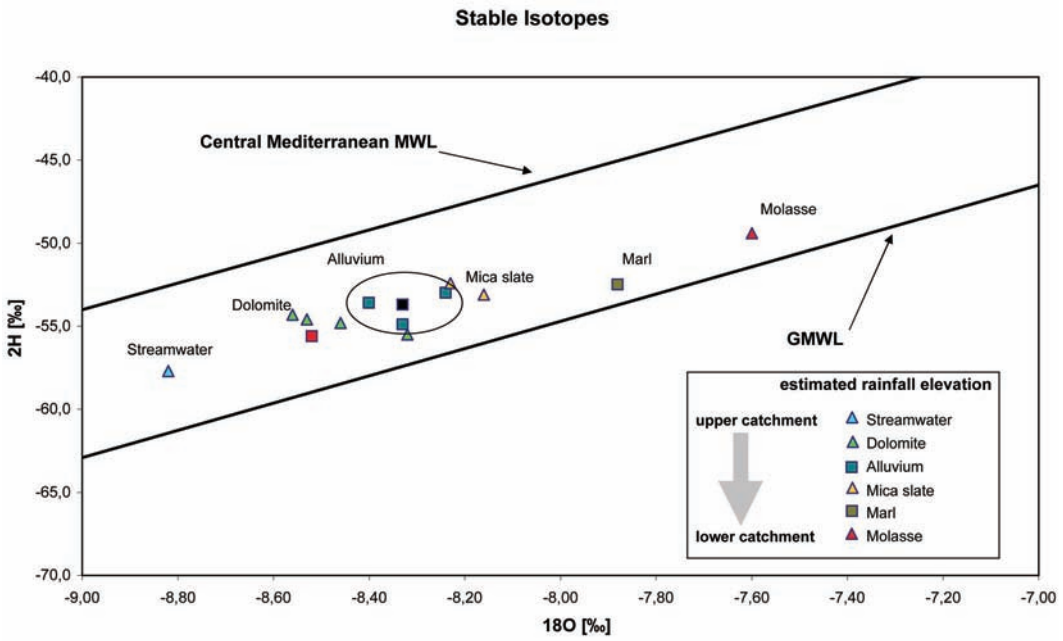


Figure 4.6: Stable Isotopes from the samples taken during the field trip in September 2005. The accuracy of measurements is ± 1.5‰ in $\delta^2H$ and ± 0.15‰ in $\delta^{18}O$.

All samples plot between the Global Meteoric Waterline (GMWL) and the Central Mediterranean Meteoric Waterline (MMWL/A according to Anza et al., 1989) with the equation $\delta^2H = 8 \bullet \delta^{18}O + 18$, as the major sources of water vapor at the origin of precipitation in Spain are the Mediterranean Sea and the Atlantic ocean. Isotopic characteristics like δ-values and deuterium values, can be considered as discriminating tools for such origins.

Deuterium excess in rainfall of Mediterranean origin generally has a relatively high value. This is due to a strong kinetic isotopic effect during evaporation in the summer above the Mediterranean Sea because of the low relative humidity of the atmosphere (Vandenschrick, G. et al 2002). Conversely, Atlantic precipitation has a deuterium excess around +10 ‰.

Consequently, Rio Andarax Basin either benefits from rain events of different meteorological conditions or the rain results from a mixing between water vapors of Mediterranean and Atlantic origins.

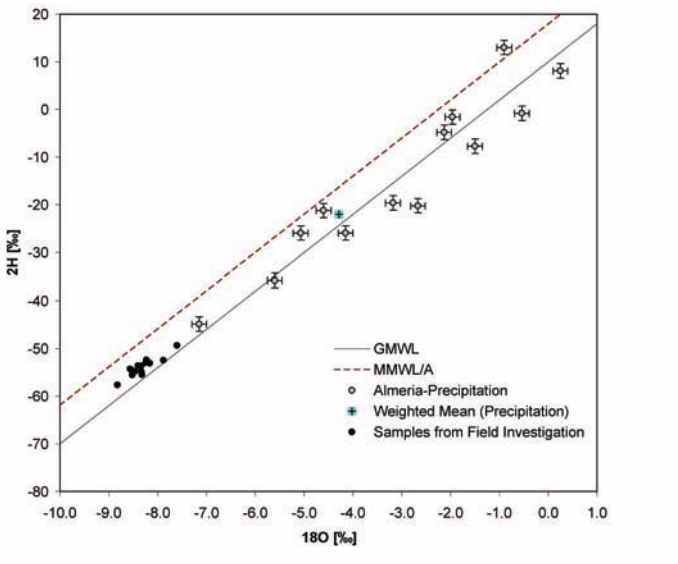


Figure 4.7: $\delta^2H$ - $\delta^{18}O$ relationships from preipitation records at Almeria-Airport and their weighted mean (IAEA/WMO, 2004), in comparison to the isotope data collected on the field trip in September 2005.

In figure 4.7, values of the stable isotopes $\delta^2H$ and $\delta^{18}O$ from precipitation records at the Airport of Almeria (21 m asl) are plotted next to the samples from the field investigation. The δ-values for precipitation from April 2000 to December 2001 were obtained at the free available database in the framework of the global network of isotopes in precipitation (IAEA/WMO, 2004). Precipitation data is aligned on a regression line with a slope close to 8 (7.4). It can be seen in the plot that groundwater, spring and river samples are highly depleted compared to the δ-values of precipitation records. This fact can mainly be explained by an existing orographic effect, considering that the precipitation records are taken close to sea level. Rainfall contributing to the stream water and recharging aquifers of Rio Andarax Basin however occurs up to 2500 m asl.

A good correlation of $\delta^{18}O$ with altitude for the Sierra de Gador is reported by Vallejos et al (1997). The orographic effect of stable isotopes of groundwater samples however can only be seen were local recharge is dominant compared to lateral flow.

In figure 4.8, $\delta^{18}O$-values from all samples are plotted against the altitude of the sampling point. A regression line taking all samples into consideration does not coincide with the expected diminution of heavy isotope values with increasing height, that should lie between -0.25 and -0.5 ‰ / 100 m for $^{18}O$. Therefore only data samples where the mean recharge elevation coincides approximately with the elevation of the sampling point were taken into account. The most reliable data samples were: W005, the river sample of Rio Andarax, 779 m asl, with an estimated mean recharge elevation of 1500 m asl; W011, the sample taken at the foothills of Sierra de los Filabres, 657 m asl, with an estimated mean recharge elevation of 1200 m asl; W012, the sample taken in the plain in the east of Tabernas, 551 m asl, with an estimated mean recharge elevation of 640 m asl.

The recharge elevations were assumed by computing the mean catchment elevations above the sampling points, respectively.

The three samples assumed to be most reliable plot well on a regression line close to the expected diminution with height, according to the deviation between the altiude of the sampling point and the mean recharge elevation.

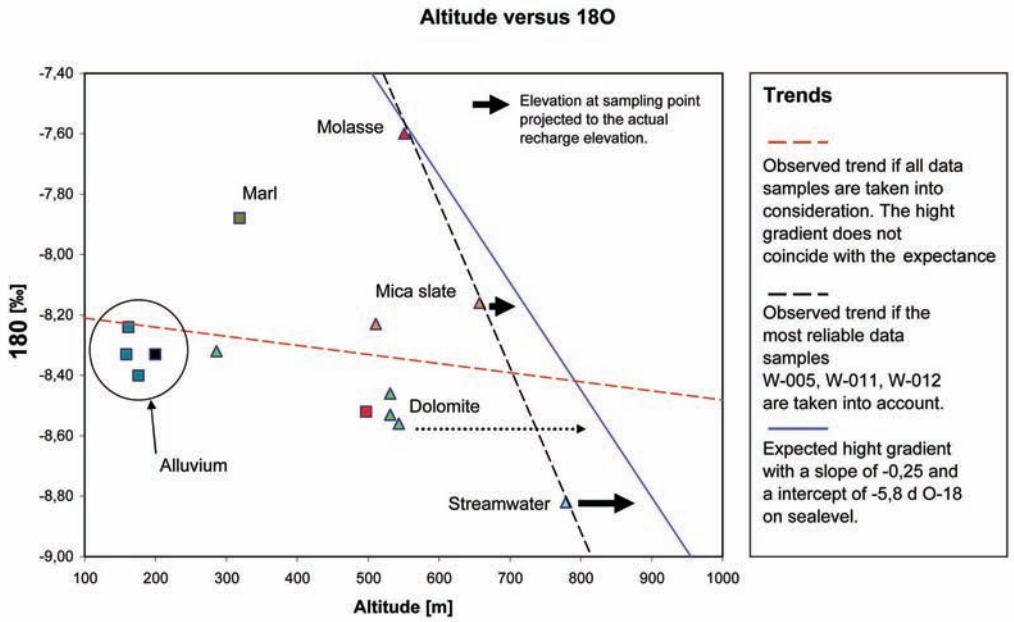


Figure 4.8: Orographic effect and correlation of $\delta^{18}O$-values with altitude.

Based on the fact, that the orographic effect was already reported by studies of the area and can also be seen in figure 4.8, most groundwater samples taken during the field trip in September 2005 can be determined as not having been recharged at the elevation of sampling. The strongest deviation is shown by the samples taken from the alluvium. This rules out any local source contributing significantly to the replenishment of the alluvial aquifer. The aquifer is either recharged further upstream or by indirect recharge processes during floods.

### *4.4.3.2 Temporal behavior at selected sampling sites*

The analysis of stable isotopes of selected sampling sites for the investigation on their temporal behaviour were done at the Institute of Hydrology Freiburg (IHF). The accuracy of the measurements is ± 1.0‰ in $\delta^2H$ and ± 0.2‰ in $\delta^{18}O$.

For the sampling, five locations were chosen for the reasons mentioned in chapter 4.2. The sampling is done by members of the project WADE on site, on a time interval of 2 to 4 weeks. In this work, first results are presented comprising 3 to 5 samples for each sampling location from September 2005 to January 2006.

The $\delta^2H$ - $\delta^{18}O$ relationships for river water at the sampling point W005a, for the deep detritic aquifer at W013 and the shallow detritic aquifer both, below the river bed of Rio Andarx W001 and below the plantation on the upper terrace level W014/W014a are not subject to major variability for the period of investigation. This can be seen in figure 4.9. Variability almost lies within the accuracy of measurment.

Simply the reverse behavior of water from the shallow aquifer W001 to water from the deep aquifer W013 attracts attention. However, three samples taken from W013 from September to December are insufficient to confirm a coherence.

Nevertheless three sampling locations, that have been monitored without major discontinuance point to interesting behaviors.

As shown in figure 4.9, a plot of $\delta^{18}O$ with time, δ-values of the shallow detritic aquifer below the river bed of Rio Andarax behave different, almost reverse to the δ-values of the shallow aquifer below the plantation.

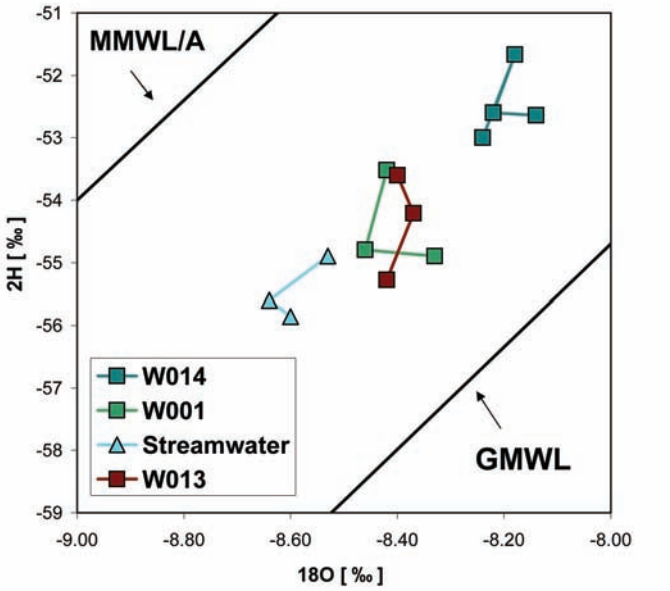


Figure 4.9: Temporal behavior of $\delta^2H$ - $\delta^{18}O$ relationships. Accuracy of the measurements is ± 1.0‰ in $\delta^2H$ and ± 0.2‰ in $\delta^{18}O$.

It is important to mention that both sampling points are 900 m away from each other, which is little compared to the stream water sample of Rio Andarax, taken around 24 km upstream of W001. δ-values from the shallow aquifer below the river bed behave similar to δ-values from the stream water sample. In January, W001 and W005a conform to the same value (marked with a black circle). Floods from Rio Andarax reaching the area of investigation were reported during this period by the WADE-Team on site. It can be concluded that indirect recharge from flood water of Rio Andarax to the shallow detritic aquifer has occured. The reverse behavior of δ-values on the plantation can be explained by direct or indirect recharge from local rainfall on lower altitudes.

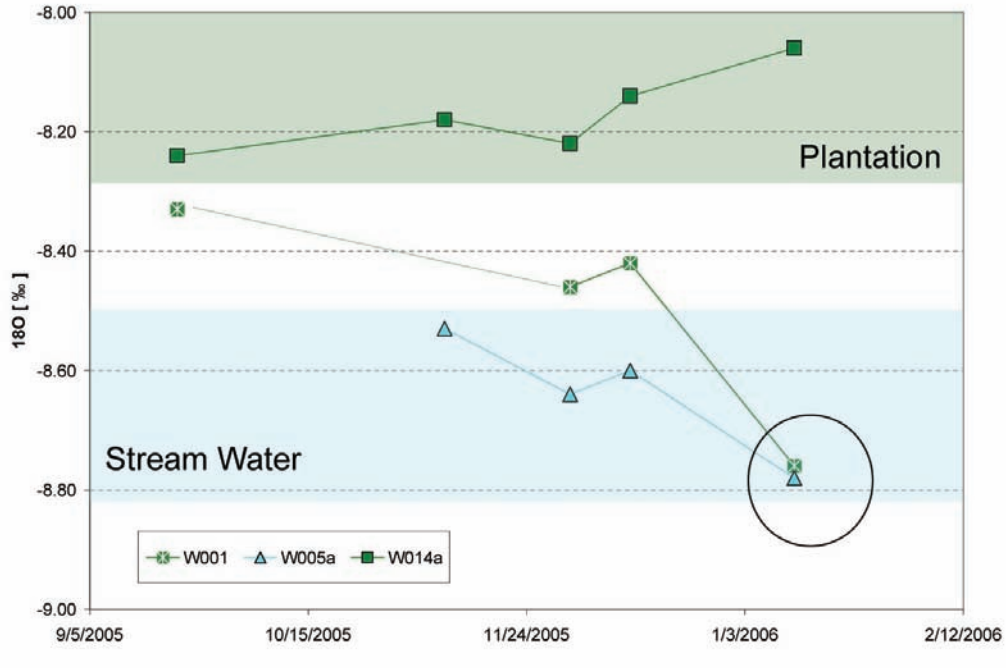


Figure 4.9a: Temporal behavior of $\delta^{18}O$ - values for three selected sampling locations. Accuracy of the measurements is ± 1.0‰ in $\delta^2H$ and ± 0.2‰ in $\delta^{18}O$.

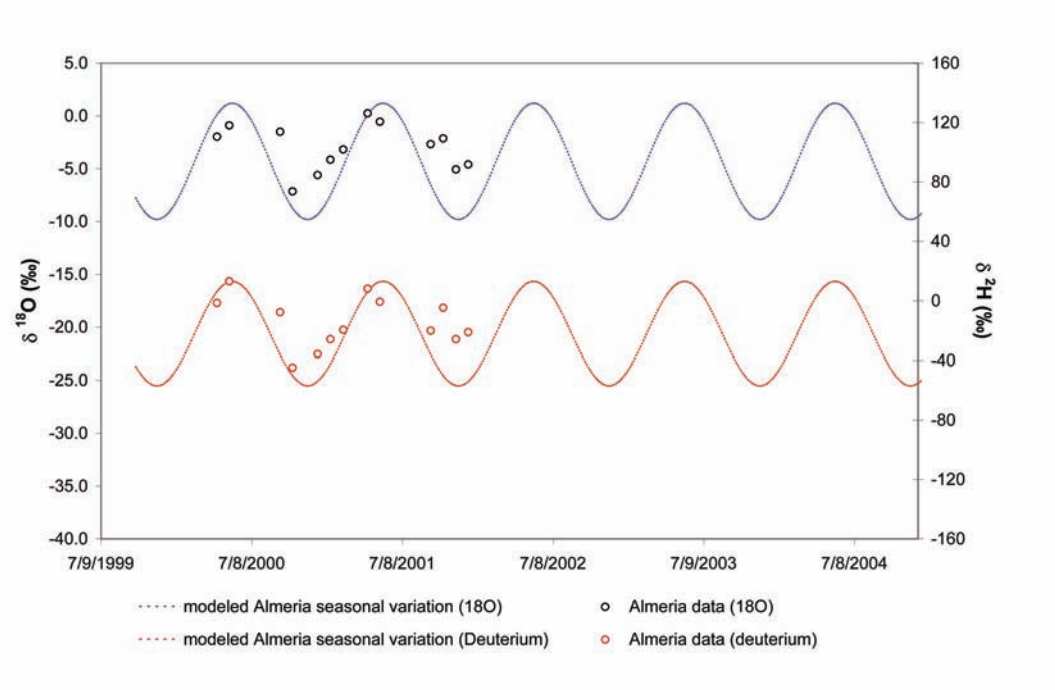


Figure 4.10: Modeled seasonal variation for $\delta^2H$ and $\delta^{18}O$ in precipitation records obtained from the GNIP database (IAEA/WMO, 2004).

Time series of $\delta^2H$- and $\delta^{18}O$ - values in groundwater at that time are too short to be evaluated on their annual variation. For the determination of seasonal and annual variation time series of at least one year should be available. Hence $\delta^2H$- and $\delta^{18}O$ - values presented in figure 4.8 and 4.9 are not plotted in figure 4.10.

The annual variation of stable isotopes in precipitation however was modeled, using the data records at Almeria Airport from April 2000 to December 2001 obtained from IAEA/WMO, 2004 and is presented in figure 4.10. It shows a mean of -4.3 $\delta^{18}O$ with an amplitude of 5.5 and a mean of -22 $\delta^2H$ with an amplitude of 35. The fact that some precipitation samples do not plot well to the modeled annual variation could be indicating a seasonal anomaly in terms of temperature or rainfall for that year.

Groundwater samples from Rio Andarax Basin and their variation of stable isotopes can be added to the model to determin the damping and shift of seasonal variation within the different aquifers.

### 4.4.4 Tritium

Long term measurments of Tritium in precipitation at Madrid and Barcelona reveal a continous decreasing as it can be observed worldwide. The evaluated Tritium data of Barcelona, obtained from the GNIP database (IAEA/WMO, 2004) shows that values around 5 TU have been reached in 1991 (fig.4.11). Such values represent todays natural background in winter season, formed in the atmosphere by reaction of nitrogene and neutrons. In summer Tritium reaches values around 10 TU.

Two values of Tritium in precipitation could be obtained from the GNIP database for Almeria Airport as well. It must be noticed, that these two Tritium records are yearly

weighed values for the years 2000 and 2001, 4.4 TU and 4.31 TU respectively. Tritium ($^3$H) values in figure 4.11 are given in Tritium Units (TU) whereas 1 TU equals a ratio of $^3H/^1H = 0.118$ Bq/l.

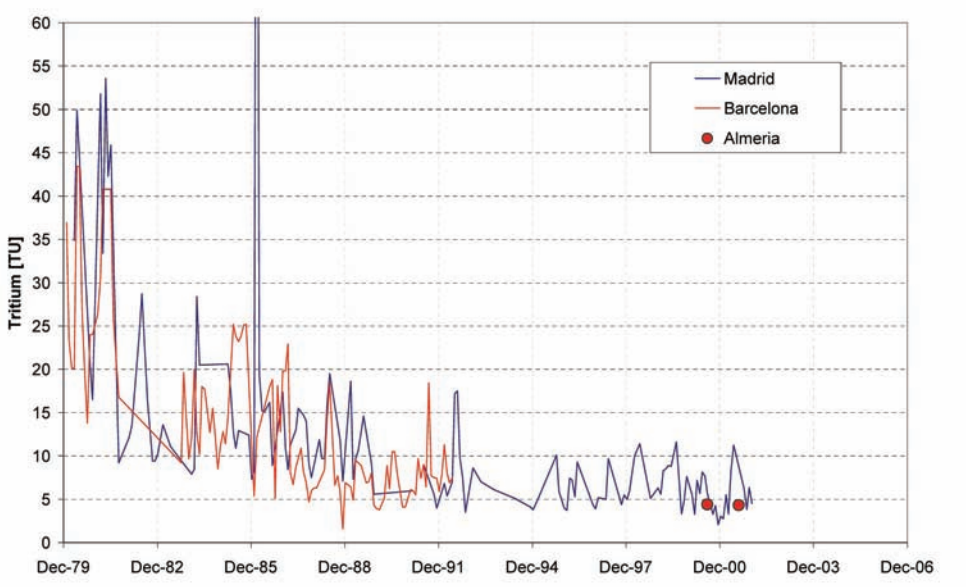


Figure 4.11: Monthly Tritium ($^3$H) concentrations in precipitation records from Madrid and Barcelona, and yearly weighted $^3$H-values from Almeria Airport (GNIP data: IAEA/WMO, 2004).

The well documented decrease of high $^3$H-values resulting from nuclear weapon tests of the early sixties, makes age dating of groundwater using this radioactive isotope with a half-life period of 12.34 years nowadays more and more difficult. It is recommended to monitor a sampling point for 2 or 3 years to be able to determine mean residence times with sufficient accuracy, as groundwater containing little $^3$H concentrations can either be old (dating from before the Tritium-Peak) or recently recharged. In case of a long time monitoring, the decay of $^3$H gives evidence about whether groundwater has long or short residence times.

Nevertheless, Tritium is still an essential tool facilitating the estimation of mean residence times in groundwater and the determination of groundwater age.

Tritium values for the sampling locations investigated on the field trip in September 2005 are shown in figure 4.12. Values vary from <0.6 TU at sampling points W002, W006 and W012 to 4.3 TU at the sampling W014. Generally all groundwater samples taken from the alluvium and the upper terrace level of Rio Andarax, as well as the samples taken at the foothills of Sierra de los Filabres show $^3$H-values close to the yearly weighed average of input from precipitation. Samples out of the deep molasse aquifer and the dolomite aquifer have values close to the limit of detection. Three samples however show an interesting behavior. W002 and W003 are samples taken out of the deep detritic aquifer below the river bed of Rio Andarax. They both show values that are significant lower compared to the sample W013 stemming from the deep detritic aquifer as well. W009, the sample out of the deep detritic aquifer below the river bed of Rio Tabernas with a $^3$H-value of 2.5 TU and is the only sample showing neither values close to the natural input nor close to the limit of detection.

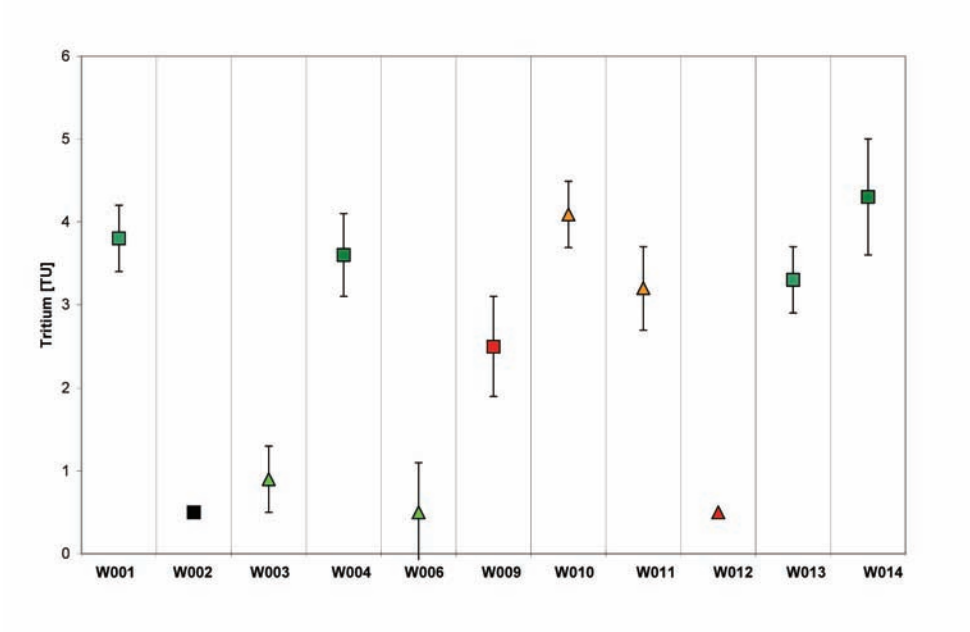


Figure 4.12: $^{3}$H-values for the samples taken on the field trip in September 2005. For the sample W002 and W012 no accuracy of measurments are given as they have values <0.6 TU. Data was analyzed by Hydroisotop GmbH, Schweitenkirchen.

Stemming primarily out of the alluvium, groundwater with $^{3}$H-values close to the yearly weighed average of input from precipitation is determined to be recently recharged. Groundwater from the molasse aquifer and the dolomite aquifer is determined to have mean residence times >40 years. The sample W009 could indicate a mixing of recently recharged water from the foothills of Sierra de los Filabres (W010, W011) with water from the molasse aquifer. The sample W003 indicates to be influenced from groundwater of the dolomite aquifer and groundwater from the alluvium of Rio Andarax.

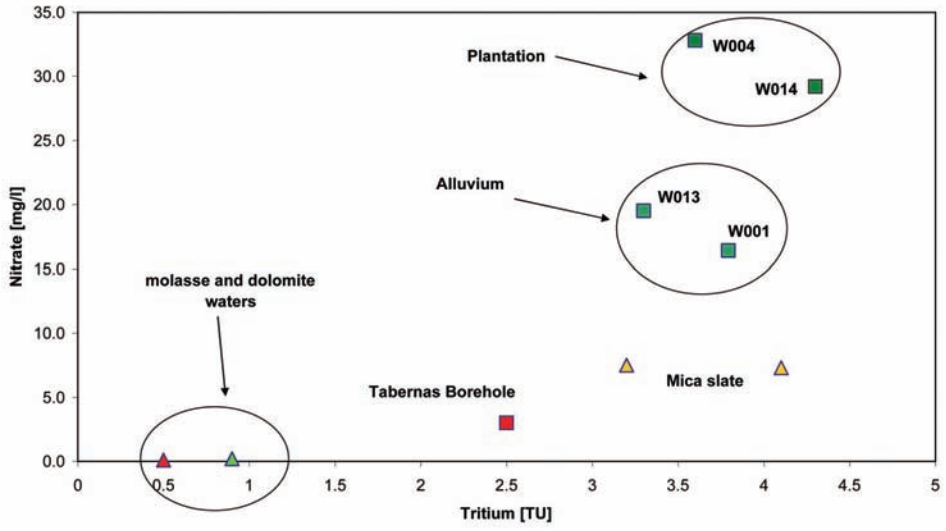


Figure 4.13: Comparison of $^{3}$H-values with nitrate contents. Groundwater with long residence times shows low nitrate contents whereas recently recharged groundwater shows nitrate contents up to 33 mg/l.

A closer look to the comportment of Tritium in groundwater from the deep detritic aquifer and the shallow detritic aquifer below Rio Andarax is shown in figure 4.13. The comparison of $^3$H-values of groundwater with nitrate contents varies from old groundwater with low nitrate content to recently recharged groundwater with nitrate contents around 30 mg/l.

Groundwaters taken from below the plantations show the highest nitrate contents. It should be noted that samples were taken from the shallow detritic aquifer (W014) and from the deep detritic aquifer (W004). Groundwaters taken from below the river bed of Rio Andarax have nitrate contents that coincide with the stream water sample having a nitrate content of 13.2 mg/l. Here as well, groundwater has been sampled from the deep detritic aquifer and from the shallow detritic aquifer.

Groundwater from the deep detritic aquifer (W004, W013) seems to have lower $^3$H-values than groundwater from the shallow detritic aquifer (W001, W014). The deviation of $^3$H-values however lies within the accuracy of measurment.

The comparison of $^3$H-values with nitrate contents helped to associate water with high $^3$H concentrations to recently recharged groundwater. High nitrate contents in groundwater only developed recently since agricultural production in this area has been encouraged through subsidies.

### 4.4.5 CFCs and $SF_6$

Chloro-Fluoro-Charbons (CFC-11, CFC-12, CFC-113) and Sulphur Hexafluoride ($SF_6$) were measured at nine locations in the Rio Andarax basin according to the sampling procedure described in chapter 4.3. Figure 4.14 gives a first impression about the comportment of industrial gases in comparison to Tritium.

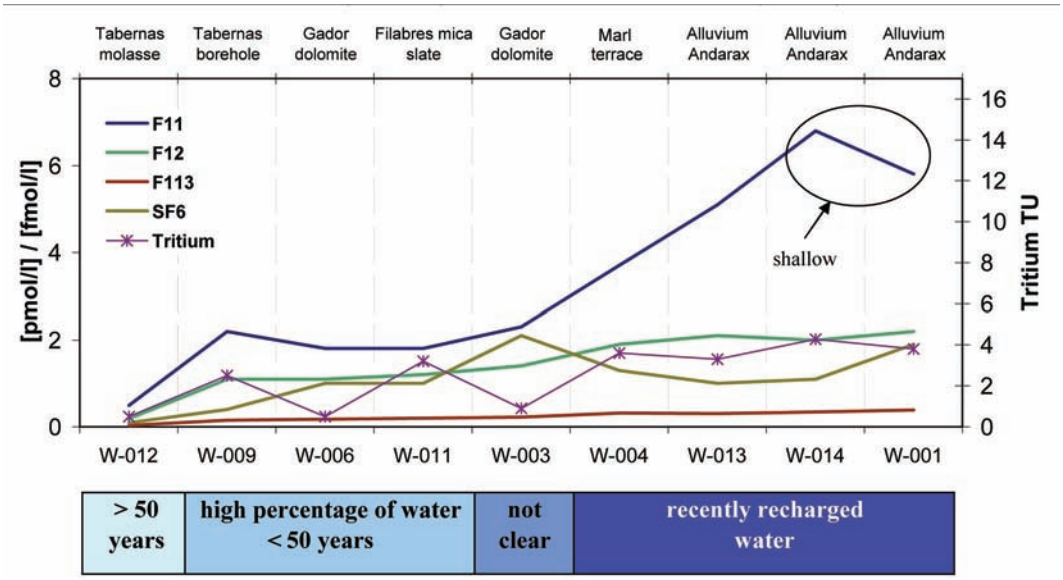


Figure 4.14: CFCs and $SF_6$ in comparison to the comportment of Tritium for 9 sampling points within the Rio Andarax basin. $^3$H-values generally coincide with the comportment of the industrial gases CFC-11, CFC-12, CFC-113 and $SF_6$. An incoherence can be seen at W006 and W003.

A rough classification of CFC-, $SF_6$- and $^3H$-concentrations determines three major age groups of groundwater: groundwater with a mean residence time of more than 50 years, groundwater containing a high percentage of water with residence times smaller than 50 years and finally recently recharged groundwater.

Derived from all concentrations plottet in figure 4.14, the groundwater from the deep molasse aquifer (W012) is determined to have a mean residence time of more than 50 years. W009, W006 and W011 are samples representing the deep detritic aquifer at Tabernas, the dolomite aquifer and groundwater stemming from the foothills of Sierra de Gador, mica slate respectively. They show concentrations of CFC and $SF_6$ that derive a mean residence time of <50 years. The behavior of $^3H$ is incoherent for the sampling point W006 and therefore estimates water of the dolomite aquifer to be older. A second incoherence of $^3H$-values and CFC- / $SF_6$-concentrations can be seen at W003. It is groundwater out of the deep detritic aquifer below the river bed of Rio Andarax which seems to be influenced from the karstic aquifer as it was already shown in all precedent analyses. Finally a group of recently recharged groundwaters is derived from all components used for age dating in this work. They contain the sampling points W001, W004, W013 and W014 taken from the alluvium of Rio Andarx, below the river bed and on the upper terrace level.

Reliable and accurate estimates of groundwater age depend mainly on the kowledge of recharge temperature, pressure (recharge elevation) and the amount of excess air. The Rio Andarax basin has a difference in elevation of approximately 2500 meters and consequently a considerable variation in temperatures. Figure 4.15 shows a sensitivity analysis that has been done for all samples. Uncertainty in recharge temperature of ± 5°C leads to uncertainty in apparent CFC ages of 4 years for water beeing recharged prior to 1970. However, as the air mixing ratios of CFCs peaked after 1990, age dating with CFC became extremely sensitive to uncertainties in recharge temperature.

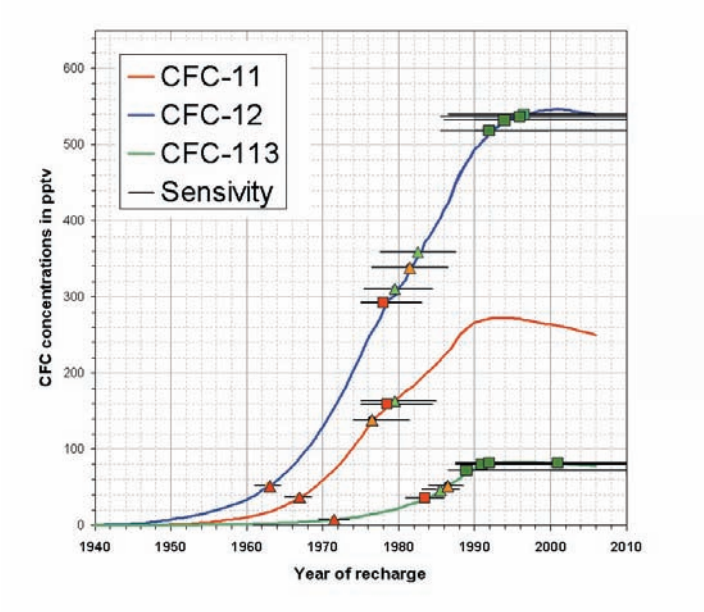


Figure 4.15: Sensitivity analysis of apparent CFC ages with regard to recharge temperature and recharge elevation. The analysis is done with an uncertainty of ± 5°C for the temperature and ± 300 m for the elevation. Recently recharged groundwater is more sensitive to uncertainties.

The information on recharge temperature and recharge elevation for the sampling points in Rio Andarax basin was estimated on the basis of all precendent investigations and hydro-chemical analyses mentioned in chapter 3 and 4. Recharge temperature was assumed to be less than the annual temperature average of 18°C regarding the rainy season from October to December and from March to May. It was therefore in a first set to values between 13°C and 16.5°C , depending on the hydrological processes assigned to the sample location. The recharge elevations were assumed by computing the mean catchment elevations above the sampling points and considering indirect recharge processes occurring along the ephemeral streams.

Atmospheric mixing ratios of CFC-11, CFC-12 and CFC-113 were calculated for the piston flow model and for the exponential model, corrected on a standard temperature of 8°C and a standard altitude of 200 m a.s.l.. The samples were corrected to the same standards.

The piston flow model (PM) is based on translation of an input signal, that is a time displacement without deformation, following the system function

$$h(t) = \delta(t - t_\alpha) \qquad \text{equation 4.2}$$

where $t_\alpha$ is the mean residence time of water. Regarding the fact that no mixing occurs in this model belief, the flow time of tracer particles (in that case CFC) between the input and output of the system correspond to the mean residence time of water in the system. In hydrology, the PM is often applied on karstic systems or on aquifers with little storage capacities and selective recharge areas.

The exponential model (EM) is based on exponential distribution of flow times according to the system function

$$h(t) = \frac{1}{t_\alpha} \cdot exp\left[-\frac{t}{t_\alpha}\right] \qquad \text{equation 4.3}$$

where $t_\alpha$ is the mean residence time of water. The system reacts immediately on an input, with short flow times having the highest probability density. In hydrology, the EM is generally applied on porous aquifers with different flow distances and a widespread input.

CFC-12 and CFC-113 mixing ratios are plotted for both, the PM and EM input functions as well as for all the sampling points being investigated for CFC in the Rio Andarax basin (figure 4.16). The classification into three major ranges of residence times is reconfirmed. Young groundwater from boreholes in the alluvial aquifer of Rio Andarax, groundwater with intermediate residence times from the Pre-Cenozoic basement and the detritic aquifer in the eastern part of the basin, and finally a groundwater with no traces of recent recharge in the molasse aquifer.

All samples seem to agree well with the EM input function and show a mixture of waters with mean residence times ranging from 10 to 250 years. However, good results can as well be obtained by a binary mixing approach of young water with old water containing no CFC (figure 4.17).

However, two sampling locations point to the piston type flow. W001 and W013, both samples taken below the riverbed of Rio Andarax tend to no agreement neither with EM

input function nor binary mixing approaches. According to the PM model belief groundwater taken from the detritic aquifer below the river bed of Rio Andarax should be considered replenished significantly by a local source or recharge area. However, this trend lies within the accuracy of measurements.

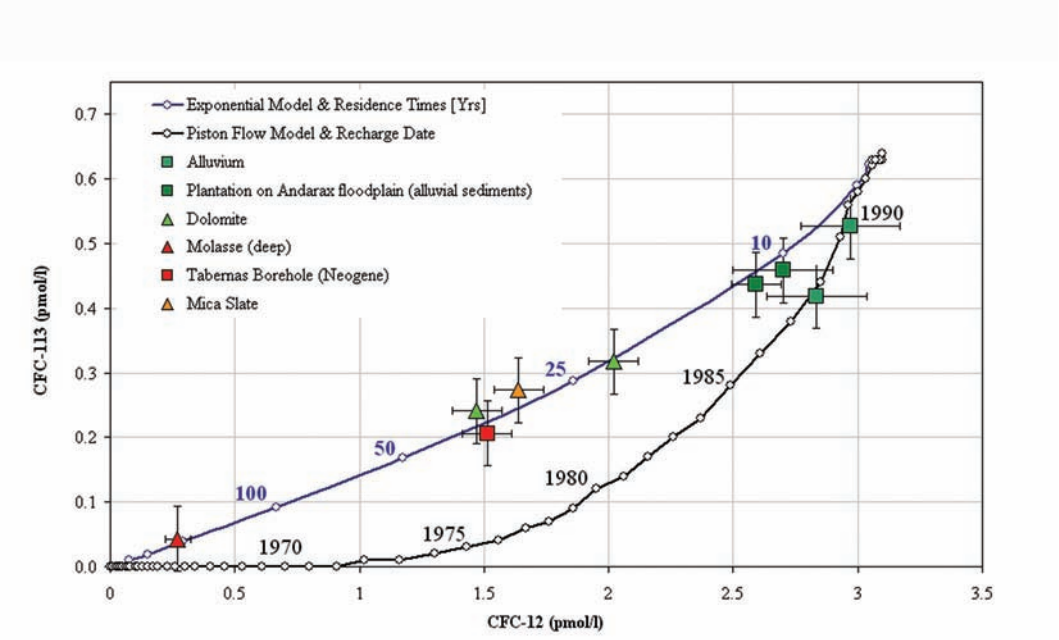


Figure 4.16: Apparent CFC age of groundwater samples from the Rio Andarax basin according to global input functions of CFC, calculated for the piston flow model and the exponential model.

Groundwater from sampling point W003, which showed an incoherence in the comparison of $^{3}H$-values with CFC- / $SF_6$-concentrations points to a mean residence time, in between residence times from the dolomite aquifer and the alluvium of Rio Andarax. A possible hydraulic interconnection between the detritic aquifers and the fissure aquifer of the Pre-Cenozoic basement at W003 results from all investigations and hydro-chemical analyses that have been done so far.

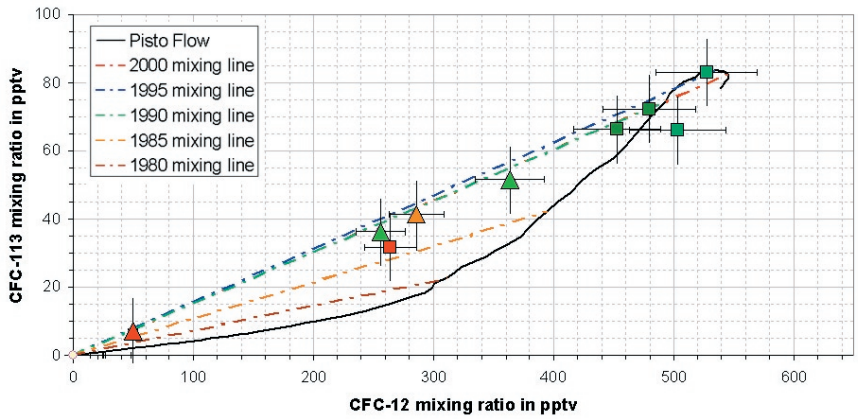


Figure 4.17: Binary mixing approach of young and old water (no CFCs) from the ratio of CFC-12 and CFC-113, calculated with the USGS spreadsheet program for preliminary evaluation of CFC data (Busenberg and Plummer, 2005). Atmospheric mixing ratios are from North America, in this spreadsheet.

Determination of CFC-based apparent groundwater age was done with mixing ratios of CFC-12 and CFC-113. In all calculations, CFC-11 turned out as not reliable for age dating purposes within the Rio Andarax basin (table 4.2). Modeled piston flow dates for CFC-11 determined the young groundwater from the alluvium to be contaminated. This results in CFC-11 concentrations of water that are greater than that possible for equilibrium with tropospheric air. In all other samples CFC-11 age is old relative to the CFC-12 and CFC-113 ages.

Table 4.2: Caculated atmospheric mixing ratios and modeled piston flow dates for all sampling points being investigated on CFCs in the Rio Andarax basin. Calculations were done with the USGS spreadsheet program (Busenberg, E., Plummer, L. N., 2005).

| Sample | Recharge Temp | Recharge Elevation | Calculated Atmospheric Mixing Ratio in pptv | | | Modeled piston dates | | |
|---|---|---|---|---|---|---|---|---|
| | [°C] | [m] | CFC-11 | CFC-12 | CFC-113 | CFC-11 | CFC-12 | CFC-113 |
| W-001 | 15,0 | 200 | 371,2 | 527,5 | 83,0 | Contam | 1993,5 | 1993,0 |
| W-013 | 15,0 | 200 | 326,4 | 503,5 | 65,9 | Contam | 1991,0 | 1988,5 |
| W-014 | 15,0 | 200 | 435,2 | 479,6 | 72,3 | Contam | 1989,0 | 1989,5 |
| W-004 | 13,0 | 900 | 232,7 | 452,6 | 66,2 | 1986,5 | 1987,5 | 1988,5 |
| W-003 | 16,5 | 300 | 160,6 | 363,4 | 51,5 | 1979,0 | 1983,0 | 1986,5 |
| W-006 | 12,5 | 900 | 110,3 | 255,9 | 36,2 | 1974,5 | 1976,5 | 1983,5 |
| W-009 | 14,5 | 400 | 140,7 | 264,2 | 31,8 | 1976,5 | 1977,0 | 1982,5 |
| W-012 | 16,0 | 600 | 35,3 | 50,0 | 7,1 | 1966,5 | 1962,5 | 1971,5 |
| W-011 | 13,0 | 900 | 113,2 | 285,9 | 41,4 | 1974,5 | 1978,0 | 1984,5 |

The USGS Reston Chlorofluorocarbon Laboratory (URL 1) lists reasons for differences in modeled groundwater ages, depending on the CFC used for dating. For an assignment of apparent CFC age, the most reliable results are obtained, if the apparent ages from all three CFC compounds agree.

If the CFC age is old relative to the CFC-12 and CFC-113 ages, CFC-11 may be degraded. CFCs are degraded by microbial processes under unaerobic conditions, primarily by dechlorination reactions that produce hydrochlorofluorocarbons (HCFCs). CFC-11 degradation is found to be nearly 16-fold that of CFC-12 and CFC-113 (Deipser and Stegmann, 1997).

When the CFC-11 and CFC-12 ages agree and the CFC-113 age is younger, mixing of old and young water has likely occured, due to CFC-113 mixing ratios having a modest increase relative to CFC-11 and CFC-12.

The differences in modeled piston flow ages for the samples of Rio Andarax basin are shown in figures 4.18 to 4.19. It can be seen, that modeled CFC-11 and CFC-12 ages agree relatively well, CFC-11 tends to be older. However, CFC-11 compared to CFC-113 reveals older ages. All the samples were taken from deep aquifers, and consequential unaerobic conditions are feasible. CFC-11 is therefore likely to be degraded as mentioned above. The comparison of CFC-12 to CFC-113 ages determines groundwater dated with CFC-113 to be younger relative to CFC-12 which reveals mixing of young and old water as mentioned above.

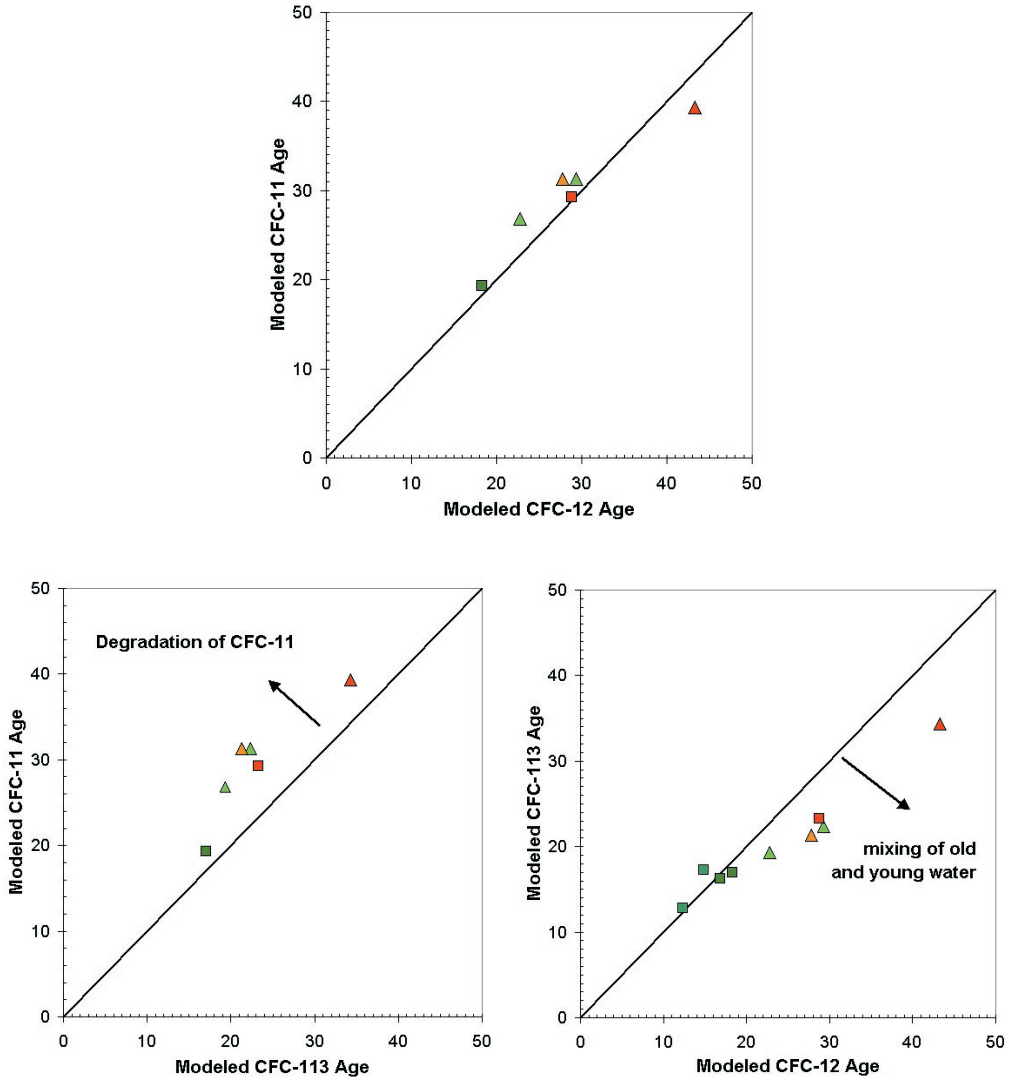


Figure 4.18 to 4.19: Correlation between modeled CFC ages for CFC-11, CFC-12 and CFC-113. For plots with CFC-11 only non-contaminated concentrations are shown.

A closer look to the correlation between modeled CFC-12 and CFC-113 ages shows, that ages of samples taken from the alluvium agree well. Mixing of young and old water is rather assigned to the samples from the dolomite aquifer and the dry eastern part of the basin. Results from the comparison of modeled CFC ages coincide with the results shown in figure 4.16.

Sulphur hexafluoride ($SF_6$) generally has promise as an alternative to CFCs for dating of groundwater, as its atmospheric concentration is still increasing with a current growth rate of approximately 7 % per year (Geller et al., 1997). $SF_6$ is primarily of anthropogenic origin. Nevertheless it also occurs naturally in minerals, rocks, and volcanic fluids. Harnish and Eisenhauer (1998) found significant concentrations of $SF_6$ in hydrothermal mineral deposits and relatively high concentrations of $SF_6$ in sedimentary dolomite.

Because of its low solubility $SF_6$ is also more sensitive to excess air compared to CFCs (chapter 2). Both the natural existence of $SF_6$ and the sensitivity of $SF_6$ to excess air determined $SF_6$ as not reliable for age dating purposes within the Rio Andarax basin.

Nevertheless, the comparison of $SF_6$ with CFC-12 is shown in figure 4.20. It can be seen that some samples plot relatively well, for instance the sample W012 from the molasse aquifer, W009 from the deep detritic aquifer below Rio Tabernas and samples taken from the alluvium of Rio Andarax. The rough classification of apparent ages of these samples coincides with determinations done with other CFCs and gives evidence of a correct sampling procedure without air contamination.

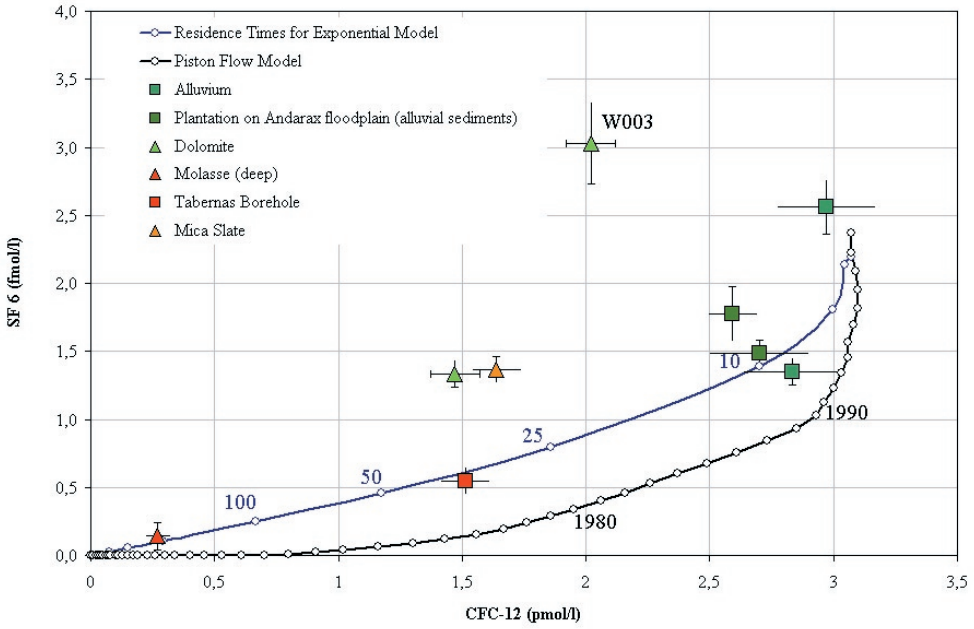


Figure 4.20: Apparent CFC-12 age compared to apparent $SF_6$ age of groundwater samples from the Rio Andarax basin according to global input functions of CFC-12 and $SF_6$, calculated for the piston flow model and the exponential model.

However, three sampling points show very high $SF_6$ concentrations. They are W006 from the dolomite aquifer of the Pre-Cenozoic basement, W011 taken from the foothills of Sierra de los Filabres, mica slate respectively, and W003 from the deep detritic aquifer below the river bed of Rio Andarax.

As described in chapter 4.2 an exposure of fault could be observed at the sampling location W006 with hydrothermal shale stratum overlaying a conglomerate with dolomite embedment. The existence of natural $SF_6$ is therefore feasible at this sampling point. W003, which was derived from preceding analyses to be influenced by W006 shows a much higher $SF_6$ concentration of 3.03 fmol/l (corrected to a standard temperature of 8°C and a standard elevation of 200 m). This concentration exceeds the atmospheric mixing ratio of modern air for $SF_6$.

Correcting both samples by the amount of natural $SF_6$ could be conceivable. However, the remaing excess of $SF_6$ in the sample from W003 is difficult to be interpreted. Uncertainties in the estimation of recharge temperature and recharge elevation are too big.

Analyses of noble gases could give useful information about recharge temperature and recharge elevation, and determine the amount of excess air in the sample.

### 4.4.6 Excess Air

Introduction of excess air adds CFCs and $SF_6$ to groundwater. If therefore, the amount of excess air is not accounted for, the apparent age of groundwater will be estimated too young. Generally, the effect is considered to be small and excess air usually less than 6 $cm^3/l$ can be ignored in most groundwater cases (Busenberg and Plummer, 1992). The calculation of apparent ages given in table 4.3 confirms that uncertainties in excess air between 0 and 6 $cm^3/kg$ result in deviations smaller than 3.6 years of apparent groundwater age.

Table 4.3: The impact of excess air on apparent groundwater age estimated with CFCs. The table compares modeled piston ages for 0 and 6 $cm^3/kg$ STP of excess air in groundwater of the Rio Andarax basin. Recharge temperatures and elevations are kept the same as in table 4.2.

| Sample | Excess Air | Piston Flow Age Excess Air corrected | | | Excess Air | Piston Flow Age Excess Air corrected | | |
|---|---|---|---|---|---|---|---|---|
| | [cc/l] | CFC-11 | CFC-12 | CFC-113 | [cc/l] | CFC-11 | CFC-12 | CFC-113 |
| W-001 | 0,0 | Contam. | 12,3 | 12,8 | 6,0 | Contam. | 15,8 | 15,3 |
| W-013 | 0,0 | Contam. | 14,8 | 17,3 | 6,0 | Contam. | 17,3 | 17,8 |
| W-014 | 0,0 | Contam. | 16,8 | 16,3 | 6,0 | Contam. | 18,3 | 17,3 |
| W-004 | 0,0 | 19,3 | 18,3 | 17,0 | 6,0 | 19,31 | 19,3 | 17,8 |
| W-003 | 0,0 | 26,8 | 22,8 | 19,3 | 6,0 | 27,31 | 24,3 | 19,8 |
| W-006 | 0,0 | 31,3 | 29,3 | 22,3 | 6,0 | 31,81 | 30,3 | 22,8 |
| W-009 | 0,0 | 29,3 | 28,8 | 23,3 | 6,0 | 29,31 | 29,8 | 23,8 |
| W-012 | 0,0 | 39,3 | 43,3 | 34,3 | 6,0 | 39,31 | 43,8 | 34,8 |
| W-011 | 0,0 | 31,3 | 27,8 | 21,3 | 6,0 | 31,31 | 28,8 | 21,8 |

However, uncertainty in excess air introduces a more significant error in modeled $SF_6$ groundwater ages with values up to 2.5 years per 1 $cm^3/kg$ of excess air in water at STP (URL 2). Along with the fact that excess air content is considered to vary with the hydrogeologic environment as well as with dominant hydrological processes the high $SF_6$ concentrations of the sampling points W003, W006 and W011 could be interpreted.

Assuming the recharge temperature of W013 to be 13°C, modeled piston ages for CFC-12 would deviate from $SF_6$ apparent ages in a range of 25 years, dating the water 1980 and 2005 respectively. Deviations of that range could be explained with excess air in groundwater of about 10 $cm^3/kg$.

Excess air concentrations as high as 10 $cm^3/kg$ were found in waters from semi-arid regions, preferentially in areas where rapid, focused recharge was observed and fractured rock aquifers with high water table fluctuation (URL 2). All terms can be assigned to the sampling points showing high $SF_6$ concentrations in figure 4.20 and excess air is likely to be expected.

Nevertheless, only analyses of noble gases, for instance Neon (Ne) can give definite information about whether and how much excess air is present in groundwater of these sampling points.

## 4.5 Conclusion

Water samples could be differentiated regarding their chemical properties and assigned to different types of water of the area. The signature of waters flowing in the fissured dolomite aquifer of Sierra de Gador could be differentiated from the ones coming out of Sierra Nevada.

Two different types of water contributing to the Rambla de Tabernas could be detected. W-012, a water with low magnesium/calcium values and high sodium/potassium values flowing probably in a molasse aquifer and a more balanced type of water coming out of Sierra de los Filabres in the north of Tabernas.

Samples that were taken in the investigation area around the village of Gador show different properties. It is therefore to be expected, that the detritic aquifer around Gador does not only benefit from one source of recharge. It is further to be expected that different sources of recharge contribute with variable intensities depending on tectonic/geologic faults in the area. Water samples of the detritic aquifer with positive thermal anomalies indicate a probable recharge from the dolomite aquifer to the detritic aquifer.

Analyses of the stable isotopes $^{2}H$ and $^{18}O$ gave information of recharge elevations and recharge processes. Most groundwaters exhibit an altitude shift, meaning that rainfall occured at elevations higher than the actual sampling point. This altitude shift is most pronounced for groundwater in the alluvium of Rio Andarax. The higher part of the basin is the major source of water generating direct recharge to the fissured dolomite aquifer and flood runoff that recharges the alluvial aquifers. The temporal behavior of stable isotopes gave evidence, that the shallow detritic aquifer below the river bed of Rio Andarax is recharged by floods.

Chemical analyses provided useful information needed for the interpretation of dissolved gases in groundwater. CFC-analyses determined three major ranges of residence times in groundwater. Young groundwater with residence times around 15 years could be found in the active channel of Rio Andarax. Groundwater from the Pre-Cenozoic basement and the detritic aquifer in the eastern part of the basement showed intermediate residence times around 30 years. Finally a groundwater with no traces of recent recharge was found in a molasse aquifer.

In addition, CFC-analyses determined groundwater with intermediate and long residence times to be mixing waters composed of young and old water. Groundwater from the detritic aquifers below the river bed of Rio Andarax point to a piston-type flow distribution. The shallow detritic aquifer is probably recharged along reaches with preferential infiltration. In some river sections, the shallow aquifer recharges the underlying Pliocene conglomerates that also contain groundwater from the Pre-Cenozoic sequence.

Analyses of $SF_6$ indicated the presence of high excess air concentrations in fissured aquifers and aquifers with rapid, focused recharge.

# 5 Experimental Investigations

## 5.1 Introduction

From March 6th to March 8th 2006, experimental invesitgations on the impact of recharge processes on gaseous components in groundwater were undertaken at the Institute of Hydrology Freiburg (IHF) in cooperation with the Insitute of Environmental Physics Heidelberg (IUP). In a column experiment, two relevant hydrological recharge processes were simulated representing direct and indirect recharge to groundwater. The objective was to get a better understanding of the comportment of gases in groundwater and to allign possible differences to hydrological recharge processes that can be found in semi-arid regions.

Numerous studies of groundwater have shown significant different behaviors of gaseous components, that were associated with different hydrogeologic environments and hydrological processes. All observations convene to the existence of variable excess air concentrations in groundwater. However, the understanding of the formation of excess air is poorly understood or scientifically proven.

The column experiment was designed at the IHF, investigations were carried out in cooperation with the IUP, and analyses were done at the Edelgas-MS Laboratory of IUP, Heidelberg.

## 5.2 Experimental Setup

The investigations on the comportment of gaseous components in groundwater were performed in three experimental setups. The first experiment was designed to simulate direct recharge to groundwater with a precipitation rate smaller or equal to the infiltration rate of the sand used for the investigations. The experiment goes by the name of „Irrigation“ throughout this chapter. Two other experiments simulated indirect recharge processes to groundwater, more precisely ponded conditions that result from focused, rapid recharge in ephemeral streams during floods. These two experiments will go by the name of „Ponded Condition -160 cm“ and „Ponded Condition -300 cm“, throughout this chapter, representing an applied hydrostatic pressure of 160 hPa and 300 hPa, respectively.

### 5.2.1 Experimental Design

The three experiments were performed in composed acrylic glass columns with each a lenght of 50 cm and an inner diameter of 9 cm. Columns for all experiments were filled up to 100 cm above the bottom with fine sorted quartz sand with grain sizes ranging from 0.08 mm to 0.2 mm. All columns were filled with the same packing technique, using the same amount of sand (3940 g per column), and filling the columns under constant tapping. A sampling port was installed at the bottom of each column experiment consisting of a ball valve to control inflow and outflow. A copper tube sampler was connected to the valve in order to sample noble gas concentrations in water flowing out of the column. A fluorimeter was connected subsequent to the copper tube sampler, measuring fluorescence tracers added to the water to determine appropriate times for sampling and cont-

rolling outflow temperature. At the outflow of the fuorimeter, an electronic balance was positioned to weigh the cumulated amount of outflow per time.

Additionally, for the ponded condition experiments, a pressure sensor was installed at the bottom of the column measuring hydrostatic pressure in a ten seconds interval, just above the lower valve controlling inflow and outflow. In addition, a ball valve on top of the sand-filled columns was installed, connecting them to an empty column to be filled with water, only.

The concept of experimental investigations was to have a saturated zone representing groundwater at the bottom of the columns, ranging from 0 cm to approximately 60 cm from above the bottom, and a dry unsaturated zone on top ranging from 60 cm to 100 cm from above the bottom. Using dry sand to represent the unsaturated zone was justificated by preliminary tests. Even after two weeks, flushed sand inside the columns was found to be still too wet, and therefore not representing sand of the unsaturated zone being observed on the field trip to Rio Andarax basin, Spain.

Depending on the experiment, the unsaturated part of the column was then either constantly irrigated or exposed to focused, rapid recharge with a defined hydrostatic pressure by opening the upper ball valve.

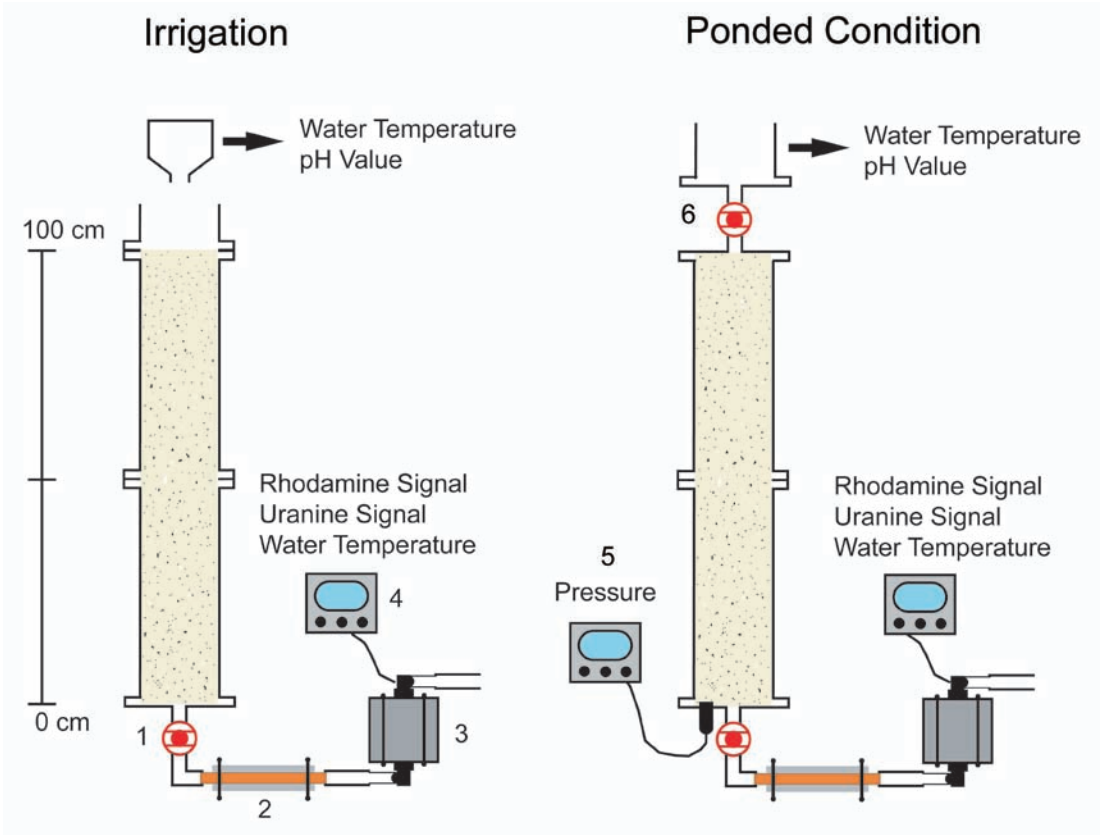


Figure 5.1: Experimental design showing the setup for the irrigation experiment on the left, and the setup for the ponded condition experiments on the right. 1.: ball valve to control inflow and outflow from the column. 2.: copper tube sampler. 3.: fluorimeter. 4.: online monitoring. 5.: pressure sensor. 6.: ball valve to apply rapid, focused recharge to the column, representing ponded conditions as they occur in ephemeral river beds of arid and semi-arid regions during floods.

### 5.2.2 Procedure

As mentioned above the simulation of two different hydrological recharge processes were conducted, direct and indirect recharge, irrigation and ponded conditions, respectively. However the sampling procedure was kept constant for all experiments and shall therefore be explained with the column setup of a ponded condition experiment.

Water for all experiments was brought into equilibrium with air. For this purpose, approximately 80 liters of de-ionized water were brought into steady circulation inside an open barrel. Stirring was conducted with a small circulation pump at the bottom of the barrel for a duration of ten weeks to make sure that the amount of water can equilibrate with the air of the laboratory environment. Electric conductivity, water temperature, air temperature and relative humidity inside the laboratory were regularly controlled. Before starting the experimental investigations, a sample of air and a sample from the water of the barrel were taken to be analyzed on local atmospheric composition of noble gases, and to confirm the equillibrium of water with atmospheric ratios.

Columns were packed with sand right before starting the experimental investigations, to make sure that entrapped air is of the same composition than current air in the laboratory environment.

Preparing the experiments, a water level was raised to approximately 60 cm above the bottom in a first, by saturating the sand-filled column from bottom to up with air satured water. The ball valve on top of the sand-filled columns was kept open, so that air could escape during the saturation process. After the waterlevel was set, both valves on top and at the bottom of the columns were closed. Air saturated water was then filled into the upper column (with no sand inside) above the ball valve and connected to a vessel of bigger diameter to keep a constant hydrostatic head throughout the experiment.

Water of the saturated zone was traced with 0,1 mg/l of uranine. Infiltrating water was traced with 0,1 mg/l of rhodamine (1 mg/l rhodamine in some experiments). Both fluorescence tracers were to be measured online with the fluorimeter in a ten seconds interval during the sampling, aiming at which water was sampled. The fluorescence of uranine decreases rapidly with acescent pH-values. To obtain good results, 1 ml of NaOH (sodium hydroxide) was added to the air saturated water in advance to stabilize the pH-value.

Starting the experiments, the upper ball valve was now opened to let the water from above infiltrate into the unsaturated zone ranging from 60 cm to 100 cm (measured from the bottom of the column). The lower valve at the sampling port was kept closed, until the expected hydrostatic head and the measured pressure at the bottom coincided.

Having reached the applied hydrostatic pressure, the system was kept untouched to allow entrapped air in the sand-filled columns to dissolve, according to the experiment.

Sampling was then undertaken by opening the lower ball valve and keeping the inflow to the columns constant. Three to five samples were taken into copper tubes, depending on the experiment. Temperatures of water flowing into the system and out of the system were continously measured as well as the pressure at the bottom of the column. Measured cumulated outflow and fluorescence signals helped to determine the origin of water being sampled.

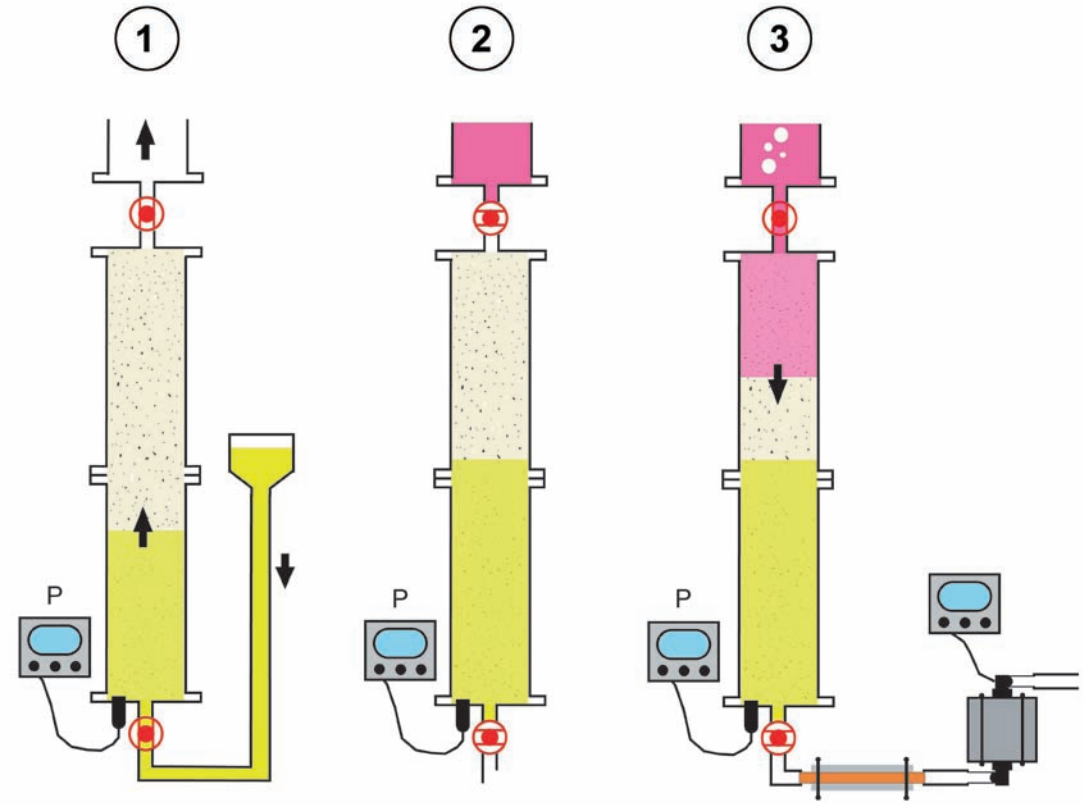


Figure 5.2: Preparational steps of the experiment, before sampling was undertaken. Water of the saturated zone was traced with 0.1 mg/l of unranine (yellow). Infiltrating water was traced with 0.1 mg/l (1 mg/l) of rhodamine (magenta). To trace water, fuorescence tracers were chosen, knowing that saline tracers have an impact on the solubility of gases in water. 1.: filling the saturated zone from bottom to up, the upper valve is open to avoid a raise of pressure inside the column. 2.: closing the valves after the waterlevel is set, and filling water into the column on top. 3.: opening the upper valve to the let water infiltrate into the system. The lower valve is kept closed until the expected hydrostatic pressure is reached. Air bubbles escaping occasionally from the system can be observed.

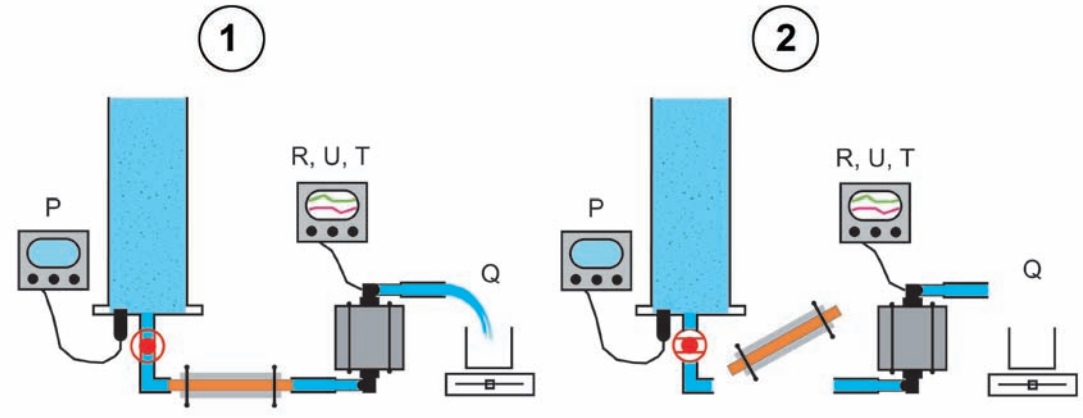


Figure 5.3.: The conduct of the sampling procedure. 1.: determining the appropriate time for sampling, then fusing the copper tube. 2.: closing the lower valve and then exchanging the fused copper tube into a new one. Therby, careful prevention of contamination with air bubbles was taken, considering that this would falsify results and also affect the reliability of fluorescence measurements. P = pressure, R = rhodamine signal, U = uranine signal, T = water temperature, Q = cumulated outflow, gravimetrically determined.

Figure 5.4: Picture of the experimental setup. In front: data logger, storage batteries and laptop for the monitoring of hydrostatic pressure, water temperature and fluorescence signals. In the back: experimental columns. In front of the columns from left to right: Dr. Laszlo Palcsu (IUP), Dr. Christoph Külls (IHF), Prof. Dr. Werner Aeschbach-Hertig (IUP).

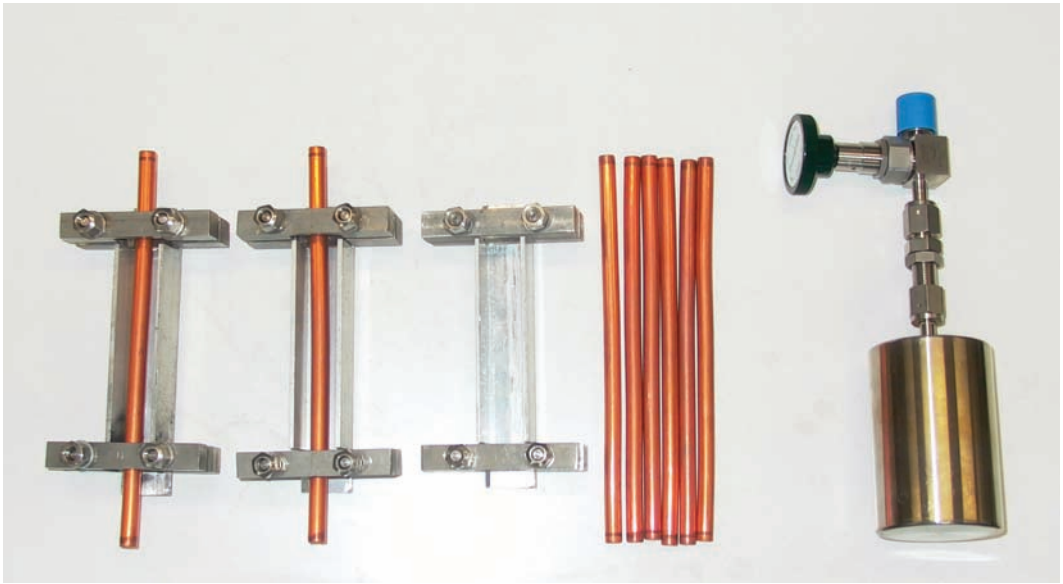

Figure 5.5: Photograph showing from left to right: Two copper tube samplers, consisting of metal sampler with screwable clamps on both sides, and copper tubes, respectively. Copper tubes are fused inside the sampler by screwing the clamps, and removed together with the sampler from the sampling port. On the right: air sampler with vacuum can, when opened air of the environment is sucked into the can abrupt.

## 5.3 Preliminary Tests

Preliminary tests were conducted to obtain a better understanding of the system implemented on the experimental investigations, as well as to determine soil properties. Therefore, several quartz sands of different particle size ranges were tested. The target was, to use a sand with properties, coinciding with soil properties of the hyporheic zone in semi-arid and arid regions. On the other hand, soil properties such as infiltration rate, hydraulic conductivity and outflow rate had to be convenient for experimental purposes.

A fine sorted quartz sand with grain sizes ranging from 0.08 mm to 0.2 mm was finally found to agree best with both, natural conditions and experimental requirements. Two preliminary tests were conducted, an infiltration experiment and a retention experiment.

### 5.3.1 Infiltration Experiment

For the infiltration experiment, the same column setup was used to keep boundary conditions constant. Three liters of water were filled into the upper column, then the ball valve was opened. As soon as water started infiltrating into the dry sand, the decreasing waterlevel in the upper column was read off in an interval of 30 seconds. The outflow was collected in a vessel, positioned on an electronical balance to weigh the water flowing out of the column. The cumulated outflow was also read off in an interval of 30 seconds.

Figure 5.6 shows the setup of the infiltration experiment on the left and the measured data on the right. One can see, that the waterlevel is rapidly decreasing at the start of the experiment, representing a high initial infiltration rate with respect to the unsaturated zone. As soon as water starts flowing out at the bottom of the column, the water level decrease remains constant, corresponding to the hydraulic conductivity for the saturated sand used in this experiment. The cumulated outflow increases constantly, the small shift can be explained with a decreasing hydrostatic pressure in the upper column.

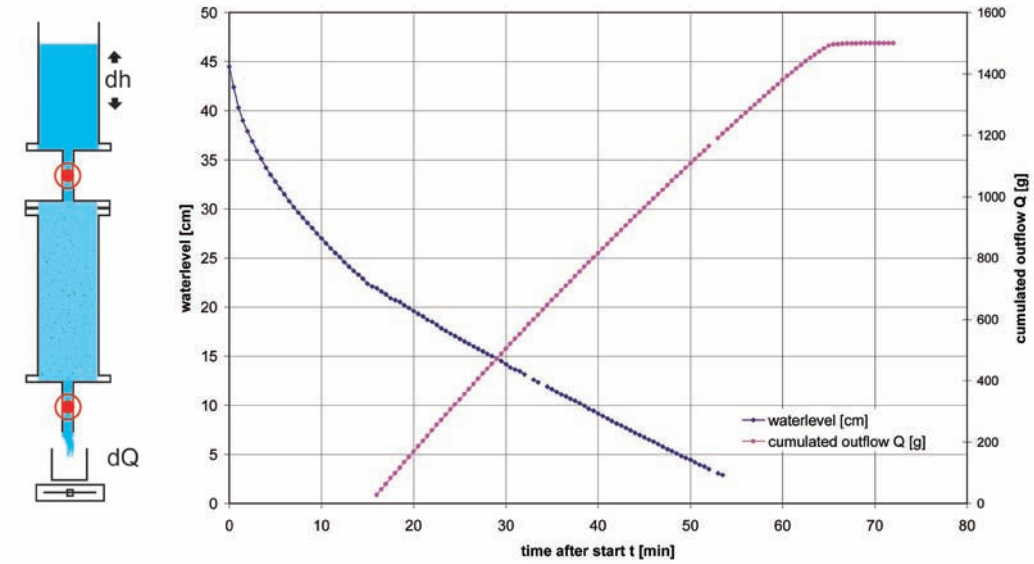


Figure 5.6: Infiltration Experiment, showing on the left the experimental setup and on the right the measured data. Decreasing water level (cm) and cumulated outflow (g) were read off in an time interval of 30 seconds.

Infiltration characteristics were described using the Green & Ampt equation. The Green & Ampt approximation to Richard's equation assumes ponded water at the ground surface and a wetting front that extends to a depth, L, moving downward as a sharp interface (equation 5.1). The soil is assumed to be saturated above the wetting front and the water content is assumed to be equal to the porosity. The rate of infiltration into unsaturated systems can be approximated by the following equation:

$$f(t) = K_{sat} \cdot \frac{H_0 + L + h_{wf}}{L} \qquad \text{equation 5.1}$$

where f(t) is the infiltration rate at time t (cm/hr), Ksat the saturated hydraulic conductivity (cm/hr), H0 is the level of water in the pond or infiltration facility, L is the depth of the wetting front below the bottom of the pond, and hwf the average capillary head at the wetting front. Equation 5.1 shows, that the initial infiltration rates are higher than the saturated hydraulic conductivity for small L, meaning that high gradients occur for shallow wetting fronts. With increasing depth (L) of the wetting front, the gradient decreases and infiltration rates approach Ksat.

Observed infiltration rates from the experiment, and infiltration rates modeled with Green & Ampt are compared with each other in Figure 5.7. The Green & Ampt model was fit using the parameters θs (saturated moisture content = porosity), Sf (wetting front soil suction), and Ksat (saturated hydraulic conductivity). It can be seen, that initial infiltration rates are sligthly overestimated by the Green & Ampt model, whereas saturated hydraulic conductivity is slightly underestimated. The parameter set coincides with literature values given in Table 5.1. The application of the Green & Ampt model helped to validate the infiltration experiment and to determine soil properties.

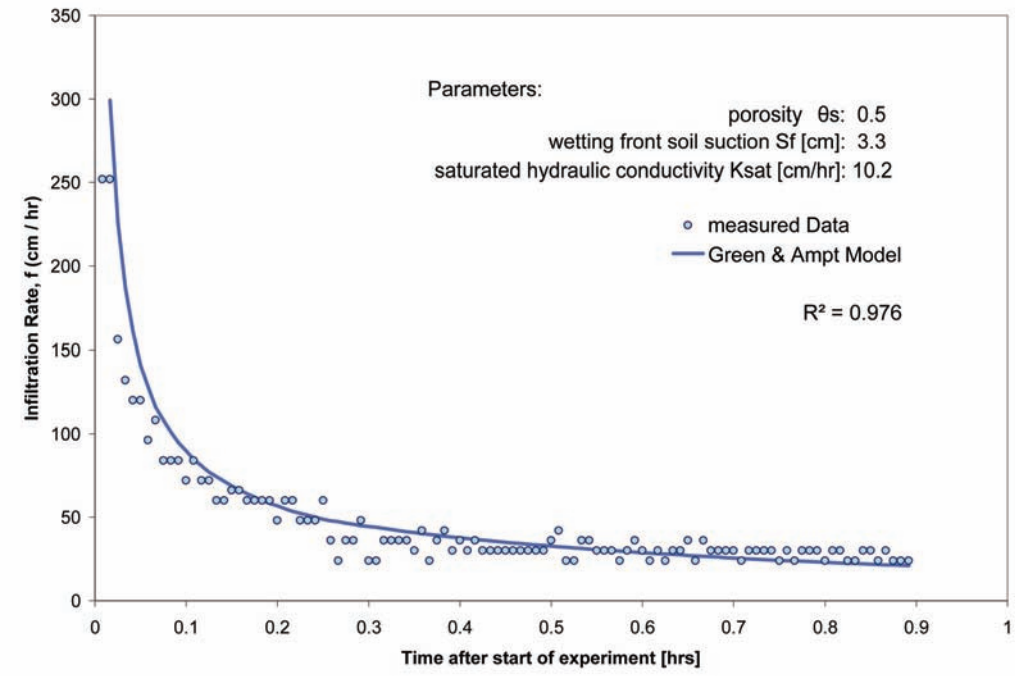


Figure 5.7: Measured infiltration rates f (cm/hr) and infiltration rates modeled with the Green & Apmt equation. Initial infiltration rates are slightly overestimated, saturated infiltration rates are slightly underestimated by the Green & Ampt model.

Table 5.1: Green & Ampt Infiltration Parameters and their ranges (Rawls et al., 1983). The Green & Ampt parameter Ksat can be taken Kast*2 for the saturated hydraulic conductivity for bare ground conditions.

| Porosity | Wetting front soil suction | Saturated hydraulic conductivity |
|---|---|---|
| θ | Sf [cm] | Ksat [cm/hr] |
| 0.437 | 4.95 | 11.78 |
| (0.374 - 0.5) | (0.97 - 25.36) | - |

### 5.3.2 Retention Experiment

In a second preliminary test, a Time Domain Reflectrometry sensor (TDR) was installed on the top of a column, to measure the volumetric water content, and to determine, if possible, the soil water retention curve. Measurements started immediately after the ponded condition experiment, on the same column, to determine the saturated water content. In addition, the cumulated outflow was measured with an electronical balance and read off for a period of 6 days. Figure 5.8 shows the setup of the retention experiment on the left and measured data on the right for the first 60 minutes of the experiment. It can be seen, that soil moisture decreases rapidly within the first five minutes, from values around 49 % to values of approximately 25 %. After the first five minutes, soil moisture decreases moderatley, and reaches a value of 17.2 % after 60 minutes.

Figure 5.9 gives the results of measurements from 1 hour to 6 days, on an hourly scale. After two days, soil moisture has reached a value of 10.1 %, this coincides well with known moisture contents of sand with field capacity. By then, the measured cumulated outflow has reached an amount of 895 ml, and does not increase significantly any more for the following 4 days.

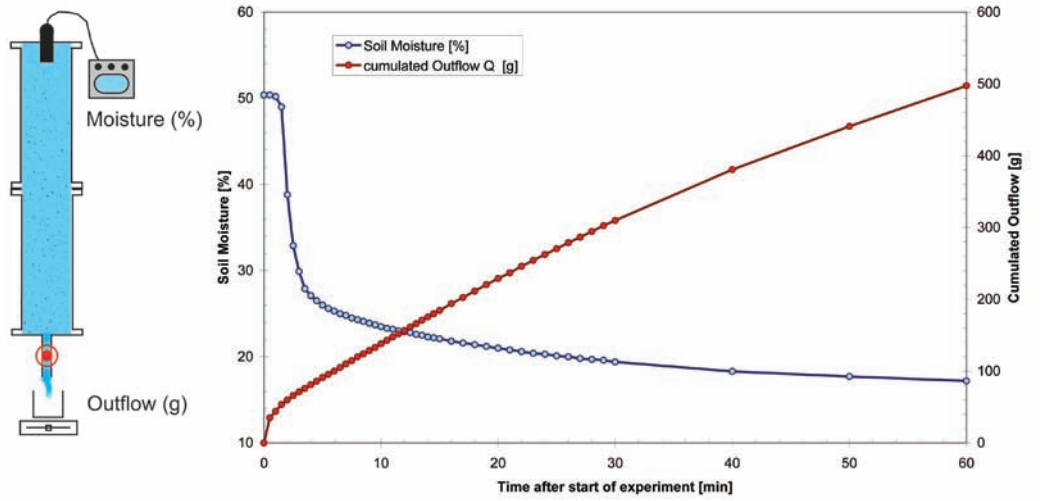


Figure 5.8: Rentention Experiment, showing on the left the experimental setup, and on the right the measured data for the first 60 minutes of the experiment. Soil moisture (in %), measured with a TDR-sensor decreases rapidly within the first five minutes.

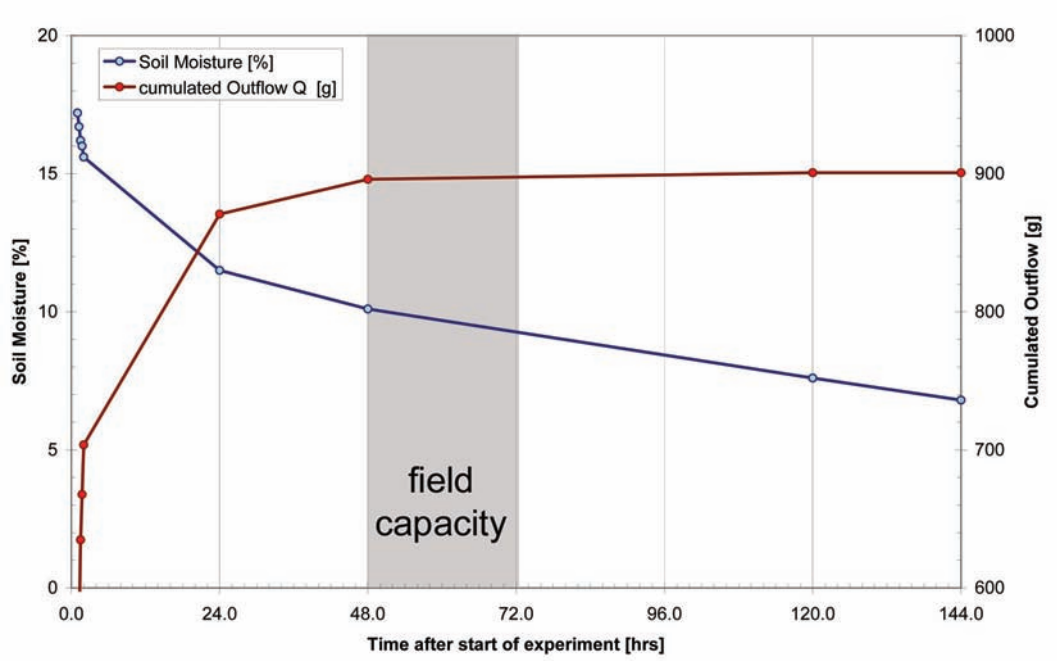


Figure 5.9: Measured data for the retention experiment from 1 hour to 6 day after start of the experiment. After two days, the amount of outflow does not increase significantly any more. However, measured soil moisture continues decreasing from 10.1 % to 6.8 % after 6 days.

A comparison between residual soilmoistures, measured with TDR on top of the column and estimated volumetrically through the cumulated outflow, shows a big discrepancy. As a matter of fact, after finnishing the experiment and emptying the column, only sand from the upper 15 cm was found to be dry. Consequently, the amount of outflow measured at the bottom of the column can not be compared to the soil moisture on top.

Table 5.2: Comparison of soil properties, estimated with different methods, for the fine sorted quartz sand with particle size range from 0.08 mm to 0.2 mm.

| | Method of estimation | | |
|---|---|---|---|
| Porosity θ | modeled (Green & Ampt) | volumetrically | gravimetrically |
| | 0.500 | 0.496 | 0.504 |
| Saturated hydraulic conductivity Kf [cm/hr] | modeled (Green & Ampt) | calculated (from decreasing water level) | calculated (from cumulated outflow) |
| | 20.4 | 24.0 | 25.2 |
| Soil suction Sf [cm] | modeled (Green & Ampt) | | |
| | 3.3 | - | - |
| Saturated soil moisture [%] | measured (TDR) | volumetrically | |
| | 49.0 | 49.6 | - |
| Residual soil moisture [%] | measured (TDR) | volumetrically | |
| | 6.8 | 35.5 | |

## 5.4 Experimental

As mentioned above, three experiments were undertaken to investigate the comportment of gaseous components in water. Firstly, observations made during the experiments, as well as boundary conditions, that have been monitored online shall be presented.

### 5.4.1 Experiment 1: Irrigation

The irrigation experiment was set up for the simulation of direct groundwater recharge, meaning the large surface infiltration and percolation of precipitation at its point of origin. The unsaturated sand column was therefore drop irrigated, until water began to pond. Sampling was then started by opening the lower ball valve, and keeping the irrigation rate equal to the amount of outflow from the column at approximately 22 ml/min, corresponding to an irrigation rate of 2 mm/hr.

Three samples were taken into copper tubes for the investigation on noble gases. The time of sampling is shown in Figure 5.10. The first sample was taken short after opening the lower ball valve to make sure to sample water from the very bottom of the column, water that was filled from bottom to up, respectively. The second sample was taken from water being initially infiltrated into the unsaturated zone, before the start of the experiment. Finally a third sample was taken from water steaming out of the drop irrigation after the start of the experiment, percolating from up to down without stagnation.

Knowing the amount of water inside the column, derived from the preliminary tests, the monitored cumulated outflow helped to determine sampling time. However, the monitored fluorscence tracer signals reveal a more detailed insight.

As mentioned above (chapter 5.2.2), water from the saturated zone was traced with 0,1 mg/l of uranine. To avoid a decay of this light-sensitive substance, the column, representing the saturated zone, was covered with tin foil. In this experiment, water from the unsaturated zone (infiltrating water) was traced with 1 mg/l of rhodamine. The higher concentration of rhodamine was justified by too low signals, obtained in the preceeding experiments. Rhodamine acts sorptive on soil, most of its pigment remained in the upper 10 cm of the unsaturated zone.

Observations of tracer time-variation curves do not coincide with the expectance. As shown on the left (figure 5.10), a mixture of water seems to appear right after the start of the experiment. The rhodamine curve increases, with a slight retardation, right after opening the ball valve. Its further developing can be described as rather inconstant, showing several peaks, whereas uranine shows a rather constant decrease. Possible reasons for this comportment will be discussed in the conclusions of this chapter (5.6). However we may rest assured that sample Nr.1 does not only contain water from the satured zone traced with uranine. The turbidity signal, also measured with the fluorimeter, was found to be very high and developing in agreement with the rhodamine signal. Both signals might therefore have an influence on each other.

As final remark, it must be added by way of explanation that the irrigation experiment did not only serve for investigations on direct recharge processes, but also provides a reference for the two column experiments with applied hydrostatic pressure.

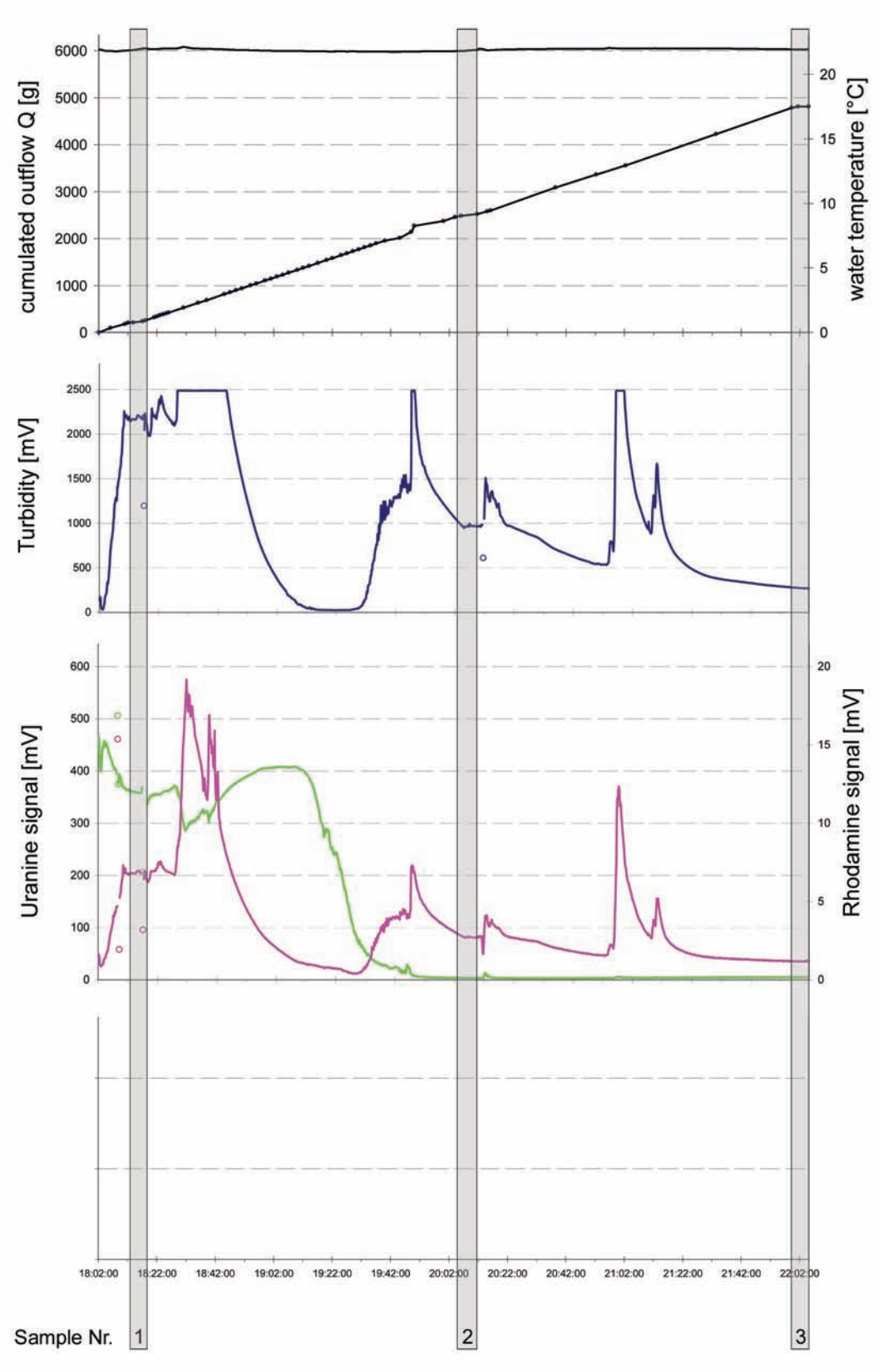


Figure 5.10: Boundary conditions for the irrigation experiment, showing from up to down: water temperature and cumulated outflow, turbidity signal, fluorescence signals of uranine (green) and rhodamine (magenta). Temperature, turbidty and tracer signals were monitored online in a 10 sec interval. Cumulated outflow was read off from an electronical balance.

### 5.4.2 Experiment 2: Ponded Condition - 160 cm

In Experiment 2, a total hydrostatic pressure head of 160 cm was applied on the system, with a constant ponded water level of 60 cm above the soil, and a total pressure of 160 hPa at the bottom of the column, respectively. During the preparation of the experiment, the pressure was already monitored at the bottom of the column, and the results are shown in Figure 4.11. Filling the saturated zone from bottom to up is not shown in this figure, but it can be seen, that pressure remained constant at 2.6 hPa before opening the upper valve, to let the ponded water infiltrate. This fact indicates, that soil suction was big enough, to hold the approximately 1.6 liters of water (60 cm of pressure head) against the gravitational force. Actually, a rising water level could be observed after ending the filling procedure.

After opening the upper ball valve to let water in the pond infiltrate into the soil, pressure monitoring showed four essentially different behaviors. An abrupt rise of pressure at the beginning (marked in gray) indicates that pressure is transmitted through the unsaturated zone to the bottom of the column. Thereupon, pressure is subject to variation, moderate increases are followed by abrubt decreases. At this period of time, with every decrease of pressure, air bubbles rising up were observed. The following phase is characterized by a stagnation of pressure. A constant increase approaching to the applied hydrostatic pressure is not observed until the wetting front has reached the water level of the saturated zone. The applied hydrostatic head remains constant, 3.5 hours after opening the upper ball valve.

In Experiment 2, four samples were taken into copper tubes, according to figure 4.12. Water of the saturated zone was traced with 0.1 mg/l of uranine, water that infiltrated during the preparation of the experiment was traced with 0.1 mg/l of rhodamine. Water, that was filled into the pond after the start of the experiment was additionaly traced with 0.1 mg/l of uranine. The putflowrate was determined to be approximately 37 ml/min.

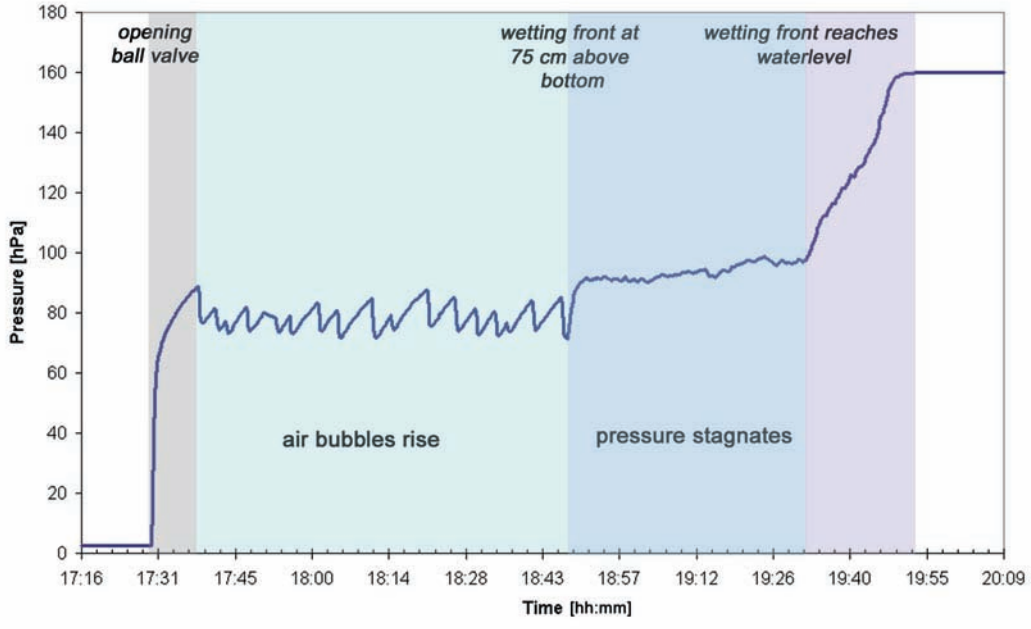


Figure 5.11: Monitoring of hydrostatic pressure during the preparation of the experiment.

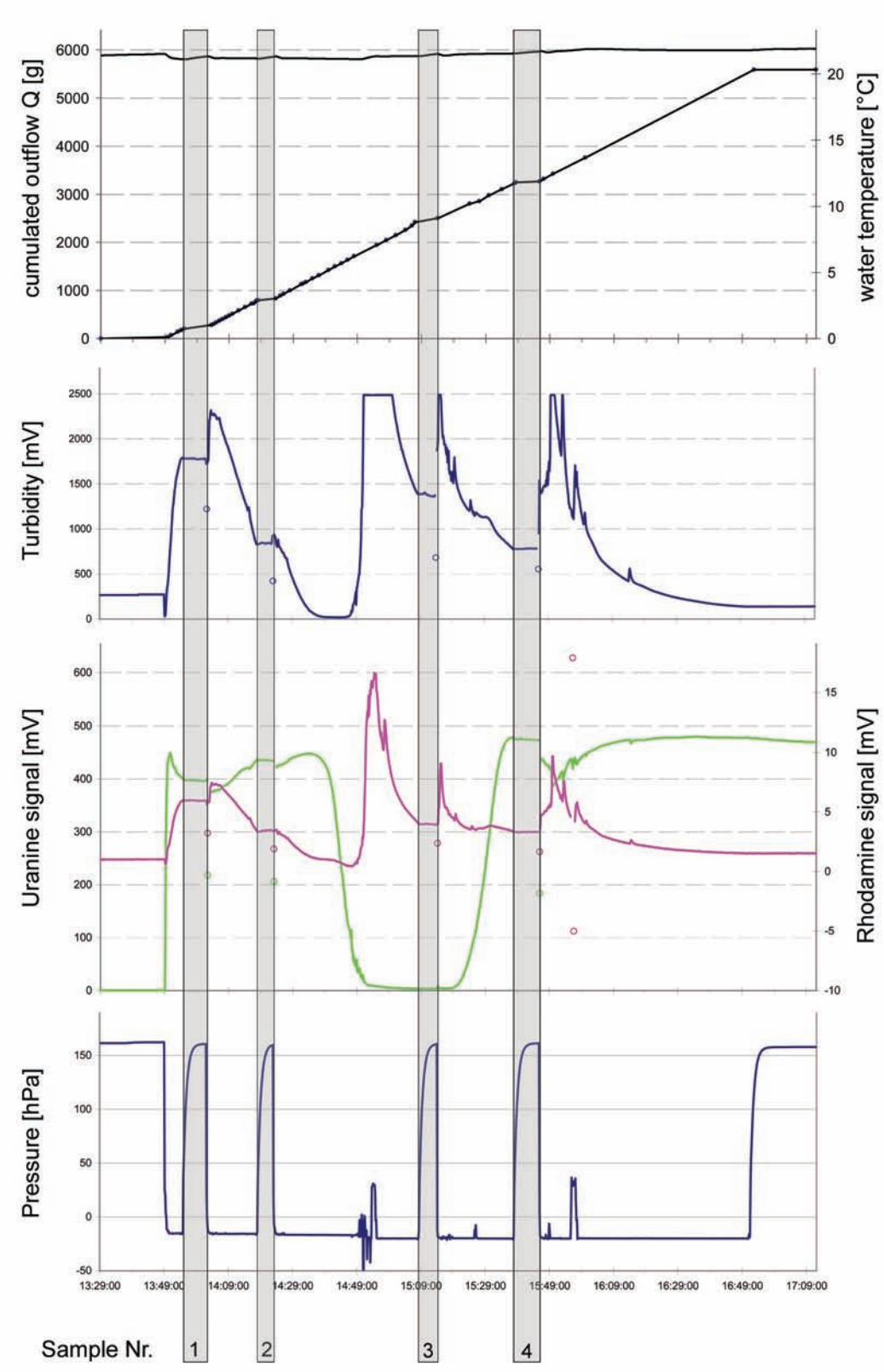


Figure 5.12: Boundary conditions for the ponded condition - 160 cm experiment. The turbidity seems again to develop in agreement with the rhodamine signal. An increase of rhodamine right after start, followed by inconsistant behaviors with several peaks can as well be observed again. The pressure decreases to values below zero, when the lower ball valve is open. Variations of pressure between the sampling times are a result of flushing the tubes at the sampling port.

### 5.4.3 Experiment 3: Ponded Condition - 300 cm

Implementing a total hydrostatic pressure of 300 hPa (200 cm in the pond) to the system, the setup of Experiment 3 was moved to the stairway of IHF. To keep air mass exchange as low as possible, experimental preparations and the sampling were undertaken over night. Additionally, a sample was taken from the air saturated water vessel right after the experimental investigations, to document possible variations of water in equilibrium with air of its new environment.

The air saturated water barrel was directly connected to the upper column with a tube. The advantage of this method was to use the diameter of the barrel, relatively big compared to the diameter of the column, to keep the hydrostatic pressure constant. Despite applying almost a 3-fold pressure head (200 cm in pond compared to 60 cm in pond), the infiltration process took about the same time as in Experiment 2, 3.5 hours respectively. Small complications occurred during the preparation of the experiment. Ascending air bubbles concentrated in the upper column, and did not escape through the tube into the barrel. Therefore, the tube had do be removed several times from the column, to let air escape.

After reaching the applied hydrostatic pressure of 300 hPa, the system was kept untouched for 3 hours, to allow entrapped air in the sand-filled columns to dissolve. Five samples were taken into copper tubes, according to figure 5.13.

Both, infiltrating water and water in the pond were traced with 1 mg/l of rhodamine. The fluorescence tracer curve of rhodamine shows a similar behavior to the preceeding experiments. However peaks seem to be less pronounced, a relatively strong signal could be measured throughout the experiment. The observation of preceeding experiments, that the rhodamine curve increases right after the start of the experiment, with a slight retardation, can be confirmed again. In addition, another tendency becomes apparent. Uranine, whose signal is highly present at the start of the experiment, seems to decrease for a while before increasing again to its maximum, and then having its defenite peak off. The contrary comportment of the rhodamine time-variation curve is most pronounced for the experiment Nr. 3, and indicates, that mixing of water occured within the saturated zone.

The monitored pressure at the bottom of the column, shows the same behavior as in Experiment 2. Values switch abruptly from high pressure, when the lower ball valve is closed, to low pressure, when the lower valve is opened. The rather slow increase of pressure for the inverse operation, can be explained by the sampling procedure. Copper tubes are fused inside the sampler by screwing the clamps, and as a consequence of, flow process is stopped relative slowly. Unlike Experiment 2, low pressure values in Experiment 3 show positive values of approximately 20 hPa. This difference could be associated with the cumulated outflow rate, which also differs.

In Experiment 3, an outflow rate of approximately 57 ml/min was observed. This outflow rate exceeds the outflow rate of Experiment 2 by 20 ml/min, and the outflow rate of Experiment 1 by 35 ml/min. Pressure values around 20 hPa in the running system determine the soil to drain not fast enough, compared to the amount of water, forced to infiltrate by a high hydrostatic head.

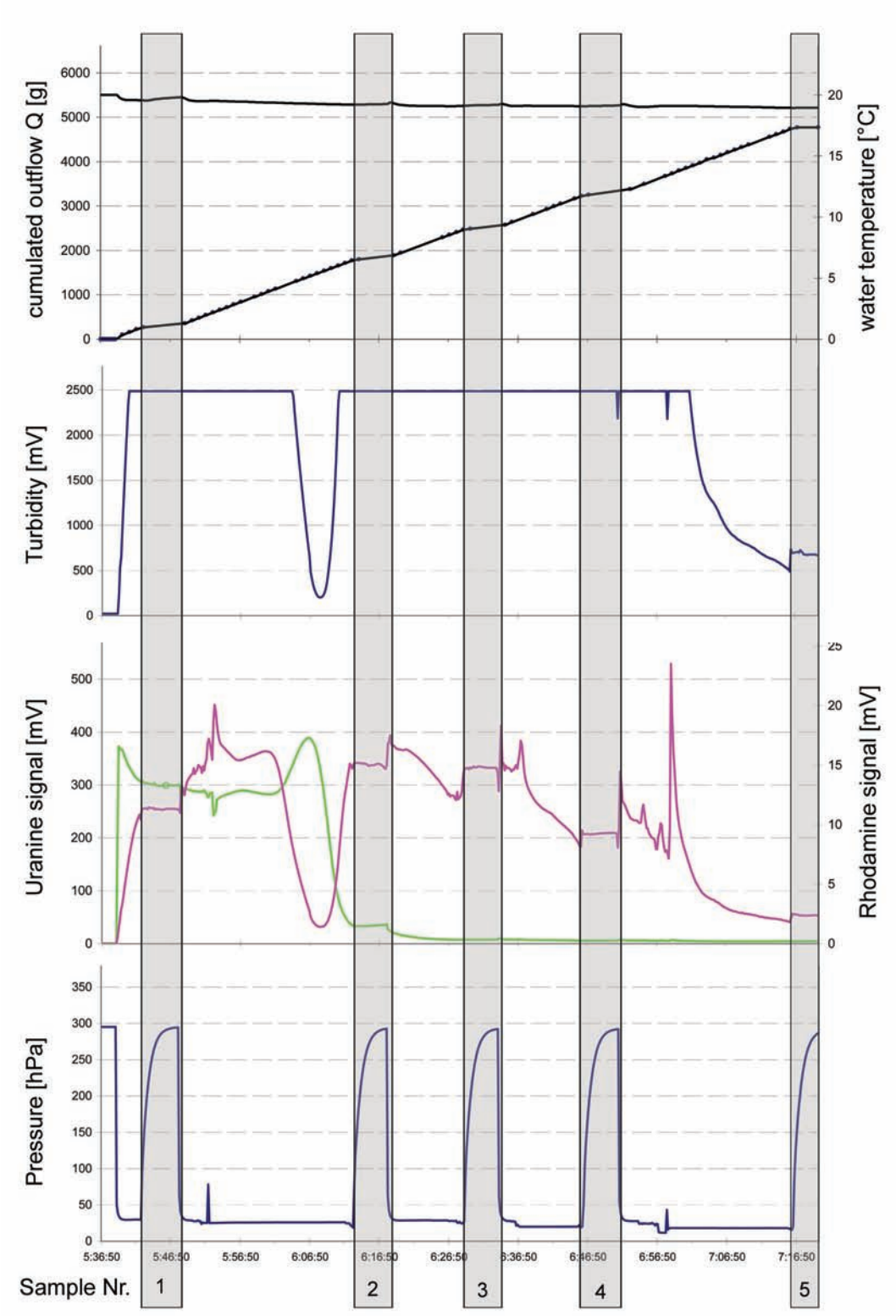


Figure 5.13: Boundary conditions for the ponded condition - 300 cm experiment. The rhodamine curve shows a more constant development compared to the preceding experiments. The time-variation curve indicates that rhodamine is already occuring in the saturated zone of the columns, where only uranine is expected. Online monitored pressure shows values of approximately 20 hPa, when the sytem is running. When fusing the copper tubes, pressure increases up to its originally set value of 160 hPa. Irregularities during low pressure records are a cause flushing tubes at the sampling port.

## 5.5 Noble Gas Analyses

All together, fourteen samples of water were sealed off into copper tubes, and analyzed for dissolved He, Ne, Ar, Kr, and Xe, at the Edelgas-MS Laboratory of IUP, Heidelberg. In addition, one sample of noble gas concentrations in the laboratory air was as well analyzed at IUP, to verify that the noble gas abundance corresponds to atmospheric composition. The accuracy of measurements is ±1% for Ne and Ar, and ±2% for He, Kr and Xe.

Air temperature and water temperature were constantly monitored, the atmospheric pressure during experimental investigations is given by the elevation of IHF, 278 m a.s.l.

First results of noble gas analyses were obtained on Saturday, April 15th for the ponded condition - 160 cm experiment. Figure 5.14 a) to e) shows the concentrations of measured noble gases, corrected to standard temperature and pressure (STP), 20 °C and 1 atm respectively. Figure 5.14 f) compares the amount of supersaturation, expressed in (%), of all noble gases measured in the experiment.

Noble gas concentrations of all samples (except He in sample Nr. 4) show a supersaturation, relative to air saturated water. Consequently, excess air in water could successfully be simultaed for Experiment 2.

Noble gases with low solubility, He and Ne respectively, show a constant decrease in concentrations with time. However, concentrations of sample Nr. 3 and sample Nr. 4 differ less, relative to samples taken at the beginning of the experiment. Sample Nr. 3 was clearly determined to steam from water of the unsaturated zone, and therefore being exposed to a hydrostatic head for the time of preparing the experiment. Sample Nr. 4 is as well clearly determined by fluorescence tracer signals, and steams from water, filled into the pond after the start of the experiment.

Noble gases with low solubility, Kr and Xe respectively have the lowest concentrations in sample Nr. 2 (saturated zone), peak in sample Nr.3 (unsaturated zone), and decrease again in sample Nr. 4 (water in pond).

Finally, Ar, which has an intermediate solubility relative to other noble gases, has decreasing concentrations in sample Nr. 2, and then constantly increases.

From this observations follows that He and Ne have the highest supersaturation in water from the staurated zone, Kr and Xe have the highest supersaturation in water from the unsaturated zone, and Ar has the highest supersaturation in water steaming from the pond.

To make a statement, the concentrations of two noble gases are compared to each other in Figure 5.15 and 5.16. In addition, the initial water in equilibrium for different temperatures, as well as changes in noble gas pattern, induced by additional pressure or dissolved air, is calculated and plotted into the same chart. An additional pressure of 0.01 atm (equal to 10.1325 hPa) affects noble gas concentrations by 1.08 %. Additional dissolved air affects concentrations by 1.24% per $10^{-4}$ $cm^3$ STP/g for He, 1.04% per $10^{-4}$ $cm^3$ STP/g for Ne, and 0.32% per $10^{-4}$ $cm^3$ STP/g (Holocher, J. et al. 2002).

The results distinguish two groups of samples. One group with relatively high Ne, He supersaturations consists of sample Nr. 1 and sample Nr. 2, from the saturated zone at the bottom of the column respectively. The other group containing sample Nr. 3 and sample

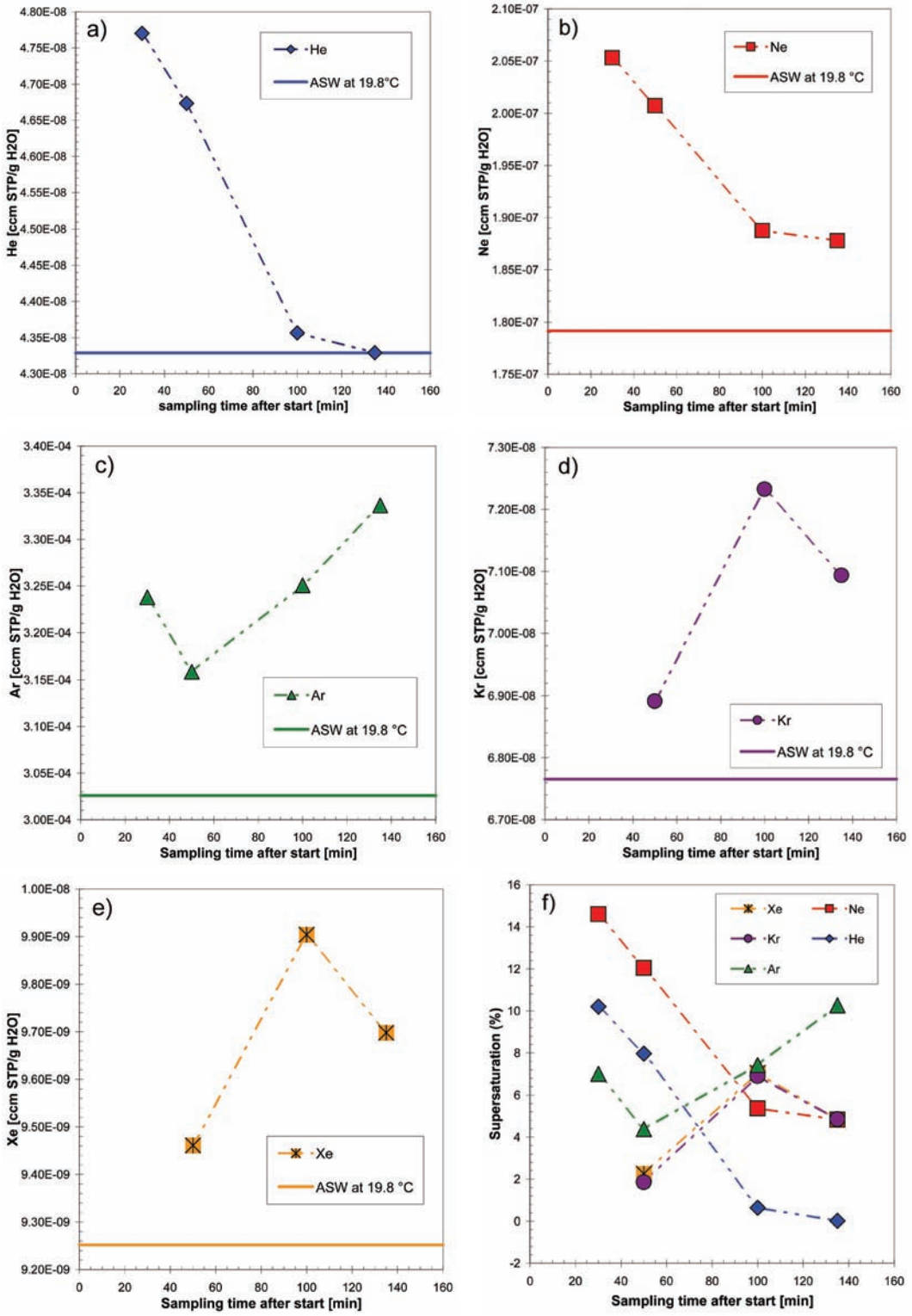


Figure 5.14: Noble gas concentrations ($cm^3$ STP/g $H_2O$) for the four samples taken from the ponded condition - 160 cm experiment. Figures a) to e) show the development of noble gas concentrations He, Ne, Ar, Kr and Xe with regard to air saturated water (ASW) at 19.8 °C, corresponding to the water used in Experiment 3. Figure f) shows the amount of supersaturation with ranges from 4.8% to 14.6% ΔNe. He and Ne concentrations decrease with time, Kr and Xe have a minimum of supersaturation in water from sample Nr. 2 and a peak in water from sample Nr. 3 (no values available for Kr, Xe concentrations in sample Nr.1). Ar has its minimum concentration in sample Nr. 2, and the highest Δ-value in the last sample, Nr. 4.

Nr. 4 shows significantly lower supersaturations of He and Ne. A high amount of excess air can therefore be found in water from the saturated zone. This water was exposed to the highest hydrostatic pressure for the longest time. Consequently, entrapped air was additionally dissolved under a high hydrostatic head, within the saturated zone.

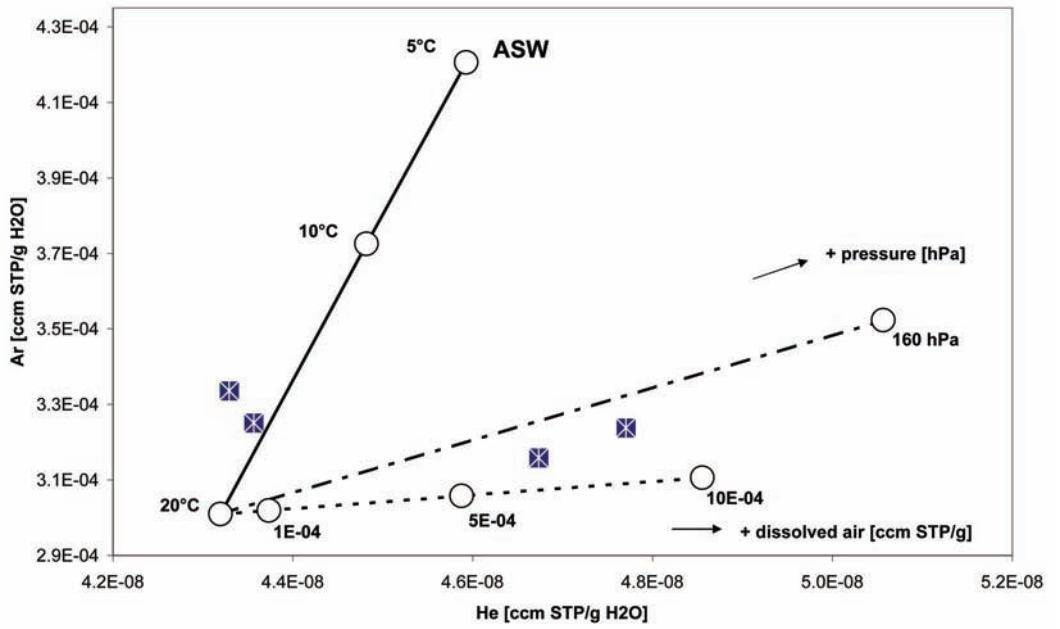


Figure 5.15: Measured He versus Ar concentrations for the ponded condition - 160 cm experiment. Water in equilibrium with air, depending on temperature (ASW) is plotted on the solid line. Changes in noble gas patterns, induced by additional pressure or additional dissolved air for ASW at 20°C are shown on dashed lines.

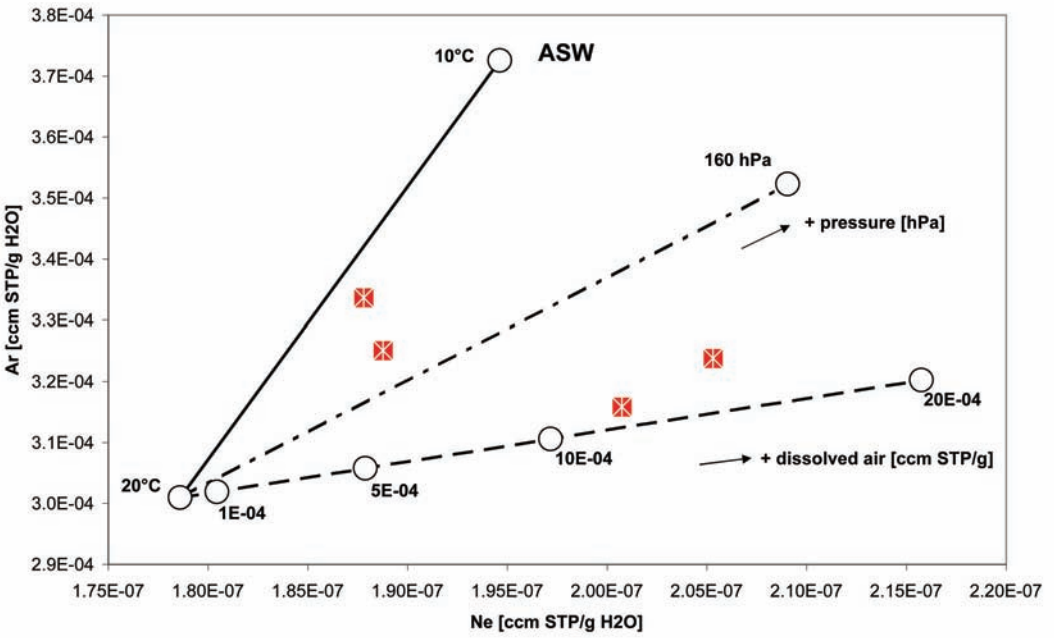


Figure 5.16: Measured Ne versus Ar concentrations for the ponded condition - 160 cm experiment. Water in equilibrium with air, depending on temperature (ASW) is plotted on the solid line. Changes in noble gas patterns, induced by additional pressure or additional dissolved air for ASW at 20°C are shown on dashed lines.

## 5.6 Conclusions

Experimental investigations on the behavior of gaseous components in water could successfully simulate the formation of excess air. Almost all samples, that have been analyzed so far show concentrations higher than water in equilibrium with air. The amount of supersaturation ranges from 4.8% to 14.6% ΔNe. A high supersaturation of water could be found in samples taken out of the saturated zone at the bottom of the column. However, no water from Experiment 2 seems to show water in equilibrium with air for the additionally applied hydrostatic pressure of 160 hPa. The fact, that sample Nr. 4 shows no relative ΔHe excess, remains remarkable as well, regarding that water from that sample has moved under the same pressure conditions to the bottom of the column.

The fact that dissolution of entrapped air has occured within the saturated zone of the column can be explained by observations, made during the experimental investigations. Monitored pressure during the preparation of the experiment has shown, that water filled into the column to raise a groundwater level to 60 cm above the bottom, has not imposed the expected hydrostatic pressure of 60 hPa. Together with the observation, that the water level was still rising after filling the column and closing the lower valve, this zone can rather be determined quasi-saturated, showing characteristics of capillary fringe above the water table of aquifers, for instance.

Fluorescence tracer signals circumstantiate the assumption mentioned above. Probable rhodamine signals in water flowing out of the column at the start of the experiment, indicate, that water traced with uranine has filled pores with small diameter and higher suction. Water traced with rhodamine could therefore percolate into the lower cloumn, filling pores of bigger diameters and lower suction. A relatively high amount of entrapped air within the quasi-saturated zone is therefore likely to occur. To validate this observation and assumption, further investigation, for instance on the interaction of rhodamine signals and turbidity signals, are suggested.

A final determination of relevant processes contributing to the formation of excess air, is not feasible at the present state of investigations. Results of the irrigation experiment, as well as results of the ponded condition - 300 cm experiment need to be evaluated and compared to the results within this work. Nevertheless, further analyses might contribute to a better understanding of the impact of groundwater recharge processes on gaseous components in water.

# 6 Discussion

Dissolved gases in groundwater, more precisely the inert noble gases as well as CFCs and $SF_6$, seem to be applicable and reveal useful information for investigations in catchment hydrology.

The measurements of CFCs and $SF_6$ concentrations in groundwater from different aquifers within the Rio Andarax basin have demonstrated that a determination of mean residence times in groundwater bodies is possible, with a relatively high precision, compared to a one-time sampling of $^3H$. However, the recently peaking atmospheric mixing ratios of CFCs show that determination of apparent ages in young groundwaters is afflicted with uncertainties. Boundary conditions, such as temperature of water at the time of recharge, elevation of recharge and amount of excess air, therefore have to be determined with high accuracy in order to achieve good results. $SF_6$, which is considered to offer an alternative to CFCs for dating of young groundwater did not give reliable results for all the samples. Though its atmospheric mixing ratios are constantly increasing, the estimation of residence times with $SF_6$ relies on major uncertainties, such as natural occurance as well as a high sensitivity to excess air.

It is therefore suggested to measure all CFCs and $SF_6$ in order to better interpret dinstinct behaviors and obtain objective results. Actually, the comparison of all measured gases reveals even further information on dominant processes in aquifers. That way, the potential presence of high excess air concentrations could be shown for some samples, and as a consequence, the accuracy of modeled apparent age of these sample can be discussed in the evalutaion of measurements. In addition, the comparison of CFCs among each other has revealed potential anaerobic environments within some aquifers, which could for instance determine them to be of confined character. Finally, the application of mass transport models has indicated potential recharge processes, such as exponential mixing of waters in aquifers beside the river (direct recharge), and focused recharge in aquifers below the river bed of Rio Andarax (indirect recharge). However, these suggestions have to be verified by further investigations in order to consider CFCs and $SF_6$ measurements as tracing methods for the processes mentioned above.

A distinct excess air pattern in samples from Rio Andarx basin, derived from the sensitive measurements of $SF_6$ could not be detected, regarding the fact that some samples showed a potential of high excess air concentrations, however, other samples below the river bed of Rio Andarax did not. But the existence of excess air and distinct concentration patterns, can definitely only be detected by the measurements of noble gas concentrations. It is therefore suggested to investigate noble gas patterns in samples from the same wells and boreholes in order to verify the field observations dealed within this work and confirm the belief of higher excess air concentrations below the river bed of Rio Andarax.

To our knowledge, the simulation of direct and indirect recharge processes in laboratory columns and the impact of these processes on noble gas patterns was for the first time conducted under defined, variable hydrostatic pressures. Excess air could successfully be generated and the first results are promising. High noble gas concentrations in the first two samples indicate a major impact of hydrostatic pressure on excess air. It can be seen from observations during the experiments that the effective hydrostatic pressure does not

necessarily correspond to the applied hydrostatic head. Hydrostatic pressure was observed to rise even by transmisson through air within the unsaturated zone of the columns. Little hydrostatic pressure was observed whenever the lower valve was open, resulting in small supersaturation of water from samples taken at the end of Experiment 2. These observations might not be reflected in nature and show a potential discrepancy between nature and laboratory. Nevertheless, the assumed influence of hydrostatic pressure on the formation of excess air has probably been laboratory-confirmed. In further steps, results of all experiments need to be compared among each other. In order to derive distinct excess air patterns (complete or partial dissolution) for direct and indirect recharge processes, measured concentrations of all noble gases need to be modeled according to the methods presented in chapter 2.

In conclusion one can say that this work has shown the importance of integrating conventional hydrologic methods in the use of gases as environmental tracers. Gained information from insitu parameters and water chemistry as well as supporting data from Tritium and stable isotopes $^{18}O$ and $^{2}H$ remain crucial to reliably interpret CFCs, SF6 and noble gas measurements. In addition, field investigations on catchment boundaries, potential recharge areas, geological and hydrogeological units, etc., as well as construction properties of the sampled wells and boreholes avoid a misinterpretation.

I would like to end the discussion, recommending further investigations on the necessarily challenging and auspicious impact of hydrological processes on gaseous components in groundwater. Measurements of noble gases in the study site, or laboratory investigations including measurment of $SF_6$ would be options to link investigations done within this work and to enhance knowledge.

## References

Aeschbach-Hertig, W.; Peters, F.; Beyerle, U.; Kipfer, R. (1999): Interpretation of dissolved atmospheric noble gases in natural waters. Water Resources Research, Vol. 35(9), pp. 2779-2792.

Aeschbach-Hertig, W.; Peters, F.; Beyerle, U.; Kipfer, R. (2000): Palaeotemperature reconstruction from noble gases in ground water taking into account equilibration with entrapped air. Nature 405, pp. 1040 - 1044.

Aeschbach-Hertig, W. (2004): Excess air in groundwater: problems and opportunities. Presentation at: GSA, Denver, 2004, special session: Dissolved gases as indicators of geochemical and hydrogeologic processes.

Anza, S.; Dongarrà, G.; Giammanco, S.; Gottini, V.; Hauser, S.; Valenza, M. (1989): Geochimica dei fluidi dell‘ Etna: le acque sotterranee. Miner. Petrogr. Acta, Vol. XXXII, pp. 231-251.

Alvargonzales, D. (1967): Mapa Geologico de la Provincia de Almeria formado por el ingeniero de minas. Instituto Geologico y Minero de Espana.

Benson, B. B.; Krause Jr, D. (1976): Empirical laws for dilute aqueous solutions of nonpolar gases. The Journal of Chemical Physics - January 15, 1976 - Volume 64, Issue 2, pp. 689-709.

Bernini, M.; Boccaletti, M.; Gelati, R.; Moratti, G.; Papani, G.; Tortorici, L. (1990): Geological-Structural Map of Ugijar and Canjayar Basins, Betic Cordillera. S. EL. CA., Florence.

Beyerle, U.; Aeschbach-Hertig, W.; Hofer, M.; Imboden, D. M.; Baur, H.; Kipfer, R. (1999): Infiltration of river water to a shallow aquifer investigated with 3H/3He, noble gases and CFCs. Journal of Hydrology, 220, pp. 169-185.

Busenberg, E.; Plummer, L. N. (2005): CFC-2005-2a. USGS spreadsheet program for preliminary evaluation of CFC data. In: IAEA Guidebook on the Use of Chlorofluorocarbons in Hydrology. International Atomic Energy Agency, Vienna, in press.

Busenberg, E.; Plummer, L. N. (1992): Use of chlorofluorocarbons (CCl3F and CCl2F2) as hydrologic tracers and age-dating tools: The alluvium and terrace system of central Oklahoma. Water Resour. Res. 28: 2257-2284.

Busenberg, E.; Plummer, L. N. (2000): Dating young groundwater with sulfur hexafluoride: Natural and anthropogenic sources of sulfur hexafluoride. Water. Res. Res., Vol 36(10), pp. 3011-3030.

Deipser, A.; Stegmann, R. (1997): Biological degradation of VCCs and CFCs under simulated anaerobic landfill conditions in laboratory test digesters. Environ. Sci. Pollut. Res. Int. 4(4), pp. 209-216.

Faybishenko, B. A. (1995): Hydraulic behavior of quasi-saturated soils in the presence of entrapped air: Laboratory experiments. Water Resources Research, Vol. 31(10), pp. 2421-2435.

Geller, L. S.; Elkins, J. W.; Lobert, J. M.; Clarke, A. D.; Hurst, D. F.; Buttler, J. H.; Meyers, R. C. (1997): Tropospheric SF6: Observed latitudinal distribution and trends, derived emissions and interhemispheric exchange time. Geophys. Res. Lett. 44(6), pp. 675-678.

Harnish, J.; Eisenhauer, A. (1998): Natural CF4 and SF6 on Earth. Geophysical Research Letters, Vol 25, No. 13, 1998, pp 2401–2404.

Heaton, T. H. E.; Vogel, J. C. (1981): „Excess air“ in groundwater. J. Hydrol. 50, pp. 201-216.

Holocher, J.; Peeters, F.; Aeschbach-Hertig, W.; Hofer, M.; Brennwald, M.; Kinzelbach, W.; Kipfer, R. (2002): Experimental Investigations on the formation of excess air in quasi-saturated porous media. Geochimica et Cosmochimica Acta, Vol. 66, No. 23, pp. 4103-4117.

IAEA/WMO, (2004): Global Network for Isotopes in Precipitation. The GNIP Database. Accessible at http://isohis.iaea.org.

IGME-IRYDA , (1977): Estudio hidrogelógico de la Cuenca Sur-Almeria. Informe Técnico n° IV. Plan Nacional de Investigatión de Aguas subterráneas, 7. vol.

Katz, B. G.; Lee, T. M.; Plummer, L. N.; Busenberg, E. (1995): Chemical evolution of groundwater near a sinkhole lake, nothern Florida. Fow patterns, age of groudwater, and influence of lakewater leakage. Water Resources Research, Vol. 31(6), pp. 1549-1564.

Lázaro, R.; Rodrigo, F. S.; Gutiérrez, L.; Domingo, F.; Puigdefábregas, J. (2001): Analysis of a 30-year rainfall record (1967–1997) in semi–arid SE Spain for implications on vegetation. Journal of Arid Environments, 48, pp. 373-395.

Leibundgut, Ch.; Demuth, S. (Eds) (1997): Grundwasserneubildung. Beiträge zum Workshop «Grundwasserneubildung» im Rahmen des neuen Hydrologischen Atlasses von Deutschland (Oktober 1996). Freiburger Schriften zur Hydrologie, Bd. 5, Freiburg i. Br., 121 S.

Massman, J.; Butchart, C. (2001): Infiltration characteristics, performance and design of storm water facilities. Washington State Transportation Center, VSA.

Mazor, E. (1972): Palaeotemperatures and other hydrological parameters deduced from gases dissolved in groundwaters, Jordan Rift Valley, Israel. Geochimica Cosmochimica Acta 36, pp. 1321-1336.

Mazor, E. (2004): Chemical and isotopic groundwater hydrology, third edition. Marcel Dekker, Inc, New York.

Mochalski, P. (2002): Chromatographic measurement of permanent gases in water. Report No 1906/Ch, Institute of Nuclear Physics, Kraków.

Oster, H. (1994): Datierung von Grundwasser mittels FCKW: Voraussetzungen, Möglichkeiten und Grenzen. Inaugural-Dissertation, University of Heidelberg.

Ozima, M.; Podosek, F. A. (1983): Noble Gas Geochemistry. Cambridge University Press, New York, 367p.

Peeters, F.; Beyerle, U.; Aeschbach-Hertig, W.; Holocher, J.; Brennwald, M. S.; Kipfer, R. (2002): Improving noble gas based paleoclimate reconstruction and groundwater dating using 20Ne/22Ne ratios. Geochim. et Cosmochim. Acta, Vol. 67, No 4, pp. 587-600.

Plummer, L. N.; McConnell, J. B.; Busenberg, E.; Drenkard, S.; Schlosser, P.; Michel, R.L. (1998): Flow of river water into a karstic limestone aquifer. Tracing the young fraction in groundwater mixtures in the Upper Floridan aquifer near Valdosta, Georgia. Apll. Geochem. 13(8), pp. 1017-1043.

Plummer, L. N.; Busenberg, E. (2000): Chlorofluorocarbons. In: Environmental tracers in subsurface hydrology. Cook P, Herczeg AL (ed) Kluwer Academic Publishers, Boston, pp. 441-478.

Price, R. M.; Top, Z.; Happell, J. D.; Swart, P. K. (2003): Use of tritium and helium to define groundwater flow conditions in Everglades National Park. Water Resources Research, Vol. 39, No. 9, 1267p.

Rawls, W. J.; Brakensiek, D. L. (1983): A Procedure to Predict Green Ampt Infiltration Parameters. Adv. Infiltration, Am. Soc. Agric. Eng., pp. 102-112.

Solomon, D. K.; Hunt, A.; Poreda, R. J. (1996): Source of radiogenic helium 4 in shallow aquifers: Implications for dating young groundwater. Water Resources Research, Vol. 32, No. 6, pp. 1805-1813.

Solomon, D. K.; Cook, P. G.; Sanford, W. E, (1998): Dissolved gases in subsurface hydrology. In: Isotope tracers in catchment hydrology. Kendall, C.; McDonnell, J. J. (ed), Elsevier, New York, Chapter 9.

Stute, M.; Schlosser, P. (1993): Principlesand applications of the noble gas paleothermometer. In: Climate Change in Continental Isotopic Records, (ed. P. K. Swart, K. C. Lohmann, J. McKenzie, and S. Savin) Vol. 78, pp. 89-100. American Geophysical Union.

Stute, M.; Talma, A. S. (1998): Glacial temperatures and moisture transport regimes reconstructed from noble gases and delta 18O, Stampriet aquifer, Namibia. In: Isotope techniques in the study of environmental change, edited by IAEA, Vienna, pp. 307-318.

UNEP, (1987): Montreal Protocol to reduce substances that deplete the ozone layer. Final report, UNEP, 1987.

Vandenschrick, G.; van Wesemael, B.; Frot, E.; Pulido-Bosch, A.; Molina, L.; Stiévenard, M.; Souchez, R. (2002): Using stable isotope analysis ( D – 18O) to characterize the regional hydrology of the Sierra de Gador, south east Spain. Journal of Hydrology, 265, pp. 43-55.

Volk, C. M.; Elkins, J. W.; Fahey D. W.; Dutton, G. S.; Gilligan, J. M.; Loewenstein, M.; Podolske, J. R.; Chan, K. R.; Gunson, M. R. (1997): Evaluation of source gas lifetimes from stratospheric observations. J. Geophys. Res. - Atmos. 102(D21), pp. 25543-25564.

Ward, J. (1963): Hierarchical grouping to optimize an objective function. J. American Stat. Assoc., 58: 236-245.

Weiss, R.F. (1971): Solubility of Helium and Neon in Water and Seawater. J. Chem. Eng. Data, 16(2), pp. 235-241.

Weiss, R. F. (1970): The solubility of nitrogen, oxygen, and argon in water and seawater. Deep-Sea Research, v. 17, pp. 721-735.

Zukowskyj, P.; Alexander, R.; Teeuw, R.; Faulkner, H.; Sullivan, M.; Ruiz, J. L. (2004): Changing vegetation density and a comparison with agricultural clearances in Sorbas, south east Spain. ARSF Workshops, Natural Environment Research Council.

URL 1: http://water.usgs.gov/lab/clorofluorocarbons/lab/assigning_age/, 9.2.2006

URL 2: http://water.usgs.gov/lab/sf6/sampling/, 13.2.2006

URL 3: http://water.usgs.gov/lab/software/air_curve/, 27.1.2006

# Annex

Table A1: Sampling Locations 20 - 22 Sep. 2005

| Sample | Grad N | Grad W | Altitude [m] | Name/Specification |
|---|---|---|---|---|
| W-001 | 36.5778 | 2.3024 | 159 | Piezometer Andarax (Alluvium) |
| W-002 | 36.5845 | 2.3127 | 200 | Andarax pumping station (Deep aquifer, no clear geological assignment) |
| W-003 | 36.5907 | 2.3668 | 286 | Irrigation well in the valley, Benatrique (Dolomite) |
| W-004 | 36.5930 | 2.3683 | 319 | Irrigation well beside the valley (Marl) |
| W-005 | 36.5920 | 2.5107 | 779 | River Andarax stream sample |
| W-006 | 36.5759 | 2.3646 | 531 | Sierra Gador Pump (Dolomite) |
| W-007 | 36.5759 | 2.3646 | 531 | Sierra Gador (behing the bifurcation) (Dolomite) |
| W-008 | 36.5752 | 2.3639 | 543 | Sierra Gador (before the bifurcation) (Dolomite) |
| W-009 | 37.0503 | 2.2325 | 497 | Irrigation well, Tabernas |
| W-010 | 37.0545 | 2.2357 | 511 | Spring, Tabernas |
| W-011 | 37.0829 | 2.2531 | 657 | Well on terraces at end of the valley, Tabernas |
| W-012 | 37.0551 | 2.1481 | 551 | Pumping station (probably molasse aquifer) |
| W-013 | 36.5766 | 2.3017 | 176 | Irrigation well, Andarax stream, deep, Gador |
| W-014 | 36.5765 | 2.2948 | 162 | Irrigation well, Andarax terrace, shallow, Gador |

Table A2: Insitu Parameters 20 - 22 Sep. 2005

| Sample | Date | Time [hr:min] | Electric conductivity [µs/cm] | Temperature [°C] | pH |
|---|---|---|---|---|---|
| W-001 | 20.9.2005 | 20:00 | 1272 | 17.5 | 7.4 |
| W-002 | 21.9.2005 | 09:25 | 1432 | 24.0 | 7.4 |
| W-003 | 21.9.2005 | 16:00 | 947 | 28.0 | 7.8 |
| W-004 | 21.9.2005 | 17:30 | 2290 | 22.5 | 7.7 |
| W-005 | 21.9.2005 | 20:00 | 693 | 17.5 | 8.1 |
| W-006 | 22.9.2006 | 09:00 | 889 | 28.6 | 7.5 |
| W-007 | 22.9.2006 | 09:00 | 878 | 28.9 | 8.0 |
| W-008 | 22.9.2006 | 09:30 | 892 | 29.2 | 7.8 |
| W-009 | 22.9.2006 | 14:30 | 1455 | -999 | 7.2 |
| W-010 | 22.9.2006 | 15:00 | 830 | 22.0 | 8.1 |
| W-011 | 22.9.2006 | 15:30 | 973 | 21.7 | 7.4 |
| W-012 | 22.9.2006 | 17:00 | 1938 | 29.9 | 7.9 |
| W-013 | 22.9.2006 | 18:00 | 1335 | 19.0 | 7.4 |
| W-014 | 22.9.2006 | 19:00 | 1724 | 17.6 | 7.3 |

Table A3: Major Ions 20 - 22 Sep. 2005

| Sample | HCO3 [mg/l] | Cl [mg/l] | SO4 [mg/l] | NO3 [mg/l] | Na [mg/l] | K [mg/l] | Mg [mg/l] | Ca [mg/l] |
|---|---|---|---|---|---|---|---|---|
| W-001 | 364.7 | 69.5 | 387.9 | 16.4 | 66.6 | 6.1 | 63.4 | 158.3 |
| W-002 | 400.6 | 106.6 | 414.4 | 8.7 | 137.3 | 4.4 | 56.9 | 151.3 |
| W-003 | 440.3 | 9.9 | 255.5 | 0.0 | 13.3 | 3.6 | 64.9 | 138.3 |
| W-004 | 508.3 | 89.8 | 1086.9 | 32.8 | 96.9 | 7.8 | 170.5 | 305.7 |
| W-005 | 308.6 | 11.2 | 104.9 | 13.2 | 15.3 | 2.3 | 33.8 | 82.4 |
| W-006 | 478.5 | 8.8 | 227.4 | 0.0 | 11.7 | 3.3 | 58.6 | 150.2 |
| W-009 | 659.3 | 124.7 | 148.7 | 3.0 | 250.8 | 4.8 | 36.6 | 70.1 |
| W-010 | 366.1 | 62.4 | 157.4 | 7.3 | 112.2 | 2.3 | 34.3 | 66.9 |
| W-011 | 417.9 | 66.3 | 169.3 | 7.5 | 131.3 | 4.4 | 38.4 | 67.7 |
| W-012 | 688.3 | 305.3 | 104.4 | 0.0 | 471.0 | 13.5 | 9.7 | 15.7 |
| W-013 | 453.7 | 85.4 | 441.0 | 19.5 | 79.8 | 5.3 | 76.5 | 185.6 |
| W-014 | 555.0 | 116.0 | 590.7 | 29.6 | 96.7 | 7.3 | 111.4 | 226.4 |

Table A4: Stable Isotopes and Tritium 20 - 22 Sep. 2005

| Sample | $\Delta\ ^{18}O$ [‰] | $\Delta\ ^{2}H$ [‰] | $^{3}H$ [TU] | err. |
|---|---|---|---|---|
| W-001 | -8.33 | -54.9 | 3.8 | ±0.4 |
| W-002 | -8.33 | -53.7 | < 0.6 | |
| W-003 | -8.32 | -55.5 | 0.9 | ±0.4 |
| W-004 | -7.88 | -52.5 | 3.6 | ±0.5 |
| W-005 | -8.82 | -57.7 | | |
| W-006 | -8.53 | -54.6 | < 0.6 | ±0.6 |
| W-007 | -8.46 | -54.8 | | |
| W-008 | -8.56 | -54.3 | | |
| W-009 | -8.52 | -55.6 | 2.5 | ±0.6 |
| W-010 | -8.23 | -52.4 | 4.1 | ±0.4 |
| W-011 | -8.16 | -53.1 | 3.2 | ±0.5 |
| W-012 | -7.60 | -49.4 | < 0.6 | |
| W-013 | -8.40 | -53.6 | 3.3 | ±0.4 |
| W-014 | -8.24 | -53.0 | 4.3 | ±0.7 |

Table A5: Stable Isotopes 10 Nov. 2005 - 13 Jan. 2006

| Sample | Date | δ 18O [‰] | δ 2H [‰] |
|---|---|---|---|
| | | | |
| W-013 | 10.11.2005 | -8.37 | -54.21 |
| | 13.12.2005 | -8.42 | -55.28 |
| | | | |
| W-014a | 09.11.2005 | -8.18 | -51.67 |
| | 02.12.2005 | -8.22 | -52.60 |
| | 13.12.2005 | -8.14 | -52.64 |
| | 13.01.2006 | -8.06 | -51.49 |
| | | | |
| W-005a | 10.11.2005 | -8.53 | -54.90 |
| | 02.12.2005 | -8.64 | -55.60 |
| | 13.12.2005 | -8.60 | -55.86 |
| | 13.01.2006 | -8.78 | -56.74 |
| | | | |
| W-001 | 02.12.2005 | -8.46 | -54.80 |
| | 13.12.2005 | -8.42 | -53.52 |
| | 13.01.2006 | -8.78 | -56.94 |
| | | | |
| W-016 | 10.11.2005 | -8.23 | -52.52 |
| | 02.12.2005 | -8.46 | -54.30 |
| | 13.12.2005 | -8.38 | -53.78 |
| | 13.01.2006 | -8.56 | -55.85 |

Table A6: CFCs and SF6 20 - 22 Sep. 2005

| Sample | CFC-11 [pmol/l] | | CFC-12 [pmol/l] | | CFC-113 [pmol/l] | | $SF_6$ [fmol/l] | |
|---|---|---|---|---|---|---|---|---|
| W-001 | 5.80 | ±0.60 | 2.20 | ±0.20 | 0.39 | ±0.05 | 1.90 | ±0.20 |
| W-002 | | | | | | | | |
| W-003 | 2.30 | ±0.30 | 1.40 | ±0.10 | 0.22 | ±0.05 | 2.1 | ±0.30 |
| W-004 | 3.70 | ±0.40 | 1.90 | ±0.10 | 0.32 | ±0.05 | 1.3 | ±0.20 |
| W-005 | | | | | | | | |
| W-006 | 1.80 | ±0.20 | 1.10 | ±0.10 | 0.18 | ±0.05 | 1.0 | ±0.10 |
| W-007 | | | | | | | | |
| W-008 | | | | | | | | |
| W-009 | 2.20 | ±0.30 | 1.10 | ±0.10 | 0.15 | ±0.05 | 0.40 | ±0.10 |
| W-010 | | | | | | | | |
| W-011 | 1.80 | ±0.20 | 1.20 | ±0.10 | 0.20 | ±0.05 | 1.00 | ±0.10 |
| W-012 | 0.50 | ±0.10 | 0.19 | ±0.05 | 0.03 | ±0.05 | 0.10 | ±0.10 |
| W-013 | 5.10 | ±0.60 | 2.10 | ±0.20 | 0.31 | ±0.05 | 1.0 | ±0.10 |
| W-014 | 6.80 | ±0.70 | 2.00 | ±0.20 | 0.34 | ±0.05 | 1.1 | ±0.10 |

Table A7: Noble gases 6 - 8 Mar 2006

Measured Concentrations for Experiment 2: Ponded Conditions - 160 cm

| Sample number | He (ccSTP/g) | Ne (ccSTP/g) | Ar (ccSTP/g) | Kr (ccSTP/g) | Xe (ccSTP/g) |
|---|---|---|---|---|---|
| Sample Nr.4 | 4.329E-08 | 1.878E-07 | 3.336E-04 | 7.094E-08 | 9.698E-09 |
| Sample Nr.3 | 4.356E-08 | 1.888E-07 | 3.251E-04 | 7.233E-08 | 9.904E-09 |
| Sample Nr.2 | 4.673E-08 | 2.007E-07 | 3.158E-04 | 6.891E-08 | 9.461E-09 |
| Sample Nr.1 | 4.770E-08 | 2.053E-07 | 3.238E-04 | - | - |

Relative excess Δ noble gas for Experiment 2: Ponded Conditions - 160 cm

| Sample number | Δ He (%) | Δ Ne (%) | Δ Ar (%) | Δ Kr (%) | Δ Xe (%) |
|---|---|---|---|---|---|
| Sample Nr.4 | 0.01 | 4.82 | 10.26 | 4.85 | 4.82 |
| Sample Nr.3 | 0.64 | 5.37 | 7.43 | 6.90 | 7.05 |
| Sample Nr.2 | 7.97 | 12.04 | 4.38 | 1.86 | 2.26 |
| Sample Nr.1 | 10.20 | 14.60 | 7.00 | - | - |